Title
Metabolic regulation of intestinal stem cell function in Drosophila melanogaster

Author
Koehler, Christopher Lee

Publication Date
2016

Peer reviewed|Thesis/dissertation

UNIVERSITY OF CALIFORNIA

Los Angeles

Metabolic regulation of intestinal stem cell function in *Drosophila melanogaster*

A dissertation submitted in partial satisfaction of the

requirements for the degree Doctor of Philosophy

in Molecular Biology

by

Christopher Lee Koehler

2016

ABSTRACT OF THE DISSERTATION

Metabolic regulation of intestinal stem cell function in *Drosophila melanogaster*

by

Christopher Lee Koehler

Doctor of Philosophy in Molecular Biology

University of California, Los Angeles, 2016

Professor Dana Leanne Jones, Chair

Aging is a degenerative process characterized by the accumulation of cellular damage that results in altered tissue homeostasis, organ function, and, ultimately, death. Tissues with the potential for regeneration (muscle) or that undergo cellular turnover (intestine, blood, skin) rely on populations of adult stem or progenitor cells to divide and replace damaged cells to maintain tissue homeostasis. One hallmark of aging is reduced stem cell function, which can lead to decreased tissue homeostasis. The exact mechanisms for aging are still unclear, but recent evidence suggests an important role for adult stem cells in organismal aging. Current reports indicate that alterations in adult stem cell function via changes in stem cell metabolism can have widespread effects on tissue homeostasis and aging. Thanks to its relatively short lifespan and amenability to genetic manipulations, the model organism *Drosophila melanogaster* provides a convenient system to study the interaction between somatic stem cell metabolism and aging. A recently discovered population of intestinal stem cells in *Drosophila* bears many similarities to the stem cells of the mammalian small intestine. Genetic tractability, a simple cell lineage, and conserved pathways that regulate stem cell behavior combine to make the

Drosophila midgut epithelium a powerful model system for the study of stem cell regulation and tissue homeostasis.

Here, we show that increased mitochondrial biogenesis or enhanced electron transport chain function in the intestinal stem cells results in increased tissue homeostasis, a delay in age-related midgut phenotypes, and increased lifespan. This prompted us to study the roles of mitochondrial dynamics (fission, fusion, movement, and turnover) on intestinal stem cell function. We demonstrate that loss of either of two, mitophagy-related genes, *pink1* or *parkin*, in *Drosophila* ISCs leads to: severe alterations in mitochondrial structure, nearly complete inhibition of stem cell proliferation during aging or stress, and the appearance of senescence-associated markers within the ISCs.

The dissertation of Christopher Lee Koehler is approved.

Utpal Banerjee

David William Walker

Alvaro Sagasti

Volker Hartenstein

Dana Leanne Jones, Committee Chair

University of California, Los Angeles

2016

Table of Contents

List of Figures

Chapter 1:

Chapter 2:

Chapter 3:

Chapter 4:

List of Tables

Chapter 4:

Acknowledgements

Chapter 2 is a version of a manuscript published in *Cell Metabolism* reproduced here with permission from the Copyright Clearance Center (order number 4000091457975). [Rera, M., S. Bahadorani, J. Cho, C.L. Koehler, M. Ulgherait, J.H. Hur, W.S. Ansari, T. Lo, Jr., D.L. Jones, and D.W. Walker. 2011. Modulation of longevity and tissue homeostasis by the Drosophila PGC-1 homolog. *Cell Metabolism*. 14:623-634]. The authors M.R., S. B., and J. C. contributed equally to the manuscript. C.L.K, M.U, J.H.H., W.S.A, and T.L performed experiments and contributed to the manuscript editing. D.L.J and D.W.W. were the PIs of the study. D.L.J. is funded by the Emerald Foundation, the G. Harold and Leila Y. Mathers Charitable Foundation, the ACS, the California Institute for Regenerative Medicine (CIRM), and the NIH (R01 AG028092). C.L.K. was funded by an NIH Developmental Biology training grant (2T32HD007495, C. Kintner). M.U. is supported by a Ruth L. Kirschstein National Research Service Award (GM07185). D.W.W is funded by the National Institute on Aging (RO1 AG037514) and the Ellison Medical Foundation. D.W.W also received support from the UCLA Older Americans Independence Center, NIH/NIA Grant P30-AG028748, and the content does not necessarily represent the official views of the National Institute on Aging or the National Institutes of Health. D.W.W is an Ellison Medical Foundation New Scholar in Aging.

Chapter 3 is a version of a manuscript published in the journal *Aging*. [Hur, J.H., S. Bahadorani, J. Graniel, C.L. Koehler, M. Ulgherait, M. Rera, D.L. Jones, and D.W. Walker. 2013. Increased longevity mediated by yeast NDI1 expression in Drosophila intestinal stem and progenitor cells. *Aging*. PMID:24038661, PMCID:PMC3808699, DOI:10.18632/aging.100595]. *Aging* applies the Creative Commons Attribution License (CC BY) to all works publishes in *Aging*. The article is being reused here in accordance with the CC BY. JHH performed experiments and prepared the manuscript. SB, JG, CLK, MU, and MR performed experiments. DLJ and DWW were the

PIs of the study. DWW is supported by the National Institute on Aging (R01 AG037514, R01 AG040288) and the Ellison Medical Foundation. MU is supported by a Eureka fellowship. JG is funded by the National Institutes of Health/National Institute of General Medical Sciences (grant number NIH MARC T34 GM008563). DLJ is supported by the National Institute on Aging (R01 AG028092, R01 AG040288). CLK is supported by a National Science Foundation predoctoral training fellowship (DGE-1144087). D.W.W is an Ellison Medical Foundation New Scholar in Aging.

Chapter 4 is a version of a manuscript currently in revisions from the *Journal of Cell Biology* (*JCB*). [Koehler, C.L., Perkins, G.A., Ellisman, M.H., and D.L. Jones. 2016. Pink1 and Parkin regulate intestinal stem cell proliferation during stress and aging. *JCB* (in revisions)]. CLK performed experiments and prepared the manuscript. GAP and MHE acquired 3-D electron tomographies. DLJ was the PI of the study. This work was supported by the Eli and Edythe Broad Center of Regenerative Medicine and Stem Cell Research at the University of California-Los Angeles (D.L.J), the NIH: AG028092 and AG040288 (D.L.J.) and 5P41GM103412-28 (M.H.E.); and a graduate student fellowship from the National Science Foundation DGE-1144087 (C.L.K.)

Vita

Master of Science, 2009 - 2013

University of California San Diego, Division of Biological Sciences

Salk Institute of Biological Studies, Laboratory of Genetics

Bachelor of Science, 2003-2007

Trinity University, San Antonio, Texas

Concentration in molecular and cell biology

Summa cum laude with Honors

Advisor – Jonathan King, Ph.D.

Funding Awards

2010 NIH Developmental Biology training grant (2T32HD007495, C. Kintner)

2011-2014 National Science Foundation GRFP (DGE-1144087)

Publications

Koehler, C.L., Perkins, G.A., Ellisman, M.H., and D.L. Jones. 2016. Pink1 and Parkin regulate intestinal stem cell proliferation during stress and aging. *JCB* (in revisions).

Resnik-Docampo, M., **Koehler, C.L.**, Clark, R.I., Schinaman, J.M., Sauer, V., Wong, D.M., Lewis, S., D'Alterio, C., Walker, D.W., and D.L. Jones. 2016. Tricellular junctions regulate intestinal stem cell behavior to maintain homeostasis. *Nature Cell Biology*. (in press)

Hur, J.H., S. Bahadorani, J. Graniel, **C.L. Koehler**, M. Ulgherait, M. Rera, D.L. Jones, and D.W. Walker. 2013. Increased longevity mediated by yeast NDI1 expression in Drosophila intestinal stem and progenitor cells. *Aging*.

Rera, M., S. Bahadorani, J. Cho, **C.L. Koehler**, M. Ulgherait, J.H. Hur, W.S. Ansari, T. Lo, Jr., D.L. Jones, and D.W. Walker. 2011. Modulation of longevity and tissue homeostasis by the Drosophila PGC-1 homolog. *Cell Metabolism*. 14:623-634.

Koehler, C.L., N.P. Akimov, and R.C. Renteria. 2011. Receptive field center size decreases and firing properties mature in ON and OFF retinal ganglion cells after eye opening in the mouse. *Journal of neurophysiology*.

Barabas, P., W. Huang, H. Chen, **C.L. Koehler**, G. Howell, S.W. John, N. Tian, R.C. Renteria, and D. Krizaj. 2011. Missing optomotor head turning reflex in the DBA/2J mouse. *Invest Ophthalmol Vis Sci*.

Ryskamp, D.A., P. Witkovsky, P. Barabas, W. Huang, **C. Koehler**, N.P. Akimov, S.H. Lee, S. Chauhan, W. Xing, R.C. Renteria, W. Liedtke, and D. Krizaj. 2011. The Polymodal Ion Channel Transient Receptor Potential Vanilloid 4 Modulates Calcium Flux, Spiking Rate, and Apoptosis of Mouse Retinal Ganglion Cells. *J Neurosci*. 31:7089-7101.

Leone, A.K., J.A. Chun, **C.L. Koehler**, J. Caranto, and J.M. King. 2007. Effect of proinflammatory cytokines, tumor necrosis factor-alpha and interferon-gamma on epithelial barrier function and matrix metalloproteinase-9 in Madin Darby canine kidney cells. *Cell Physiol Biochem*. 19:99-112.

Chapter 1: Introduction

Mitochondrial function, tissue homeostasis, and the causative factors of aging

The process of aging is characterized by a time-dependent decrease in viability and concomitant increase in vulnerability. This degenerative process is characterized by the accumulation of cellular damage that results in altered tissue homeostasis, decreased organ function, and, ultimately, death. Though the process of aging is inevitable, it is also plastic. A number of interventions (both genetic and otherwise) exist that can alter the lifespan and health span of an organism. In organisms as diverse as yeast, *c. elegans*, *Drosophila melanogaster*, and mice, the mild inhibition of mitochondrial respiration is sufficient to significantly extend lifespan [1-5]. Furthermore, simple non-genetic interventions, such as caloric restriction or restricted feeding can lead to significant increases in lifespan or healthspan [6-11]. Investigating the plasticity of aging, as well as the pathways involved in the genetic and non-genetic interventions that affect lifespan, has revealed some clues as to the nature of the causative factors of aging, which, from a cellular and molecular perspective, are still poorly understood.

A number of physiological changes consistently accompany the process of aging; among them is the decline in bioenergetic efficiency. In flies, mice, and humans, the transcription of several electron transcport chain (ETC) components decreases with age, causing a decline in bioenergetic efficiency [12]. Furthermore, the organelles responsible for the majority of cellular energy production, the mitochondria, accumulate organellar damage with time [13]. These data indicate that declines in metabolic function correlate with age, but fail to determine if decreasing bioenergetic efficiency is a major driving force behind aging. Evidence suggesting that bioenergetic decline can actually cause aging came from the study of the mitochondrial mutator mouse - a model in which the exonuclease domain of the mtDNA polymerase gamma (POLG) had been inactivated, thus causing the introduction of mtDNA

mutation and deletions into the mitochondrial genome [14-16]. Mitochondrial mutator mice displayed increased mtDNA deletion loads, which led to the appearance of progeriod pheotypes including decreased lifespan, osteoporosis, hair graying, general wasting, decreased fertility, and alopecia [15, 16]. More specifically, several stem and progenitor compartments, including the hematopoietic stem cells (HSC) and neural progenitor cells (NPC), had defects including impaired self renewal and abnormal lineage differentiation [17]. The stem/progenitor cell defects manifested early in the chronological life of the mice (even as early as embryogenesis), while respiratory dysfunction in non-dividing tissues were not detected until in late in life [17]. Conversely, in a mitochondrial "deletor" model, where a dominant mutant form of replicative helicase, Twinkle, causes the introduction of large-scale mtDNA deletions in postmitotic tissue, mitochondrial defects do not minfest until late in life, and there is no decrease in longevity [18]. It is, therefore, possible that the somatic stem cell mtDNA mutations and subsequent mitochondrial dysfunction underlie the advanced aging phenotypes of these animals.

The involvement of metabolic pathways in lifespan extension, the decrease in bioenergetic efficiency with age, and appearance of progeriod phenotypes upon mtDNA mutation all point to the importance of mitochondria on the aging phenotype. Current discussions hinge around the question of whether age-dependent accumulation of mtDNA mutations are caused by free radicals from mitochondria or clonal expansion of mtDNA mutations. In the classic, free radical theory of aging, accumulated cellular damage is the result of cycles of mtDNA mutation that leads to ROS-dependent genotoxic stress, which then results in the accumulation of more mutations. However, the central role of ROS as the mutagenic element in the theory has been brought into question. In mice, knock-in mutations for a proofreading deficient PolgA [16] did not demonstrate increased levels of oxidative protein damage or age-dependent increases in mtDNA oxidative damage [19]. Furthermore, in *Drosophila*, only a small number of the mutations in the mtDNA of aged flies were GC to TA transversions, therefore excluding oxidative stress as the main mechanism for mutation [20].

Importantly, los of function (LOF) mutations in the mitochondrial superoxide dismutase (*Sod2*) or a DNA repair enzyme that removes oxidatively damaged deoxyguanosine residues (*Ogg1*), have no effect on the somatic mtDNA mutation rate [20]. An alternative theory for the spread and accumulation of mtDNA damage with age is clonal expansion in which mtDNA mutations are passed to progeny; these mutations accumulate with age until reaching a pathogenic level. Reports have shown that respiratory chain defects accumulate to significant levels in human colon [21], liver [22], stomach [23], and small intestine [24]; the accumulation appears to be caused by clonal expansion of mtDNA pools from progenitor cells, thus highlighting the importance of the maintenance of mutation-free mtDNA in stem cell progenitor cells.

The *Drosophla* posterior midgut provides an ideal system for *in vivo* studies of stem cell function and tissue homeostasis

Individually, stem cell function and metabolism have been implicated as factors that regulate aging. Until recently, fewer studies have been concerned with how the metabolism of stem cells themselves can impact tissue homeostasis, and, therefore, aging and longevity. This is a question that the following manuscript has sought to shed some light on. In this report, the system used to study this interaction between stem cell metabolism, tissue homeostasis, and aging, is the *Drosophila* posterior midgut.

Tissues with the potential for regeneration (such as the muscle) or that undergo continuous cellular turnover (such as the intestinal epithelium, the skin, or the blood) rely on populations of adult stem or progenitor cells to divide and replace damaged cells in order to maintain tissue homeostasis [25]. Similar to the mammalian intestine, the midgut of Drosophila contains intestinal stem cells (ISCs) responsible for the turnover of the gut epithelium via repeated cycles of stem cell division and daughter cell differentiation [26, 27]. Genetic tractability, a simple cell lineage, and conserved pathways that regulate stem cell behavior combine to make the Drosophila midgut epithelium a powerful model system for the study of

stem cell regulation and tissue homeostasis. Similar to the mammalian small intestine, regional differences exist along the length of the *Drosophila* midgut; therefore, this report focuses solely on the posterior midgut (modeled in Figure 1-1) [28, 29].

In the posterior midgut, the ISCs reside adjacent to the basement membrane. Here, they can either undergo symmetric division in order to increase ISC number due to the presence of nutritional cues [30], or divide asymmetrically in order to maintain turnover of differentiated epithelial cells. Asymmetric ISC division leads to self renewal of the ISC along with the generation of a daughter cell, called an enteroblast (EB) [26, 27]. Subsequent Delta/Notch signaling between the ISC and EB then dictate the direction of EB differentiation. High Notch signaling causes EBs to differentiate into large, polyploidy, absorptive cells, called enterocytes (ECs). Alternatively, Low Notch signaling directs EB differentiation to the secretory, enteroendocrine (EE) cell lineage [31-33]. Recent reports indicate that EEs can also derive directly from ISCs [34-36].

In a young, homeostatic midgut milieu, the epithelium of the posterior midgut undergoes slow turnover due to sparse ISC mitoses [26, 27]. Mitogenic stimuli such as the presence of pathogenic bacteria, chemical induces DNA damage, disruption of the basement membrane, or bacterial dysbiosis can cause drastic increases in ISC mitotic rate, leading to increased gut turnover (modeled in Figure 1-1) [37-48]. While the adaptive proliferation after injury can maintain tissue homeostasis via replenishment of damaged cells, uncontrolled ISC proliferation or altered differentiation programs can lead to los of tissue homeostasis.

Aging in the *Drosophla* midgut results in the manifestation of a number of easily scored, ISC-related phenotypes. Loss of epithelial monoloayer morphology occurs due to the accumulation of non-terminally differentiated cells (Figure 1-2A-A'). Additionally, the midgut displays an age-related block in terminal differentiation whereby ISC/EB-specific markers such as Escargot (Esg), or EB-specific markers such as GBE.Su(H)LacZ, are expression in polyploidy ECs (Figure 1-2B-B'). Lastly, the ISCs of the posterior midgut tend to increase their

proliferation rates with age as noted by the increased presence of the mitotic marker phospho-Histone H3 (pHH3) (Figure 1-2C-C'). The *Drosophila* posterior midgut, therefore, presents an ideal system in which to study age-related or stress-specific changes in stem cell function, its relation to tissue homeostasis, and the ultimate effect on aging.

Mitochondrial function changes with age in *Drosophila*; can metabolic dysfunction in the somatic stem cell affect aging?

In *Drosophila*, reports have indicated the presence of both age-associated changes in mitochondrial structure [49, 50] and an age-dependent decline in mitochondrial function [51, 52]. Furthermore, mtDNA deletions are detected in aging flies [53, 54], and the levels of mitochondrial transcripts are significantly reduced [55]. In Chapter 2, we demonstrate that increased mitochondrial biogenesis and function via progenitor-specific overexpression of dPGC1 leads to an increase in lifespan and prolonged tissue homeostasis in the midgut epithelium [56]. In Chapter 3, we go on to show that increased mitochondrial function via NADH Dehydrogenase Internal 1 (NDI1) overexpression in the intestinal progenitor cells of *Drosophila* is also sufficient to maintain tissue homeostasis and extend lifespan [57]. Previous results, along with those presented here in Chapters 2 and 3 indicate that enhanced mitochondrial function in intestinal progenitors can delay age-onset phenotypes in the whole organism; therefore, age-associated declines in mitochondrial function of ISC/EBs could be a causative factor in the *Drosophila* aging phenotype.

Mitochondrial dynamics and intestinal stem cell function

The results from Chapters 2 and 3 prompted us to explore the role of mitochondrial dynamics in the adult intestinal stem cell of *Drosophila*. Mitochondrial dynamics is a term that encompasses mitochondrial network fission and fusion, mitochondrial movement and trafficking, and the turnover of mitochondria via mitophagy. In Chapter 4, we complete an RNAi screen to

determine which, if any, factors involved in mitochondrial dynamics played a role in the regulation of ISC function during aging. Chapter 4 demonstrates that progenitor cell-specific loss of either of two mitophagy-related genes (PTEN-induced putative kinase 1 [*pink1*] or *parkin*) leads to: severe alterations in mitochondrial structure, nearly complete inhibition of stem cell proliferation during aging or stress, the presence of senescence-associated markers in the ISC/EBs, and a functionally senescent phenotype.

Specifically, knockdown of Pink1 or Parkin in the SICs causes some mitochondria to undergo an orthodox to condensed transition, which is associated with increased OXPHOS activity and ROS production. These changes are accompanied by a significant decrease in ISC proliferation. In addition, progenitor-specific knockdown of Pink1/Parkin results in the accumulation of several senescence markers in the ISCs including senescence associated β-Galactosidase (SA-β-Gal) and heterochromatin protein 1 (HP1). In addition, we demonstrate that ISCs depleted of Pink1 or Parkin are functionally senescent; the ISCs remain proliferation-deficient after resumption of normal expression. Therefore, we conclude that loss of mitophagy-associated Pink1/Parkin in the *Drosophila* ISCs leads to a senescence-like phenotype that inhibits proliferation during aging and stress.

In a cell responsible for the replenishment of the epitheliu, reduced potential for mitochondrial turnover, via Pink1/Parkin knockdown, coupled to increased ROS production could lead to dramatically negative consequences for the ISC, midgut, and organism as a whole. However, our data reseal a novel mechanism by which ISCs halt almost all age- or stress-related proliferation in response to progenitor-specific knockdown of Pink1/Parkin. Surprisingly, this lack of division preserves tissue homeostasis with no negative impact on the lifespan of the fly. We hypothesize this could be a strategy employed by adult stem cells that have undergone irreparable damage to mitochondria to limit their negative impact on the tissue as a whole. Altogether, Chapter 4 highlights a previously unidentified role for mitophagy-related genes in the regulation of stem cell proliferation. Furthermore, we highlight the uncoupling of

cellular, tissue, and organismal aging as a ptential strategy employed by stem cells to limit tissue- and organism-wise damage as a result of stem cell dysfunction.

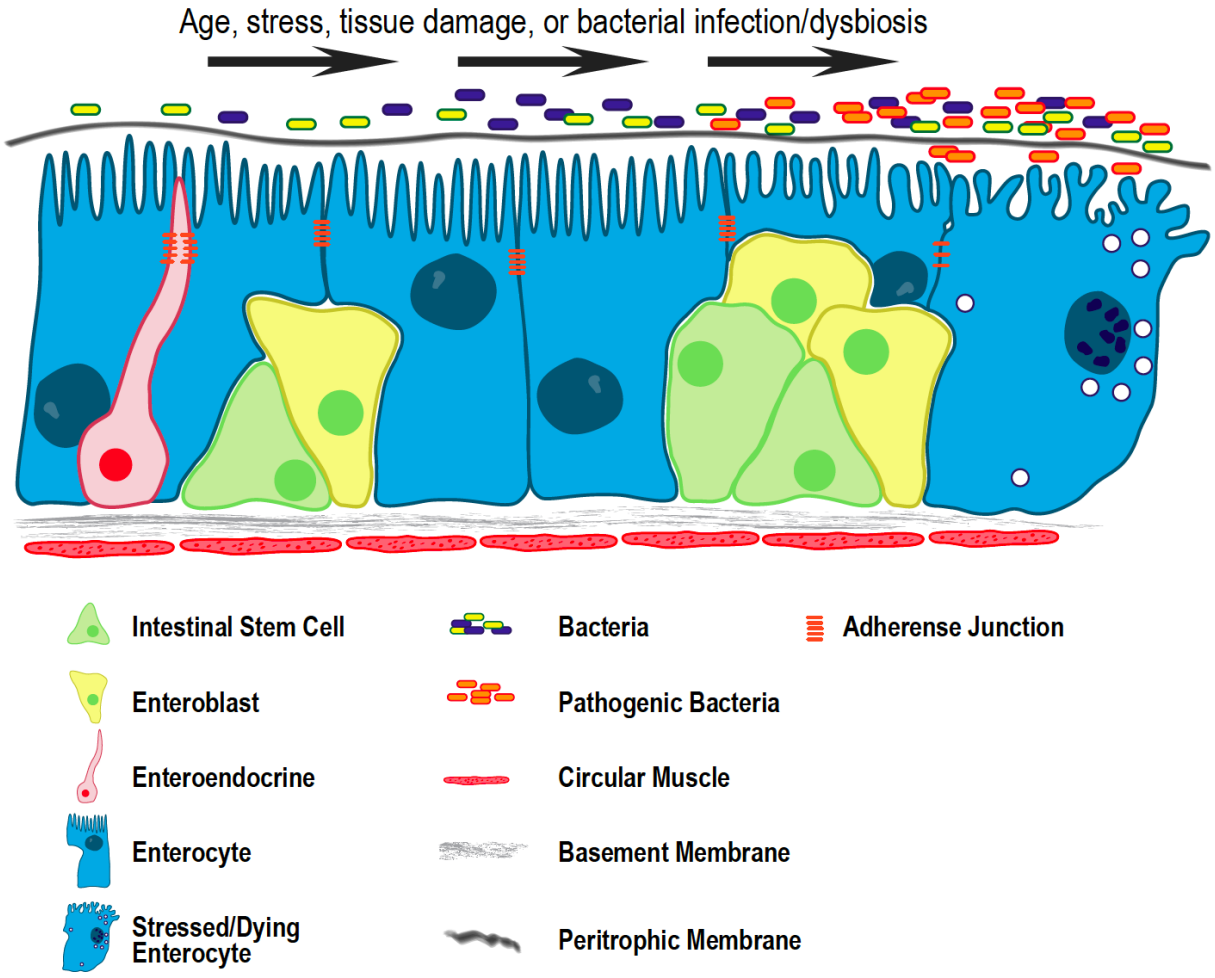

Figure 1-1. Schematic representation of the adult *Drosophila* posterior midgut under homeostatic and non-homeostatic conditions. (Left) Modeled representation of the different cell types of the young, homeostatic *Drosophila* posterior midgut epithelium. (Right) Representation of age- or stress-related phenotypes in the posterior midgut epithelium including: accumulation of non-terminally differentiated cells, increased ISC proliferation, disrupted barrier function, and altered epithelial monolayer morphology.

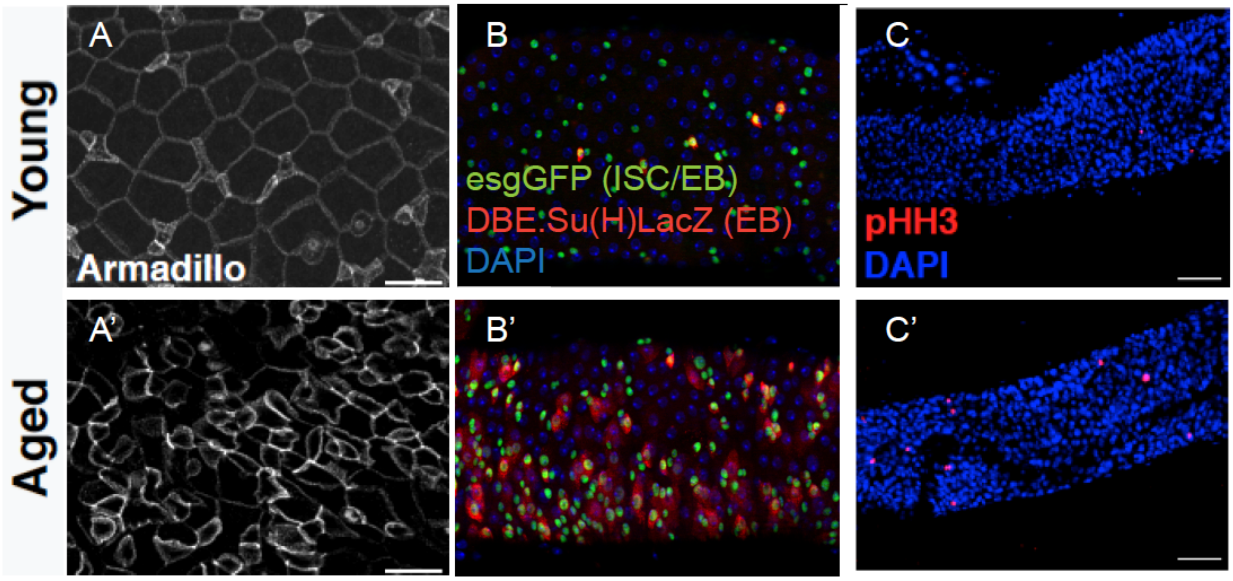

Figure 1-2. Aging phenotypes of the *Drosophila* posterir midgut. Young (A-C) or aged (A'-C') posterior midgut morphology assayed via Armadillo antibody stain (A-A'), expression of ISC/EB-specific margers (B-B'), or mitotic activity assayed via pHH3 (C-C').

References

1. Lakowski, B. and S. Hekimi, *Determination of life-span in Caenorhabditis elegans by four clock genes.* Science, 1996. **272**(5264): p. 1010-3.
2. Braeckman, B.P., et al., *Apparent uncoupling of energy production and consumption in long-lived Clk mutants of Caenorhabditis elegans.* Curr Biol, 1999. **9**(9): p. 493-6.
3. Copeland, J.M., et al., *Extension of Drosophila life span by RNAi of the mitochondrial respiratory chain.* Curr Biol, 2009. **19**(19): p. 1591-8.
4. Liu, X., et al., *Evolutionary conservation of the clk-1-dependent mechanism of longevity: loss of mclk1 increases cellular fitness and lifespan in mice.* Genes Dev, 2005. **19**(20): p. 2424-34.
5. Kirchman, P.A., et al., *Interorganelle signaling is a determinant of longevity in Saccharomyces cerevisiae.* Genetics, 1999. **152**(1): p. 179-90.
6. Gillespie, Z.E., J. Pickering, and C.H. Eskiw, *Better Living through Chemistry: Caloric Restriction (CR) and CR Mimetics Alter Genome Function to Promote Increased Health and Lifespan.* Front Genet, 2016. **7**: p. 142.
7. Choi, K.M., et al., *Enhancement of mitochondrial function correlates with the extension of lifespan by caloric restriction and caloric restriction mimetics in yeast.* Biochem Biophys Res Commun, 2013. **441**(1): p. 236-42.
8. Yamaza, H., et al., *Lifespan extension by caloric restriction: an aspect of energy metabolism.* Microsc Res Tech, 2002. **59**(4): p. 325-30.
9. Hatori, M., et al., *Time-restricted feeding without reducing caloric intake prevents metabolic diseases in mice fed a high-fat diet.* Cell Metab, 2012. **15**(6): p. 848-60.
10. Gill, S., et al., *Time-restricted feeding attenuates age-related cardiac decline in Drosophila.* Science, 2015. **347**(6227): p. 1265-9.

11. Chaix, A., et al., *Time-restricted feeding is a preventative and therapeutic intervention against diverse nutritional challenges.* Cell Metab, 2014. **20**(6): p. 991-1005.

12. Zahn, J.M., et al., *Transcriptional profiling of aging in human muscle reveals a common aging signature.* PLoS genetics, 2006. **2**(7): p. e115.

13. Brunk, U.T. and A. Terman, *The mitochondrial-lysosomal axis theory of aging: accumulation of damaged mitochondria as a result of imperfect autophagocytosis.* Eur J Biochem, 2002. **269**(8): p. 1996-2002.

14. Vermulst, M., et al., *DNA deletions and clonal mutations drive premature aging in mitochondrial mutator mice.* Nat Genet, 2008. **40**(4): p. 392-4.

15. Kujoth, G.C., et al., *Mitochondrial DNA mutations, oxidative stress, and apoptosis in mammalian aging.* Science, 2005. **309**(5733): p. 481-4.

16. Trifunovic, A., et al., *Premature ageing in mice expressing defective mitochondrial DNA polymerase.* Nature, 2004. **429**(6990): p. 417-23.

17. Ahlqvist, K.J., et al., *Somatic progenitor cell vulnerability to mitochondrial DNA mutagenesis underlies progeroid phenotypes in polg mutator mice.* Cell Metabolism, 2012. **15**(1): p. 100-9.

18. Tyynismaa, H., et al., *Mutant mitochondrial helicase Twinkle causes multiple mtDNA deletions and a late-onset mitochondrial disease in mice.* Proc Natl Acad Sci U S A, 2005. **102**(49): p. 17687-92.

19. Zhang, D., et al., *Construction of transgenic mice with tissue-specific acceleration of mitochondrial DNA mutagenesis.* Genomics, 2000. **69**(2): p. 151-61.

20. Itsara, L.S., et al., *Oxidative stress is not a major contributor to somatic mitochondrial DNA mutations.* PLoS Genet, 2014. **10**(2): p. e1003974.

21. Taylor, R.W., et al., *Mitochondrial DNA mutations in human colonic crypt stem cells.* J Clin Invest, 2003. **112**(9): p. 1351-60.

22. Fellous, T.G., et al., *Locating the stem cell niche and tracing hepatocyte lineages in human liver.* Hepatology, 2009. **49**(5): p. 1655-63.

23. McDonald, S.A., et al., *Mechanisms of field cancerization in the human stomach: the expansion and spread of mutated gastric stem cells.* Gastroenterology, 2008. **134**(2): p. 500-10.

24. Gutierrez-Gonzalez, L., et al., *Analysis of the clonal architecture of the human small intestinal epithelium establishes a common stem cell for all lineages and reveals a mechanism for the fixation and spread of mutations.* J Pathol, 2009. **217**(4): p. 489-96.

25. Jones, D.L. and T.A. Rando, *Emerging models and paradigms for stem cell ageing.* Nature cell biology, 2011. **13**(5): p. 506-12.

26. Ohlstein, B. and A. Spradling, *The adult Drosophila posterior midgut is maintained by pluripotent stem cells.* Nature, 2006. **439**(7075): p. 470-4.

27. Micchelli, C.A. and N. Perrimon, *Evidence that stem cells reside in the adult Drosophila midgut epithelium.* Nature, 2006. **439**(7075): p. 475-9.

28. Buchon, N., et al., *Morphological and molecular characterization of adult midgut compartmentalization in Drosophila.* Cell reports, 2013. **3**(5): p. 1725-38.

29. Marianes, A. and A.C. Spradling, *Physiological and stem cell compartmentalization within the Drosophila midgut.* eLife, 2013. **2**: p. e00886.

30. O'Brien, L.E., et al., *Altered modes of stem cell division drive adaptive intestinal growth.* Cell, 2011. **147**(3): p. 603-14.

31. Liu, W., S.R. Singh, and S.X. Hou, *JAK-STAT is restrained by Notch to control cell proliferation of the Drosophila intestinal stem cells.* J Cell Biochem, 2010. **109**(5): p. 992-9.

32. Maeda, K., et al., *E-cadherin prolongs the moment for interaction between intestinal stem cell and its progenitor cell to ensure Notch signaling in adult Drosophila midgut.* Genes to cells : devoted to molecular & cellular mechanisms, 2008. **13**(12): p. 1219-27.

33. Takashima, S., et al., *Development of the Drosophila entero-endocrine lineage and its specification by the Notch signaling pathway.* Dev Biol, 2011. **353**(2): p. 161-72.

34. Biteau, B. and H. Jasper, *Slit/Robo signaling regulates cell fate decisions in the intestinal stem cell lineage of Drosophila.* Cell Rep, 2014. **7**(6): p. 1867-75.

35. Guo, Z. and B. Ohlstein, *Stem cell regulation. Bidirectional Notch signaling regulates Drosophila intestinal stem cell multipotency.* Science, 2015. **350**(6263).

36. Zeng, X. and S.X. Hou, *Enteroendocrine cells are generated from stem cells through a distinct progenitor in the adult Drosophila posterior midgut.* Development, 2015. **142**(4): p. 644-53.

37. Amcheslavsky, A., et al., *Tuberous sclerosis complex and Myc coordinate the growth and division of Drosophila intestinal stem cells.* The Journal of cell biology, 2011. **193**(4): p. 695-710.

38. Amcheslavsky, A., J. Jiang, and Y.T. Ip, *Tissue damage-induced intestinal stem cell division in Drosophila.* Cell Stem Cell, 2009. **4**(1): p. 49-61.

39. Amcheslavsky, A., et al., *Enteroendocrine cells support intestinal stem-cell-mediated homeostasis in Drosophila.* Cell Rep, 2014. **9**(1): p. 32-9.

40. Biteau, B. and H. Jasper, *EGF signaling regulates the proliferation of intestinal stem cells in Drosophila.* Development, 2011. **138**(6): p. 1045-55.

41. Buchon, N., et al., *Invasive and indigenous microbiota impact intestinal stem cell activity through multiple pathways in Drosophila.* Genes & Development, 2009. **23**(19): p. 2333-2344.

42. Buchon, N., et al., *Drosophila Intestinal Response to Bacterial Infection: Activation of Host Defense and Stem Cell Proliferation.* Cell Host and Microbe, 2009. **5**(2): p. 200-211.

43. Jiang, H. and B.A. Edgar, *EGFR signaling regulates the proliferation of Drosophila adult midgut progenitors.* Development, 2009. **136**(3): p. 483-493.

44. Jiang, H., et al., *Cytokine/Jak/Stat signaling mediates regeneration and homeostasis in the Drosophila midgut.* Cell, 2009. **137**(7): p. 1343-55.

45. Lee, W.-J., *Bacterial-modulated host immunity and stem cell activation for gut homeostasis.* Genes & Development, 2009. **23**(19): p. 2260-5.

46. Li, H., Y. Qi, and H. Jasper, *Dpp signaling determines regional stem cell identity in the regenerating adult Drosophila gastrointestinal tract.* Cell Rep, 2013. **4**(1): p. 10-8.

47. Myant, K.B., et al., *Rac1 drives intestinal stem cell proliferation and regeneration.* Cell Cycle, 2013. **12**(18).

48. Tian, A. and J. Jiang, *Intestinal epithelium-derived BMP controls stem cell self-renewal in Drosophila adult midgut.* Elife, 2014. **3**: p. e01857.

49. Walker, D.W. and S. Benzer, *Mitochondrial "swirls" induced by oxygen stress and in the Drosophila mutant hyperswirl.* Proc Natl Acad Sci U S A, 2004. **101**(28): p. 10290-5.

50. Burch, G.E., R. Sohal, and L.D. Fairbanks, *Ultrastructural changes in Drosophila heart with age.* Arch Pathol, 1970. **89**(2): p. 128-36.

51. Sohal, R.S., et al., *Age-related decrease in expression of mitochondrial DNA encoded subunits of cytochrome c oxidase in Drosophila melanogaster.* Mech Ageing Dev, 2008. **129**(9): p. 558-61.

52. Ferguson, M., et al., *Age-associated decline in mitochondrial respiration and electron transport in Drosophila melanogaster.* Biochem J, 2005. **390**(Pt 2): p. 501-11.

53. Yui, R., Y. Ohno, and E.T. Matsuura, *Accumulation of deleted mitochondrial DNA in aging Drosophila melanogaster.* Genes Genet Syst, 2003. **78**(3): p. 245-51.

54. Yui, R. and E.T. Matsuura, *Detection of deletions flanked by short direct repeats in mitochondrial DNA of aging Drosophila.* Mutat Res, 2006. **594**(1-2): p. 155-61.

55. Calleja, M., et al., *Mitochondrial DNA remains intact during Drosophila aging, but the levels of mitochondrial transcripts are significantly reduced.* J Biol Chem, 1993. **268**(25): p. 18891-7.

56. Rera, M., et al., *Modulation of longevity and tissue homeostasis by the Drosophila PGC-1 homolog.* Cell Metabolism, 2011. **14**(5): p. 623-34.

57. Hur, J.H., et al., *Increased longevity mediated by yeast NDI1 expression in Drosophila intestinal stem and progenitor cells.* Aging, 2013.

Chapter 2: Modulation of longevity and tissue homeostasis by the *Drosophila* PGC-1 homolog

Michael Rera, Sepehr Bahadorani, Jaehyoung Cho, Christopher L. Koehler, Matthew Ulgherait, Jae H. Hur, William S. Ansari, Thomas Lo Jr., D. Leanne Jones, David W. Walker

Abstract

In mammals, the PGC-1 transcriptional co-activators are key regulators of energy metabolism, including mitochondrial biogenesis and respiration, which have been implicated in numerous pathogenic conditions including neurodegeneration and cardiomyopathy. Here, we show that overexpression of the *Drosophila* PGC-1 homolog (*dPGC-1*/*spargel*) is sufficient to increase mitochondrial activity. Moreover, tissue-specific overexpression of *dPGC-1* in stem and progenitor cells within the digestive tract extends lifespan. Long-lived flies overexpressing *dPGC-1* display a delay in the onset of aging-related changes in the intestine, leading to improved tissue homeostasis in old flies. Together, these results demonstrate that *dPGC-1* can slow aging both at the level of cellular changes in an individual tissue and also at the organismal level by extending lifespan. Our findings point to the possibility that alterations in PGC-1 activity in high-turnover tissues, such as the intestine, may be an important determinant of longevity in mammals.

Introduction

A progressive loss of mitochondrial energetic capacity is a common feature of multiple aspects of aging [1]. This may result from the age-related decline in the expression of genes important for mitochondrial electron transport chain (ETC) function observed in diverse organisms including humans [2, 3]. A causal relationship is suggested by the fact that alterations in ETC activity are emerging as integrating phenomena in a number of lifespan-extending manipulations including dietary restriction (DR) [4] and reduced insulin/TOR signaling [5, 6]. More specifically, DR has been observed to result in an increase in mitochondrial biogenesis and/or respiratory activity in yeast, worms, flies, mice and humans [7-13]. Furthermore, perturbation of mitochondrial ETC components has been shown to impair the ability of DR to promote longevity in yeast, worms and flies [11-14]. These findings suggest that strategies to enhance mitochondrial biogenesis and/or energy metabolism may promote healthy aging.

In mammals, the PGC-1 family of transcriptional co-activators plays a central role in the regulation of mitochondrial biogenesis, respiration and glucose homeostasis [15, 16]. Three members of this family have been identified based on sequence similarity to the founding member PGC-1α. PGC-1 family members promote mitochondrial biogenesis through co-activation of nuclear transcription factors, including nuclear respiratory factor-1 and -2 (NRF-1 and NRF-2) and estrogen-related receptor-α (ERRα) to induce the expression of genes encoding mitochondrial proteins [17, 18]. Increased PGC-1 gene activity has been associated with health benefits in a number of pathogenic conditions, including various muscular [19-21] and neurodegenerative disorders [22, 23]. Furthermore, increased expression of PGC-1α has been shown to protect against age-related sarcopenia [24] and to improve respiration and gluconeogenesis under conditions of telomere dysfunction [25]. However, the role of PGC-1 co-activators in determining longevity remains poorly understood.

The fruit fly *Drosophila melanogaster* is an excellent model system to study the role of mitochondrial activity in the aging process [26]. In addition, *Drosophila* has emerged as a premier model system to dissect the relationship between altered stem cell behavior, tissue homeostasis and aging [27]. Several discrete populations of adult stem cells have been reported in *Drosophila*, such as germline stem cells and intestinal stem cells (ISCs) in the midgut (reviewed in [27]). These stem cells reside in defined niches and play active roles in maintaining local tissue homeostasis, resembling the behavior of mammalian stem cells.

Here, we report that up-regulation of the *Drosophila* PGC-1 homolog (*dPGC-1/spargel*) leads to an increase multiple markers of mitochondrial abundance and activity both during development and also in the adult stage. Furthermore, we find that targeted overexpression of *dPGC-1* in the digestive tract, including restricted expression in somatic stem cells (including ISCs) and immediate daughter cells, can extend adult lifespan. Up-regulation of *dPGC-1* abrogates the precocious activation of ISC proliferation and delays the accumulation of mis-differentiated cells in the intestinal epithelium- two hallmark of aging in this tissue. Furthermore, *dPGC-1* up-regulation leads to improved intestinal integrity in old flies. Our findings demonstrate that *dPGC-1* gene activity is an important determinant of aging both at the tissue and organismal level.

Results

Overexpression of *Drosophila* PGC-1 leads to an increase in mitochondrial activity

The *Drosophila* genome contains a single PGC-1 homolog, CG9809/*spargel*/*dPGC-1* [28]. A loss-of-function study reported that *dPGC-1* is required for the normal expression of multiple genes encoding mitochondrial proteins in the larval fat body [29]; therefore, we predicted that increased *dPGC-1* might lead to an increase in mitochondrial abundance and/or activity. To investigate the physiologic and phenotypic consequences of overexpression of *dPGC-1*, we expressed *dPGC-1* using the GAL4/UAS system [30]. We transformed flies with

UAS-constructs containing the *dPGC-1* cDNA and performed twelve rounds of backcrossing into a w^{1118} background, which was used as a control strain in subsequent experiments. We confirmed that the *dPGC-1* transcript was up-regulated in flies carrying both the *dPGC-1* transgene and a ubiquitous GAL4 driver line, *daughterless (da)*-GAL4 (Figures S2-1A and S2-1B). Increased expression of *dPGC-1* did not produce any gross changes in body size (Figure S2-1C) or obvious differences in size, morphology or cell number of external structures, such as wings (Figure S2-1D).

To determine whether up-regulation of *dPGC-1* can increase mitochondrial activity, we measured three independent mitochondrial markers: the amount mitochondrial DNA (mtDNA), the enzymatic activity of citrate synthase, a key enzyme in the Krebs cycle and a widely used marker for mitochondrial density, and the abundance of HSP60, a mitochondrial matrix protein. Firstly, we measured the amount of mtDNA, relative to the amounts of a nuclear DNA (nDNA) amplicon, in 3rd instar larvae and observed a 2.5 fold increase in response to *dPGC-1* up-regulation (Figure 2-1A). This data is consistent with a *dPGC-1*-mediated increase in mitochondrial density per cell. Thoraxes, which consist primarily of flight muscle (a rich source of mitochondria), were used for the measurement of changes in mitochondrial abundance in adult flies: a 60% increase in mtDNA in response to *dPGC-1* up-regulation was observed in adult thoraxes (Figure 2-1B). In accordance, there was a significant increase in citrate synthase activity in both larvae (Figure 2-1C) and adult thoraxes in *dPGC-1* overexpressing animals (Figure 2-1D). Similarly, Western blots using antibodies against a mitochondrial matrix protein, HSP60, showed significant increases of HSP60 levels in both whole larvae and adult thoraxes of animals overexpressing *dPGC-1*, when normalized to loading control (Figures 2-1E and 2-1F).

Next, we sought to address whether *dPGC-1* can stimulate mitochondrial oxidative metabolism. We employed blue native polyacrylamide gel electrophoresis (BN-PAGE) to examine the impact of up-regulation of *dPGC-1* on the abundance of the respiratory chain

enzyme complexes. A significant increase in the abundance of respiratory complexes I, III, IV and V was observed in flies overexpressing *dPGC-1* (Figure 2-2A). To analyze the effect of elevated *dPGC-1* expression on respiratory chain activity, the rate of oxygen consumption was measured by using a Clark-type oxygen electrode. The steps in respiration were compared in mitochondria isolated from *dPGC-1*-overexpressing flies and controls by using substrates and inhibitors specific to individual respiratory complexes. In doing so, we observed that *dPGC-1* up-regulation confers an increase in complex I-, II- and IV-dependent respiration (Figures 2-2B and S2-1E). Moreover, the respiratory control ratio (RCR), or state 3:state 4 respiration ratio, was significantly higher in mitochondria isolated from flies with increased *dPGC-1* expression (Figure 2-2C). Taken together, our data suggest that *dPGC-1* overexpression is sufficient to increase mitochondrial biogenesis and bioenergetic efficiency.

Drosophila PGC-1 modulates metabolic stores and free glucose levels

In mammals, PGC-1α regulates glucose homeostasis [31, 32] and triglyceride (TAG) metabolism [33]. To determine whether *dPGC-1* also regulates fuel homeostasis, we examined metabolic stores and free glucose levels in *dPGC-1* overexpressing flies and controls. In *Drosophila*, metabolized nutrients are primarily stored as TAG and glycogen in the fat body, the insect equivalent of the mammalian liver and white adipose tissue. Using thin-layer chromatography, the most accurate method to measure stored TAG in *Drosophila* [34], we observed ~20% reduction in TAG levels in *dPGC-1* overexpressing flies (Figure 2-2D). In contrast, there was a significant increase in both the amount of stored glycogen (Figure 2-2E) and free glucose levels (Figure 2-2F) in *dPGC-1* overexpressing flies. Our data suggests that *dPGC-1* may play an important role in maintaining energy homeostasis in the fly-consistent with findings in mammals.

Effects of tissue-specific overexpression of *Drosophila* PGC-1 on longevity

As central regulators of energy homeostasis, PGC-1 co-activators provide an attractive target to modulate animal aging. Therefore, we examined the impact of targeted overexpression of *dPGC-1* in major tissues on *Drosophila* lifespan. Firstly, we examined the effects of ubiquitous overexpression of *dPGC-1* mediated by *da-GAL4* and observed a moderate decrease in adult survival (Figures S2-2A and S2-2B). Similar effects were observed when *dPGC-1* was ubiquitously expressed using the mifepristone (RU486) inducible driver Tubulin-Gene-Switch (Figures 2-3A and S2-2C). To begin to examine tissue-specific effects of *dPGC-1*, we used a panel of Gene-Switch driver lines with recently characterized age-related expression patterns [35]. Lifespan was significantly increased when *dPGC-1* was induced with *$S_1$106* (Figures 2-3B and S2-2D), which is expressed in abdominal fat and the digestive tract [35]. To further narrow the tissue-specific requirements for *dPGC-1*-mediated longevity, we used the *TIGS-2* driver, which is expressed in the digestive tract but not fat body [35]. Induced expression of *dPGC-1* with this driver line resulted in a 33% increase in mean lifespan and a 37% increase in maximum lifespan in female flies (Figure 2-3C) and no major effect in male flies (Figure S2-2E). Notably, adult survival was not improved when *dPGC-1* was induced with the pan-neuronal driver ELAV-Gene-Switch (Figures 2-3D and S2-2F). Similarly, muscle-specific expression of *dPGC-1* using a constitutive MHC-GAL4 driver did not promote life extension in male or female flies (data not shown). Two additional independent *dPGC-1* insertions were tested with *TIGS-2* and each resulted in enhanced longevity in female flies (Figures S2-2G and S2-2H). No major longevity effects were observed in male or female control flies exposed to RU486 (Figures S2-3A-S2-3H).

Together, the *$S_1$106* and *TIGS-2* lifespan data support the idea that the digestive tract is an important target tissue in *dPGC-1*-mediated longevity.

Overexpression of *dPGC-1* in intestinal stem and progenitor cells extends lifespan

As noted above, our tissue-specific longevity studies indicate that increased expression of *dPGC-1* in the digestive tract is sufficient to promote longevity. To validate and extend this finding, we set out to identify subsets of intestinal cells that are important in mediating this phenotype. Tissue homeostasis in the mid-gut is maintained by pluripotent intestinal stem cells (ISCs), which are distributed along the basement membrane [36, 37]. Division of an ISC gives rise to one daughter cell that retains stem cell fate and another daughter cell that becomes an enteroblast (EB), both expressing a transcription factor called Escargot (*esg*). Thus, expression of *esg* is often used as a surrogate marker for ISCs and EBs. After ISC division, the daughter EB does not divide again and differentiates into either a large, polyploid enterocyte (EC) or a small, diploid enteroendocrine (ee) cell that expresses Prospero (Pros) (Figure 2- 6A). Cell cycle arrest and differentiation of EBs are controlled by Delta-Notch signaling. While the ligand Delta (Dl) specifically accumulates in ISCs, it is quickly lost in newly formed EBs, which is accompanied by an activation of Notch signaling.

To examine the impact of targeted expression of *dPGC-1* in the ISCs and EBs, we used the constitutive *esgGAL4* driver line to overexpress *dPGC-1* and observed a significant lifespan extension in both male (Figure S2-4A) and female flies (Figure 2-4A) compared to isogenic control flies. Although *esgGal4* expression is restricted to ISCs and EBs in the intestine, it is also expressed in stem cells within malpighian tubules, germline and somatic stem cells in the testis, and in salivary glands [38]. Therefore, we made use of the recently described RU486-inducible *5961GS*, which recapitulates the *esgGal4* expression pattern in the digestive tract (ISCs/EBs and malpighian tubule stem cells) [38, 39] but is not expressed in salivary glands [38] or testis (C.K., L.J., unpublished observations). Consistent with a previous report [38], we failed to detect *5961GS* expression in the brain, thorax or abdomen. *5961GS*-mediated expression of *dPGC-1*, during both development and adulthood, resulted in a significant increase in lifespan (Figures 2-4B and S2-4B). No major longevity effects were observed in control flies exposed to RU486 (Figures S2-4C and S2-4D). Next, we took advantage of the inducible nature the

5961GS driver to determine whether adult-only induction of *dPGC-1* is sufficient to promote longevity. Indeed, *5961GS > dPGC-1* flies were significantly longer lived when exposed to RU486 exclusively in the adult stage (Figure 2-4C); again no major effects on longevity were observed in control flies exposed to RU486 (Figure S2-4E). Taken together, our data with the constitutive *esgGAL4* and the inducible *5961GS* driver support a model whereby increased expression of *dPGC-1* in stem and progenitor cells within the digestive tract of adults is sufficient to extend lifespan.

dPGC-1 extends lifespan independently of effects on reproduction or global stress resistance.

To gain further insight into *dPGC-1*-mediated longevity, we examined a number of physiological and behavioral parameters in long-lived flies overexpressing *dPGC-1*. For these studies, we used *esgGAL4* because expression in the ISCs/EBs is stronger than with *5961GS* [38], and the longevity effects are more pronounced with this driver. Importantly, there was no obvious difference in food consumption (Figure S2-5A) or body mass (Figure S2-5B) in long-lived flies compared to age-matched controls. As described earlier, we observed that ubiquitous up-regulation of *dPGC-1* leads to alterations in metabolic stores and free glucose levels (Figures 22-D- 2-2F). Therefore, we examined these parameters in long-lived *esgGAL4 > dPGC-1* flies. Interestingly, *esgGAL4*-mediated expression of *dPGC-1* is sufficient to confer a decrease in triglyceride (TAG) levels in whole flies (Figure S2-5C). Although *esgGAL4 > dPGC-1* flies display normal glycogen stores (Figure S2-5D), restricted expression of *dPGC-1* is sufficient to produce a moderate increase in free glucose levels (Figure S2-5E).

Interventions that extend lifespan are often associated with a decline in reproductive output [40]. However, long-lived *esgGAL4 > dPGC-1* flies display normal fertility compared to age-matched isogenic controls (Figure S2-5F). Interestingly, we also failed to detect fertility

defects in long-lived *dPGC-1* flies mediated by either *$S_1$106* or *TIGS-2* (SB & DW, unpublished observations). Another hallmark of extended longevity is an increase in the ability to withstand extrinsic stress [41-43]. Therefore, we tested the ability of *esgGAL4* > *dPGC-1* flies to survive under conditions of starvation and oxidative stress. However, we observed no difference in survival times when long-lived *dPGC-1* flies and controls were maintained on an agar-only diet to induce starvation (Figure S2-5G). In addition, long-lived *dPGC-1* flies displayed only a marginal increase in survival under hyperoxia (100% O_2; Figure S5H). Together, these data indicate that life extension mediated by overexpression of *dPGC-1* via *esgGAL4* acts independently of effects on reproduction or global stress resistance.

***dPGC-1* modulates mitochondrial activity and ROS levels in the aged intestine**

To better understand the relationship between *dPGC-1* gene activity and longevity, we examined *dPGC-1* mRNA levels in the intestine of young and aged flies. We observed that *dPGC-1* expression was dramatically decreased (~60%) in the intestine of aged control flies (Figure 2-5A). *esgGAL4* > *dPGC-1* flies display ~ a 2-fold increase in *dPGC-1* mRNA levels in the intestine at both time-points compared to controls (Figure 2-5A). Next, we examined whether increased *dPGC-1* expression in the intestine impacts the activities of mitochondrial respiratory chain enzymes in the target tissue. Indeed, *esgGAL4* > *dPGC-1* flies display an increase in both mitochondrial complex I (Figure 2-5B) and complex II (Figure 2-5C) activities in the aged intestine compared to controls. Interestingly, complex IV activity was increased in the intestines of *esgGAL4* > *dPGC-1* flies, compared to controls, at 10 days but not 30 days (Figure 2-5D).

The cationic dye JC-1 can be used to measure mitochondrial membrane potential at a cellular level. In healthy cells, the negative charge established by the intact mitochondrial membrane potential allows this lipophilic dye to enter the mitochondrial matrix where it accumulates and fluoresces red. When mitochondrial membrane potential is low, the dye

remains monomeric in the cytoplasm and fluoresces green. Therefore, membrane potential can be determined by the presence of J-aggregates and measured by the ratio of green: red fluorescence. Using this approach, we examined mitochondrial activity in the mid-gut epithelium. In doing so, we discovered that aging results in a progressive loss of mitochondrial membrane potential in this region of the intestine; however, intestines of long-lived *esgGAL4 >dPGC-1* flies showed significant maintenance of mitochondrial membrane potential, when compared to isogenic controls (Figures S2-6A-S2-6C).

PGC-1α is a potent regulator of reactive oxygen species (ROS) metabolism required for the induction of several ROS-detoxifying enzymes [44]. Therefore, we speculated that up-regulation of *dPGC-1* may reduce ROS levels in the target tissue. To test this idea, we examined the endogenous levels of ROS in the intestines of control and *esgGAL4 >dPGC-1* flies using dihydro-ethidium (DHE), a redox-sensitive dye that exhibits increased fluorescence intensity when oxidized [45, 46]. Targeted expression of *dPGC-1* in ISCs/EBs led to a reduction of DHE fluorescence in these cells and throughout the aged intestine (Figures 2-5E, 2-5F and S2-6D, S2-6E). Therefore, up-regulation of *dPGC-1* in stem cells and immediate daughter cells is sufficient to lower ROS levels throughout the intestinal epithelium in aged flies.

dPGC-1 modulates tissue homeostasis in the aged intestine

Given the ability of *dPGC-1* expression in the intestine to maintain mitochondrial activity and lower ROS levels, we wanted to determine whether targeted expression of *dPGC-1* in ISCs/EBs was sufficient to delay the onset of previously characterized aging-related phenotypes in the intestine. In the *Drosophila* intestine, aging or stress results in a dramatic increase in ISC proliferation, which is accompanied by an accumulation of mis-differentiated daughter cells that express markers of both ISCs and terminally differentiated daughter cells [47-49]. These cells retain expression of the stem cell markers, Esg and Dl, yet they are polyploid, suggesting that this population comprises EBs that that are blocked in the ability to terminally differentiate into

functional enterocytes [47-49]. The age-related increase in mis-differentiated cells disrupts epithelial integrity and tissue architecture, as revealed by staining for the membrane marker Armadillo (Arm), the *Drosophila* homolog of b-catenin. This leads to a loss of normal tissue homeostasis and severe deterioration of the midgut epithelium in aged flies [47], which may impact gut function or integrity.

In order to determine whether increased expression of *dPGC-1* leads to a delay in the aging-related phenotypes and improved tissue homeostasis in the gut, we quantified *esg*-positive cells (GFP^+ as a consequence of a UAS-*gfp* reporter) in guts of flies overexpressing *dPGC-1* under control of the *esg* promoter. For quantification of ISCs/EBs, GFP^+ cells were counted in control flies (genotype: *esgGAL4 , UAS-gfp/*+) or *dPGC-1* flies (genotype: *esgGAL4 , UAS-gfp/+ ; UAS-dPGC-1/*+), and at least 25 guts were examined for each time point (See Experimental Procedures for details). Both the increase in mis-differentiated cells, as well as the characteristic changes in tissue architecture were delayed in older animals expressing *dPGC-1* in ISCs/EBs (Figures 2-6B and S2-7A). The average number of GFP^+ cells per FOV in 50-day old control females was 115.1±6.4 (SEM) (n=26), whereas the average for 50-day old *dPGC-1* females was 69±5.5 (n=27) (Figure 2-6C). The same trend was observed in male flies (Figure S2-7B).

In addition to a decrease in the accumulation of mis-differentiated cells, we also observed a delay in the precocious activation of ISC proliferation, as measured by phosphorylation of histone H3 (pHH3), a marker of cell cycle progression through mitosis. Forty-eight day old female flies expressing *dPGC-1* under the control of the inducible *5961GS* driver, induced from the onset of adulthood, contained significantly fewer $pHH3^+$ cells, when compared to uninduced age-matched sibling controls (Figure 2-6D). No difference in the number of $pHH3^+$ cells was observed in 10 day old flies, indicating that the expression of *dPGC-1* delays the age-related increase in ISC proliferation. Furthermore, our data demonstrates that *dPGC-1* acts during the adult stage to abrogate the precocious activation of ISC proliferation,

which occurs during aging.

Finally, we sought to determine whether *dPGC-1* expression in the digestive tract affects intestinal integrity as a function of age. To develop an assay of intestinal integrity, we examined flies of different ages that had consumed a non-absorbable blue food dye (F D & C Blue Dye no. 1). As expected, we observed that in young flies (10 days) the dye is restricted to the proboscis and digestive tract post-feeding (Figure 2-7A). However, in aged flies (>30 days) we observed a fraction of animals that displayed a strikingly different phenotype. In these animals, the blue dye was clearly visible throughout the body post-feeding; subsequently, these flies were referred to as 'Smurf' flies (Figure 2-7B). To exclude the possibility that this phenotype was due to a unique property of this dye, we fed aged flies a different non-absorbable red food dye (F D & C Red Dye no. 40) and observed a fraction of individuals that displayed red food dye throughout the body post-feeding (MR & DW, unpublished observations). Therefore, we interpret the 'Smurf' phenotype, ie., the leakage of dye into the haemolymph and consequently all tissues, to reflect a defect(s) in intestinal integrity.

We next quantified the increase in 'Smurf' flies as a function of age in control and long-lived *esgGAL4* > *dPGC-1* flies (Figure 2-7C). In control flies, the fraction of 'Smurf' flies in the population increases dramatically with age; from 0% at 10 days to ~35% at 45 days of age. Strikingly, *esgGAL4*-mediated activation of *dPGC-1* retards the age-related onset of the 'Smurf' phenotype. Therefore, an increase in *dPGC-1* expression within the digestive tract results in improved intestinal integrity in aged flies, which is consistent with the delay in disruption of apical-basal polarity in intestines from aging flies, as revealed by Arm staining (Figure 2-6B). Together, our analysis of proliferative homeostasis and tissue integrity strongly support a model whereby *dPGC-1* activity in somatic stem cell lineages within the digestive tract regulates tissue homeostasis in the aged intestine.

Discussion

Aging is associated with a decline of function at the organismal level that has origins in cellular deterioration and the loss of tissue homeostasis. Considerable attention has been focused separately on the roles of stem cells [50] and mitochondria [1, 4] in the aging process, yet fundamental questions remain regarding the interplay between mitochondrial metabolism, stem cell behavior and lifespan determination. In this study, we demonstrate that the *Drosophila* PGC-1 homolog is a potent inducer of mitochondrial activity and that overexpression in somatic stem cells within the digestive tract can slow aging at both the tissue and organismal level.

It is interesting to speculate upon the tissue-specific requirements for *dPGC-1*-mediated longevity. Although we failed to observe life extension in response to ubiquitous, muscle or neuronal activation of *dPGC-1*, we cannot exclude the possibility that expression in subsets of muscle and/or neuronal cells or different levels of expression in these tissues could promote longevity. That said, we observed robust *dPGC-1*-mediated life extension with multiple driver lines that are expressed in the digestive tract. Consistent with our own findings, it was recently reported that intestinal homeostasis correlates with lifespan in a number of different genotypes including flies with altered Jun-N-terminal Kinase (JNK) or insulin/IGF signaling (IIS) activities [38]. One plausible explanation for such findings is that maintaining healthy intestinal function and/or integrity is an important determinant of fly lifespan. In our own study, using a non-absorbed food dye, we demonstrate that there is a loss of intestinal integrity as a function of age. It is possible that this phenomenon could impact the survival of the animal by exposing the internal tissues and organs to toxins or pathogens. However, although the intestine appears to play an important role in modulating longevity, we cannot rule out the role of cell non-autonomous effects in *dPGC-1*-mediated longevity. In this regard, we observed that *esg-GAL4*-mediated expression of *dPGC-1* resulted in changes in lipid/carbohydrate metabolism in whole flies.

In this study, we report that *dPGC-1* expression declines in the aged intestine of control flies, whereas directed expression of *dPGC-1* in somatic stem cells within the digestive tract is sufficient to retard aging in this tissue. Importantly, our data indicate that manipulating *dPGC-1* in ISCs/EBs leads to maintenance of mitochondrial activity throughout the midgut, rather than exclusively in stem cells. This is not unexpected, as there is no transit amplifying population of daughter cells; the EBs differentiate directly into one of two lineages. Therefore, any manipulation of stem cell physiology could easily be passed onto directly differentiating daughter cells. The enterocytes are the predominant cell type in the intestine; therefore, changes in these cells likely account for most of the phenotypic differences that we observe. In the case of ROS levels, we observe that *dPGC-1* expression in ISCs/EBs leads to a reduction in ROS levels in the stem cells, as well as in the enterocytes (Figures 2-5E, 2-5F and S2-6D, S2-6E).

Given the diverse roles that PGC-1 plays in metabolism [15], the relative contribution of each of these processes in modulating tissue homeostasis and longevity remains to be determined. However, our finding that *dPGC-1* modulates ROS levels in the aging intestine may provide mechanistic insight. ROS levels have been demonstrated to influence stem cell self-renewal and the onset of differentiation in multiple systems [45, 51-53]. Indeed, it was recently reported that Nrf2, a master regulator of the cellular redox state, specifically controls the proliferative activity of ISCs, promoting intestinal homeostasis [54]. Our findings support a model whereby *dPGC-1*-mediated alterations in metabolism, including ROS metabolism, can retard aging of the intestine with significant consequences for animal lifespan.
It will be interesting to determine whether PGC-1 family members in other species also regulate tissue homeostasis in high-turnover tissues such as intestine.

Acknowledgments: The authors would like to thank Kevin Vu, Kent Vu, Holly Vu and Jeff Copeland for help with fly work and generation of UAS-constructs. We also thank H.

Keshishian, S. Pletcher, L. Seroude, H. Jasper and the *Drosophila* Stock Center (Bloomington) for fly stocks. D.L.J. is funded by the Emerald Foundation, the G. Harold and Leila Y. Mathers Charitable Foundation, the ACS, the California Institute for Regenerative Medicine (CIRM), and the NIH (R01 AG028092). C.K. was funded by an NIH Developmental Biology training grant (2T32HD007495, C. Kintner). M.U. is supported by a Ruth L. Kirschstein National Research Service Award (GM07185). D.W.W is funded by the National Institute on Aging (RO1 AG037514) and the Ellison Medical Foundation. D.W.W also received support from the UCLA Older Americans Independence Center, NIH/NIA Grant P30-AG028748, and the content does not necessarily represent the official views of the National Institute on Aging or the National Institutes of Health. D.W.W is an Ellison Medical Foundation New Scholar in Aging.

Experimental Procedures

Analysis of survivorship, fertility, stress resistance, food intake, lipid/carbohydrate levels, mtDNA amount, enzyme activity assays, oxygen consumption, qRT-PCR, BN-PAGE and western blotting were conducted by standard methods and are available in the Supplemental Information.

***Drosophila* strains**

Tubulin-GS was provided by S. Pletcher. *Elav-GS* was provided by H. Keshishian. *S_1106* and *TIGS-2* were provided by L. Seroude. *5961GS* was provided by H. Jasper. *esgGAL4* was provided by A. Christiansen. All other stocks were provided by the Bloomington *Drosophila* Stock Center. We transformed flies with pUAST plasmids containing *dPGC-1* and performed 12 rounds of backcrossing into a *w^{1118}* background.

Dihydroethidium (DHE) Staining

ROS levels were detected in live tissue based on previously described methods (Hochmuth et al., 2011; Owusu-Ansah and Banerjee, 2009; Owusu-Ansah et al., 2008). In brief, guts were dissected directly in Schneider's medium, then incubated, protected from light, in 60uM dihydroethidium (Invitrogen Molecular Probes) in Schneider's medium for 7 minutes (Dye freshly reconstituted each time in anhydrous DMSO). Three washes were performed for 5 minutes each in Schneider's medium at room temperature before mounting in ProlongGold antifade reagent containing DAPI (Invitrogen Molecular Probes). Midguts were imaged immediately following the staining procedure. For total ROS production from the midgut, Z-stacks of regions 200-500uM anterior to the pylorus were measured for mean signal intensity at 568nM in Image J. For ROS output of ISCs/EBs, mean intensity of DHE signal was measured only in cell clusters identified by their esgGFP expression, their size, and their basal location within the intestinal epithelium. Pixel intensities of Z-stacks, spanning from the basal to apical cell layers,

for a minimum of 10 midguts were used for each of the quantifications. Statistical analysis was conducted on mean DHE intensities averaged from each midgut using a two-tailed, unpaired Student's T-test.

Immunofluorescence, quantification of ISCs/EBs, and pHH3$^+$ cell counts

Fixation of *Drosophila* intestines was carried out according to [55], prepared according to standard procedures, and mounted in Vectashield mounting medium containing 4',6-diamidino-2-phenylindole (DAPI) from Vector Laboratories. Primary antibodies used in this study included rabbit anti-GFP (1:5,000) from Molecular Probes, rabbit anti-phospho-histone H3 (1:200) from Millipore (06-570), and mouse anti-Armadillo (N2 7A1) (1:20) and mouse anti-Prospero (MR1A) (1:100), both obtained from the Developmental Studies Hybridoma Bank at the University of Iowa. For the quantification of GFP$^+$ cells, images were acquired from sections imaged 250-500 microns anterior to the pyloric ring in the posterior midgut, and MetaMorph software (Molecular Devices, Downingtown, PA) was used to quantify GFP$^+$ cells. The average number of GFP$^+$ cells was obtained from at least 25 guts per treatment; means were compared using one-way ANOVA followed by Tukey's HSD post-test. Due to the smaller size of male posterior midgut, the field of view (FOV) was divided into 9 equal sections, and the central region was used to quantify the average number of GFP$^+$ cells. To quantify pHH3$^+$ cells, images were acquired using a 20X objective 1-2 fields of view anterior to the pylorus. The numbers of pHH3$^+$ cells were normalized to gut area for each gut (n>21 samples per treatment). Statistical significance was determined with a Kruskall-Wallis test followed by a Dunn's post hoc test.

Analysis of Intestinal Integrity

Quantification of intestinal integrity was based upon the distribution of a blue food dye (FD&C blue dye #1) post-feeding. Briefly, two vials of female flies of each genotype were transferred

onto fresh medium containing blue dye (2.5% w/v) at 9 a.m. for 150 min. Flies showing an extended blue coloration (not limited to the proboscis and crop) were considered 'Smurf' flies.

Statistical analysis

Unless indicated otherwise, significance was determined using a two-tailed, unpaired *t*-test from at least three independent experiments and expressed as P values. Unless indicated otherwise, error bars reflect standard error of the mean (SEM).

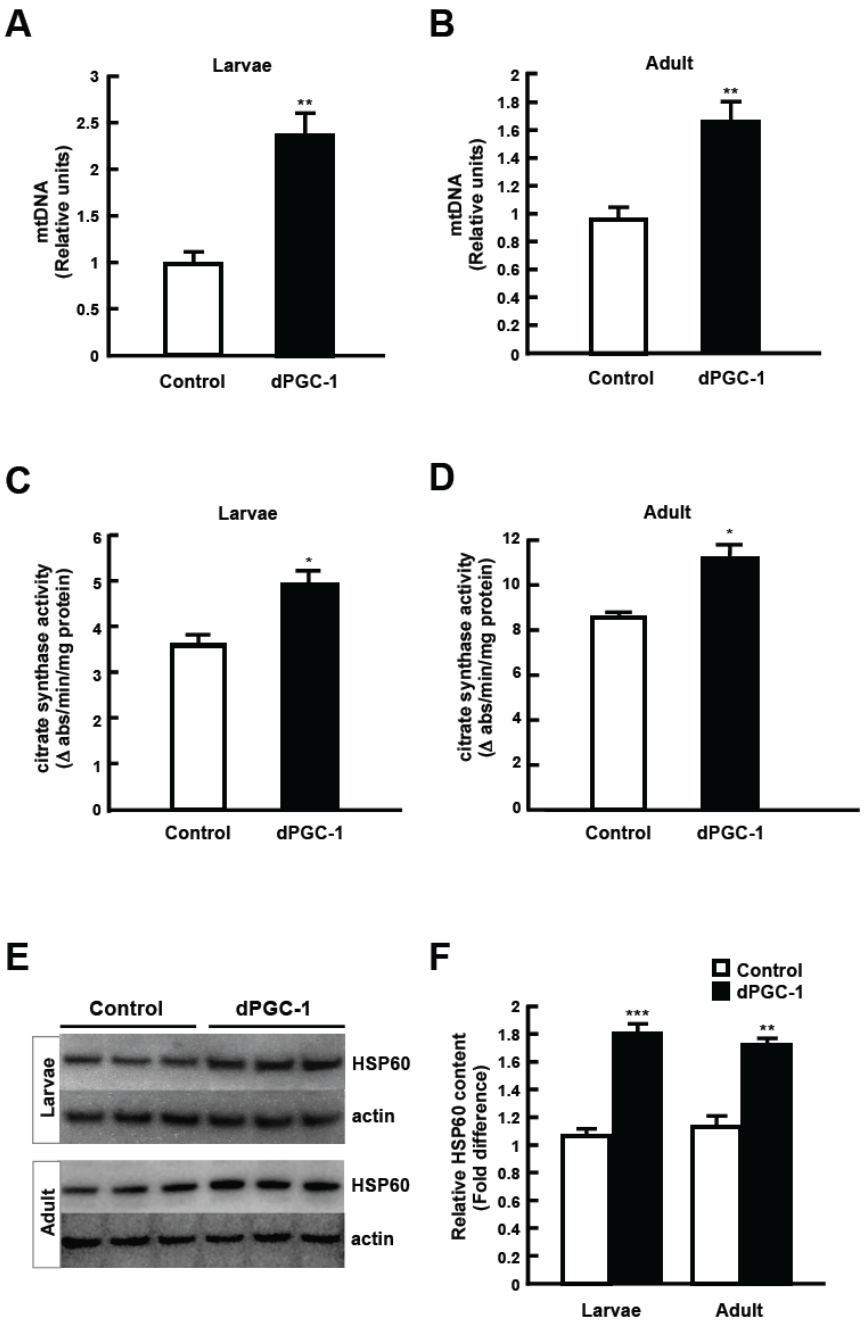

Figure 2-1. Overexpression of *dPGC-1* increases mitochondrial markers.

(A) Mitochondrial DNA (mtDNA) amount in larvae as determined by quantitative PCR (qPCR). Third instar larvae that overexpress *dPGC-1* with *daughterless*-GAL4 driver (*UAS-dPGC-1*/*da*-GAL4) show an increase in the amount of a mtDNA amplicon (**P < 0.01, *t*-test) when compared to controls (+/*da*-GAL4). Units are relative to the amounts of a nuclear DNA (nDNA) amplicon (n=3, 5 larvae per replicate).

(B) mtDNA amount in adult female thoraxes as determined by qPCR. Thoraxes of female flies that overexpress *dPGC-1* show an increase in a mtDNA amplicon (**P< 0.01, *t*-test) when compared to controls. Units are relative to the amounts of a nDNA amplicon (n=3, 5 thoraxes per replicate).

(C) Citrate synthase (CS) activity in larvae. Third instar larvae that overexpress *dPGC-1* show an increase in CS activity (*P < 0.05, *t*-test) relative to controls (n=3, 6 larvae per replicate).

(D) CS activity in adult female thoraxes. Thoraxes of female flies that overexpress *dPGC-1* show an increase in CS activity (*P < 0.05, *t*-test) relative to controls (n=3, 10 thoraxes per replicate).

(E) Western blot analysis of the mitochondrial matrix protein HSP60. Third instar larvae and thoraxes of adult female flies that overexpress *dPGC-1* show increased ratios of mitochondrial HSP60 signal to actin signal (loading control), relative to controls.

(F) Quantification of HSP60 Western blot analysis. Densitometry measurements of (E) show increases in HSP60:actin signal ratios for both larvae (***P<0.001, *t*-test) and adult thoraxes of female flies (**P<0.01, *t*-test) that overexpress *dPGC-1*, relative to controls (n=3, 5 larvae/thoraxes per replicate).

All assays in adults were carried out at 10 days of age. Data are represented as mean +/- SEM.

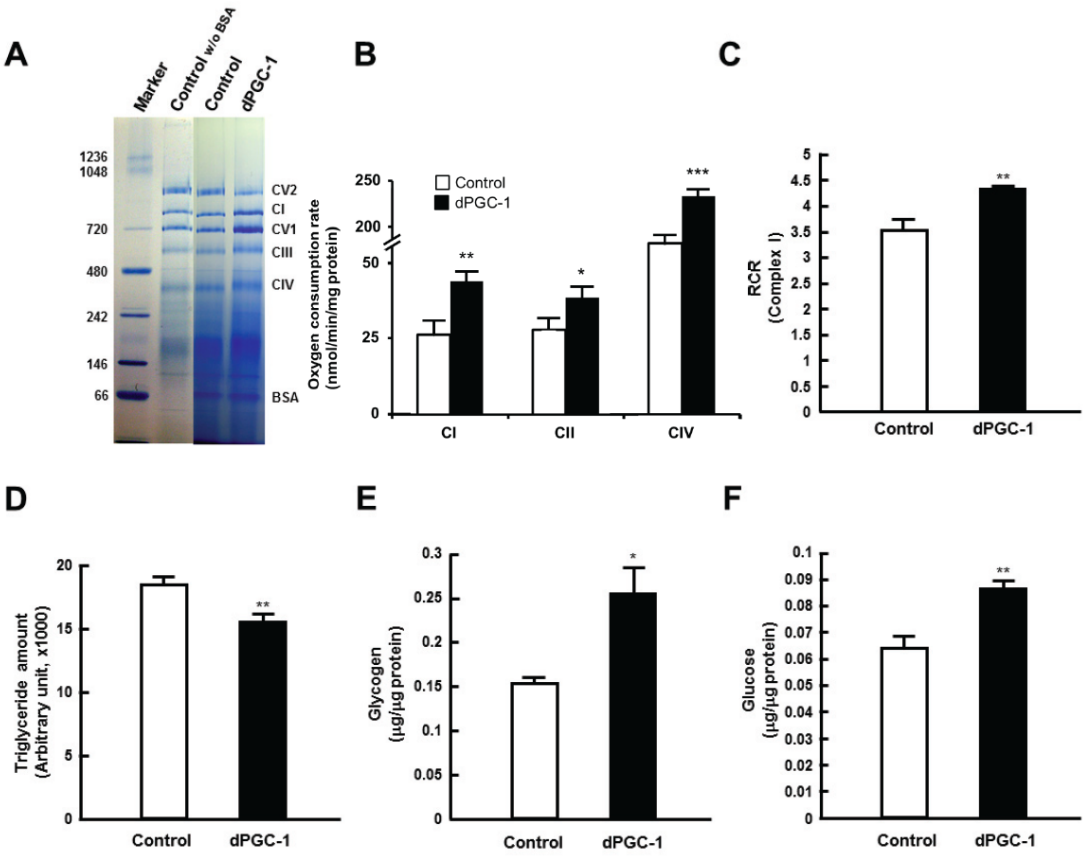

Figure 2-2. Regulation of oxidative metabolism, metabolic stores and glucose levels by *dPGC-1*.

(A) Blue-native polyacrylamide gel electrophoresis (BN-PAGE) analysis of respiratory complexes. Equal amounts of BSA (used as a loading control) were added to the total mitochondrial fraction isolated from thoraxes of female flies that overexpress *dPGC-1* (*UAS-dPGC-1*/*da*-GAL4) or controls *(+*/*da*-GAL4). Intensity of the bands corresponding to complexes I, III, IV, and V, relative to BSA, are increased in *dPGC-1* overexpressing flies compared to controls. CV2, complex V dimer; CI, complex I; CV1, complex V monomer; CIII, complex III; CIV, complex IV.

(B) Polarographic analysis of respiratory chain complex activities. Mitochondria isolated from female flies that overexpress *dPGC-1* show increased oxygen consumption by respiratory

complexes I (**P< 0.01, *t*-test), II (*P< 0.05, *t*-test), and IV (***P < 0.001, *t*-test) compared to controls (n=6, 50 flies per replicate).

(C) ADP-coupled respiration status. Mitochondria isolated from female flies that overexpress *dPGC-1* display an increased complex I respiratory control ratio (RCR) (**P < 0.01, *t*-test) relative to controls (n=3, 50 flies per replicate).

(D) Triglyceride (TAG) content. Thin-layer chromatography and densitometry of female flies that overexpress *dPGC-1* shows a decrease in TAG content (**P < 0.01, *t*-test) relative to controls (n=3, 10 flies per replicate).

(E) Glycogen content. A colorimetric glycogen assay of female flies that overexpress *dPGC-1* shows an increase in glycogen content (*P< 0.05, *t*-test) relative to controls (n=3, 5 flies per replicate).

(F) Glucose content. A colorimetric glucose assay of female flies that overexpress *dPGC-1* shows an increase in glucose content (**P < 0.01, *t*-test) relative to controls (n=3, 5 flies per replicate).

All assays in adults were carried out at 10 days of age. Data are represented as mean +/- SEM.

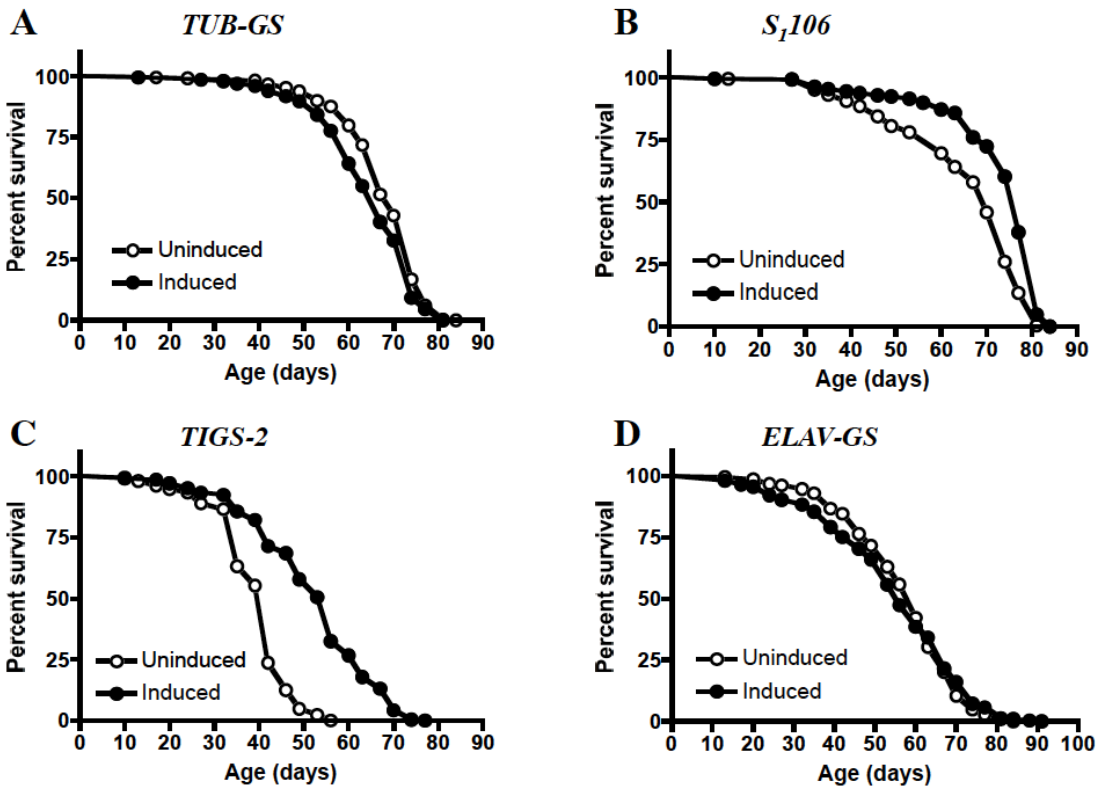

Figure 2-3. Effects of tissue-specific overexpression of *dPGC-1* on fly longevity.

UAS-dPGC-1 was crossed to Gene-Switch (GS) driver lines (A) the ubiquitous *Tubulin* (*tub*)-*GS* driver, (B) the abdominal fat and digestive tract driver *S1106*, (C) the digestive tract driver *TIGS-2* and (D) the pan-neuronal driver *ELAV-GS*, and lifespan curves are shown as induced (5 μg mL^{-1} RU486 during development and 25 μg mL^{-1} RU486 from the onset of adulthood (black circles) added on top of the food or uninduced (−RU486, open circles). (A) Lifespan curves of *UAS-dPGC-1*/*tub-GS* females. A moderate decrease in survival was observed in response to RU486 (P = 0.0029). (B) Lifespan curves of *UAS-dPGC-1*/ *S1106* females. An 11% increase in mean survival was observed in response to RU486 (P < 0.0001). (C) Lifespan curves of *UAS-dPGC-1*/ *TIGS-2* females. A 33% increase in mean survival was observed in response to RU486 (P < 0.0001). (D) Lifespan curves of *UAS-dPGC-1*/ *ELAV-GS* females. No impact on survival was observed in response to RU486 (P = 0.8). The significance of the difference between survival curves was analyzed using log-rank statistical test (n>195 flies).

Survival data for male flies can be found in Figures S2-2C-S2-2F. Survival data for independent insertions of *dPGC-1* with *TIGS-2* can be found in Figures S2-2G and S2-2H. Survival data for control flies exposed to RU486 can be found in Figures S2-3A-S2-3H.

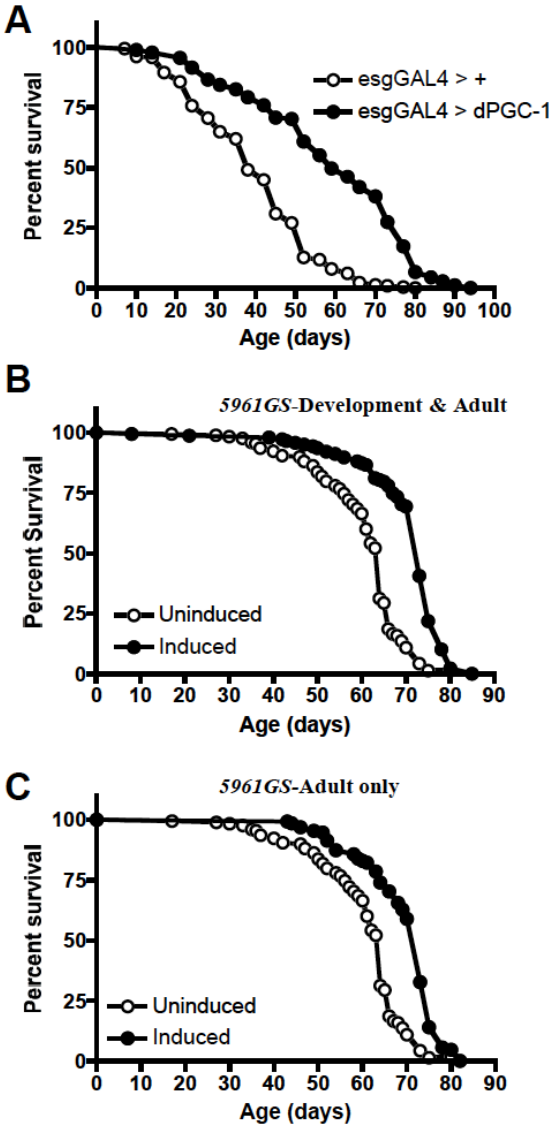

Figure 2-4. Overexpression of *dPGC-1* in intestinal stem and progenitor cells extends lifespan.

(A) Lifespan curves of *esgGAL4* > *dPGC-1* females compared to isogenic controls. *UAS-dPGC-1* and the isogenic control strain (w^{1118}) were crossed to *esgGAL4*. A 49% increase in mean survival was observed in response to *dPGC-1* activation ($P < 0.0001$).

(B) Lifespan curves of *UAS-dPGC-1*/ *5961GS* females. *UAS-dPGC-1* was crossed to the *5961GS* driver and lifespan curves are shown as induced (1 μg mL^{-1} RU486 during development and 5 μg mL^{-1} RU486 from the onset of adulthood (black circles) or uninduced (−RU486, open circles). A 19% increase in mean survival was observed in response to RU486 during both development and adulthood ($P < 0.0001$).

(C) Lifespan curves of *UAS-dPGC-1*/ *5961GS* females. *UAS-dPGC-1* was crossed to the the *5961GS* driver and lifespan curves are shown as induced (5 μg mL^{-1} RU486 from the onset of adulthood (black circles) or uninduced (−RU486, open circles). A 17% increase in mean survival was observed in response to RU486 in the adult stage ($P < 0.0001$). The significance of the difference between survival curves was analyzed using log-rank statistical test (n > 170 flies).

Survival data for male flies can be found in Figures S2-4A and S2-4B. Survival data for control flies exposed to RU486 can be found in Figures S2-4C-S2-4E.

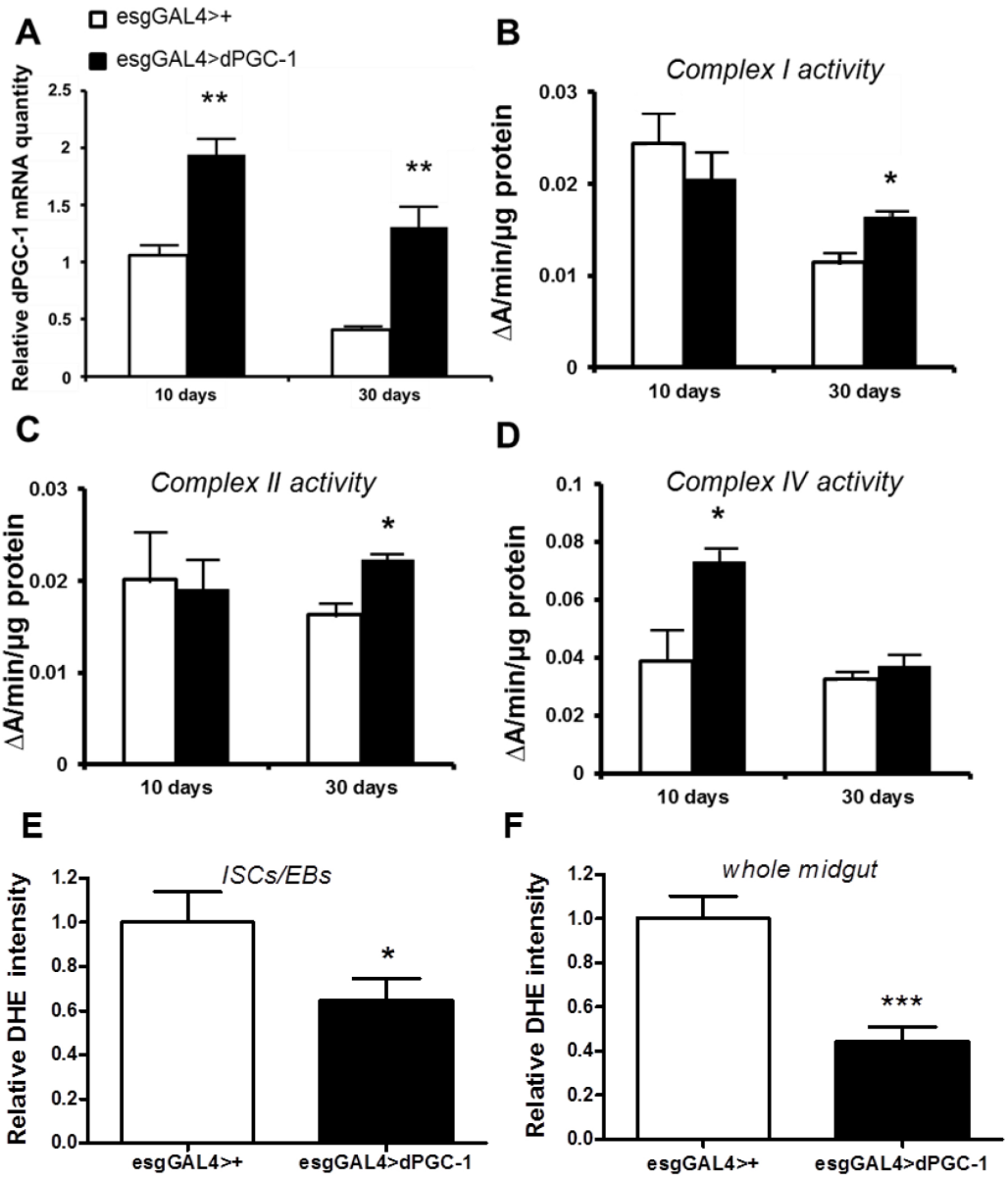

Figure 2-5. *dPGC-1* modulates mitochondrial activity and ROS levels in the aged intestine

(A) *dPGC-1* mRNA levels in the intestine at day 10 (young) and 30 (aged). *esgGAL4* > *dPGC-1* flies display increased expression of *dPGC-1* in the intestine at both ages (**$p < 0.01$, *t*-test) compared to controls (n = 3, 5 guts per replicate).

(B) Complex I activity in the intestine at day 10 (young) and 30 (aged). *esgGAL4* > *dPGC-1* flies display increased complex I activity in the aged intestine (*P< 0.05, *t*-test) compared to controls (n=3, 15 guts per replicate).

(C) Complex II activity in the intestine at day 10 (young) and 30 (aged). *esgGAL4* > *dPGC-1* flies display increased complex II activity in the aged intestine (*P< 0.05, *t*-test) compared to controls (n=3, 15 guts per replicate).

(D) Complex IV activity in the intestine at day 10 (young) and 30 (aged). *esgGAL4* > *dPGC-1* flies display increased complex IV activity in the young intestine (*P< 0.05, *t*-test) compared to controls (n=3, 15 guts per replicate).

(E) ROS levels in ISCs/EBs. Dihydro-ethidium (DHE) fluorescence was assayed in ISCs/EBs from *esgGAL4* > *dPGC-1* flies and isogenic controls at day 30. DHE fluorescence was assayed throughout the entire Z-stack and averaged to obtain a value representing the mean intensity of the entire Z-stack per gut (n>18 guts). *esgGAL4*-mediated activation of *dPGC-1* decreased DHE fluorescence in ISCs/EBs in the aged intestine (*P< 0.05, *t*-test). Representative images can be found in Figure S6D.

(F) ROS levels in midguts. DHE fluorescence was assayed in midguts (200-500uM anterior to the pylorus) from *esgGAL4* > *dPGC-1* flies and isogenic controls at day 30 (n>10 guts). *esgGAL4*-mediated activation of *dPGC-1* decreased DHE fluorescence in the aged intestine (***P<0.001, *t*-test). Representative images can be found in Figure S2-6E. Data are represented as mean +/- SEM.

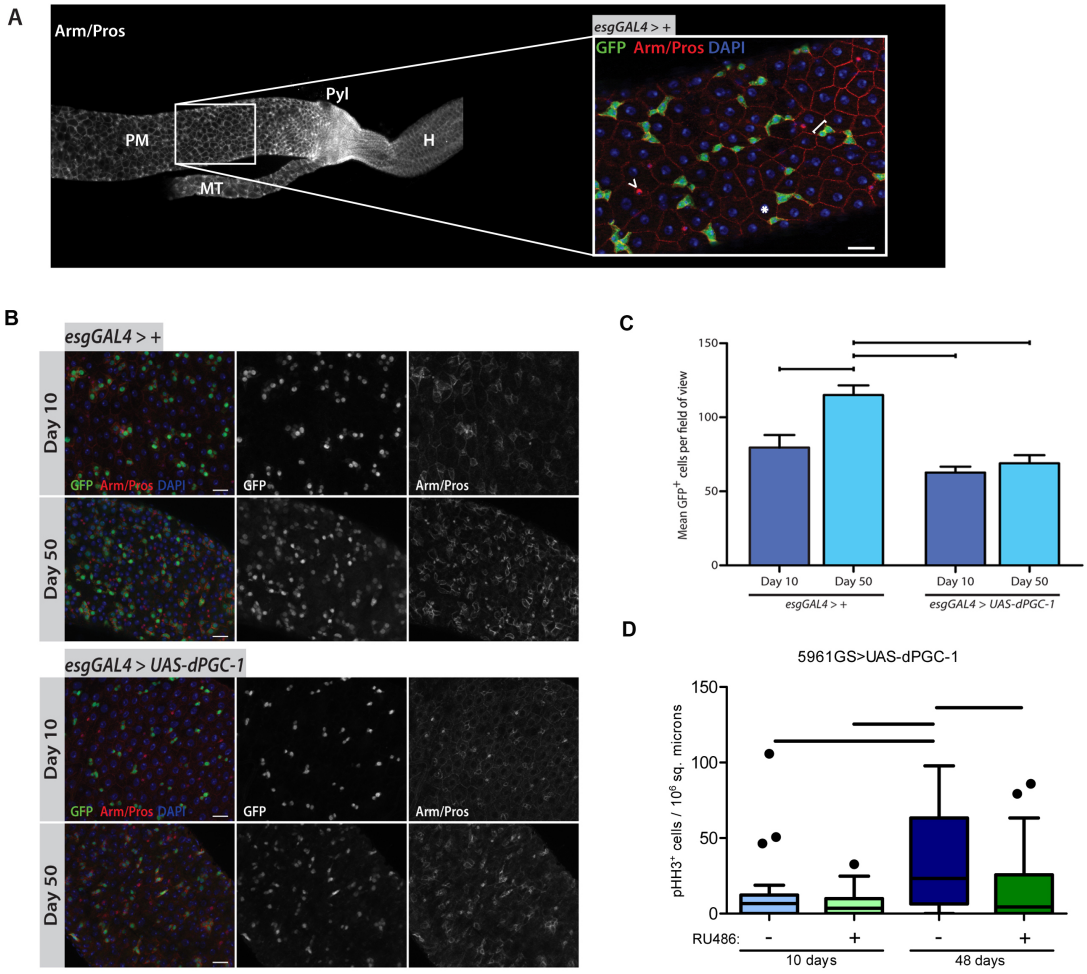

Figure 2-6. *dPGC-1* modulates tissue homeostasis in the aged intestine.

(A) Shown are: (left) adult *Drosophila* gut viewed with a 10X objective and stained with anti-Armadillo antibodies showing the posterior midgut (PM), malpighian tubules (MT), pylorus (Pyl) and hindgut (H) and (right) 40X view of the posterior midgut showing an ISC/EB nest (bracket), a polyploid enterocyte (*) and a Prospero^{+} enteroendocrine cell (arrow head). (B) Immunofluorescence images evaluating intestinal homeostasis during aging. Control (upper panels: *esgGAL4 , UAS-gfp/+*) and *dPGC-1* overexpressing (lower panels: *esgGAL4 , UAS-gfp/+ ; UAS-dPGC-1/+*) flies were aged 10 or 50 days and assayed for GFP^{+} cells. Scale bars, 20 μm. (**C**) Quantification of total number of GFP^{+} cells per field of analysis. Error bars represent SEMs with n>24 midguts per treatment. The mean number of GFP^{+} cells increased

significantly from 10 to 50 days in control but not in *dPGC-1* overexpressing flies (One-way ANOVA with Tukey's HSD post hoc test - bars indicate P<0.001). (D) Quantification of total number of $pHH3^+$ cells in guts from induced (+RU486) or uninduced (-RU486) *5961GS >UAS-dPGC-1* flies. The box plot represents medians and quartiles, and whiskers indicate 1.5 times the interquartile range with n>21 midguts per treatment. The median number of $pHH3^+$ cells increased significantly (P< 0.05) from 10 to 48 days in uninduced but not in *dPGC-1* overexpressing (induced) flies. Kruskal-Wallis test followed by a Dunn's multiple comparison test was used to assess differences between samples.

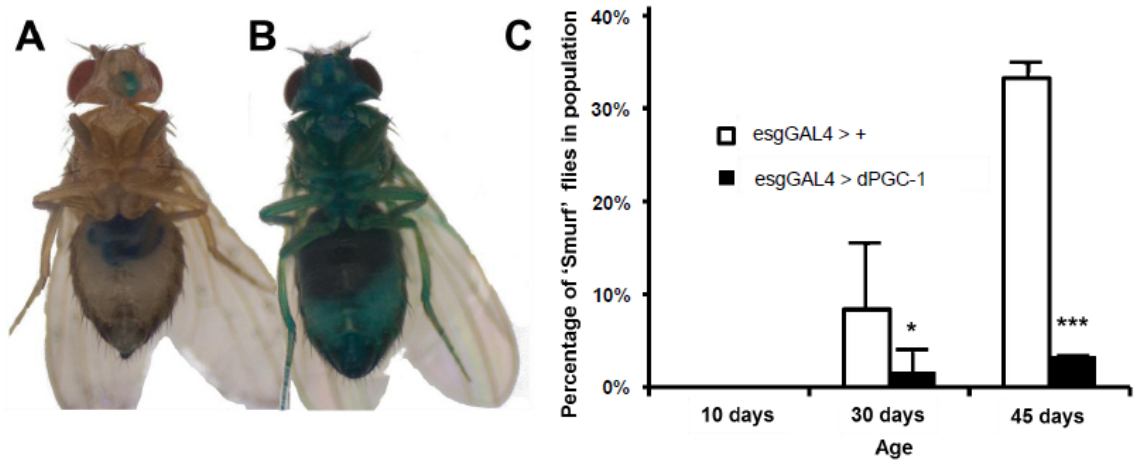

Figure 2-7. *dPGC-1* modulates intestinal integrity in old flies

Shown are (A) a 10-day old fly after consuming a non-absorbed food dye (FD&C blue dye #1). The dye is restricted to the proboscis and digestive tract. (B) A 45-day old 'Smurf' fly after consuming the same food dye. The blue dye is seen throughout the body due to loss of intestinal integrity. (C) Analysis of intestinal integrity as a function of age. In control (*esgGAL4* > +) flies, the fraction of 'Smurf' flies in the population increases with age. *esgGAL4*-mediated activation of *dPGC-1* improves intestinal integrity in aged flies. Binomial test *P < 0.05 at day 30 and ***P < 0.001 at day 45, n = 2 x 30 females for each genotype. Data are represented as mean +/- SEM.

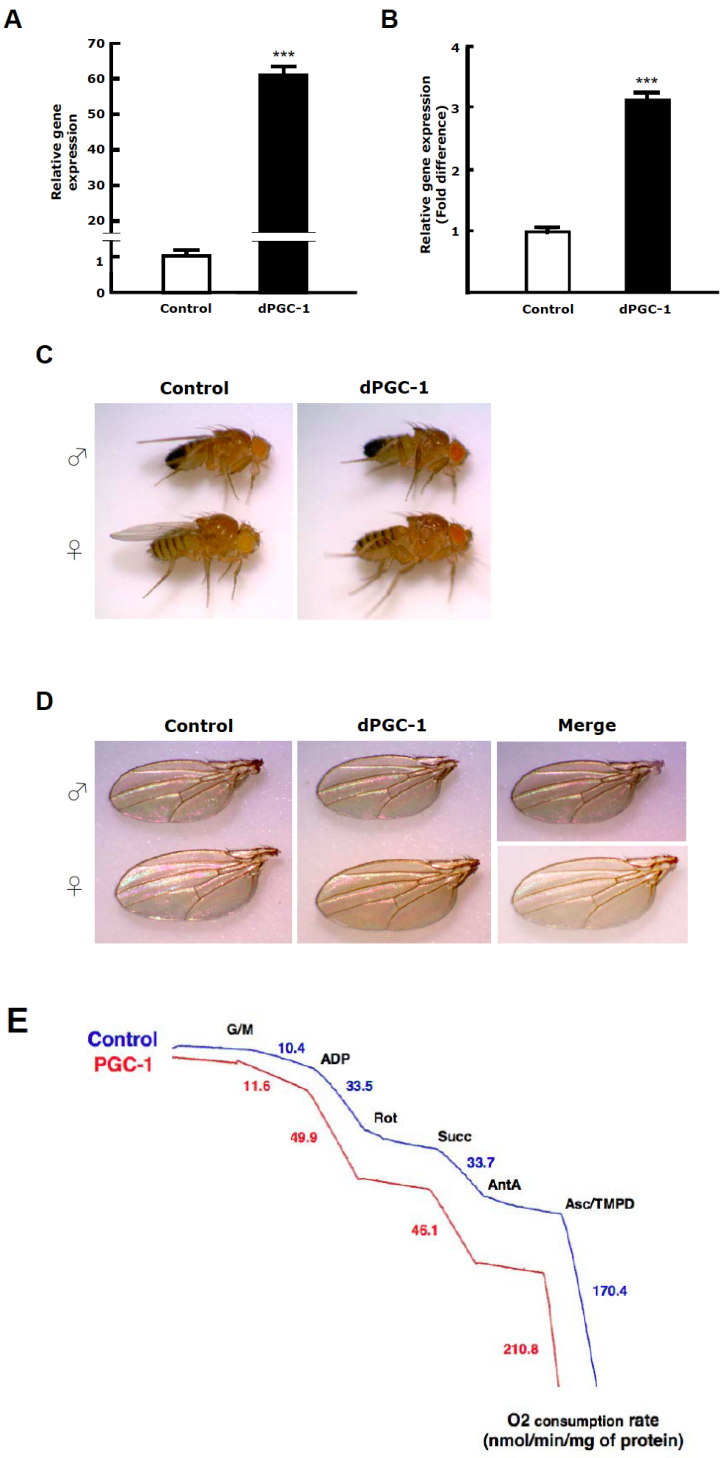

Figure S2-1. Overexpression of *dPGC-1* does not change gross morphology but stimulates mitochondrial activity.

(A) Overexpression of *dPGC-1* with *daughterless*-GAL4 driver (*UAS-dPGC-1*/*da*-GAL4) causes an approximately 60-fold increase (***p < 0.001, *t*-test) of *dPGC-1* mRNA in male flies relative to controls (w^{1118}/*da*-GAL4).

(B) Overexpression of *dPGC-1* causes an approximately 3-fold increase (***p < 0.001, *t*-test) of *dPGC-1* mRNA in female flies relative to controls.

(C) Body size. Neither male nor female flies that overexpress *dPGC-1* (*UAS-dPGC-1*/*da*-GAL4) show any significant differences in body length relative to controls (w^{1118}/*da*-GAL4).

(D) Wing morphology. No significant differences in wing size or shape were found between in male or female flies that overexpress *dPGC-1* relative to controls.

(E) Respiratory chain activity. Representative polarographic trace showing rates of oxygen consumption in mitochondria isolated from *dPGC-1*-expressing flies and controls. Female flies that overexpress *dPGC-1* (*UAS-dPGC-1*/*da*-GAL4) show increased respiration relative to controls (w^{1118}/*da*-GAL4).

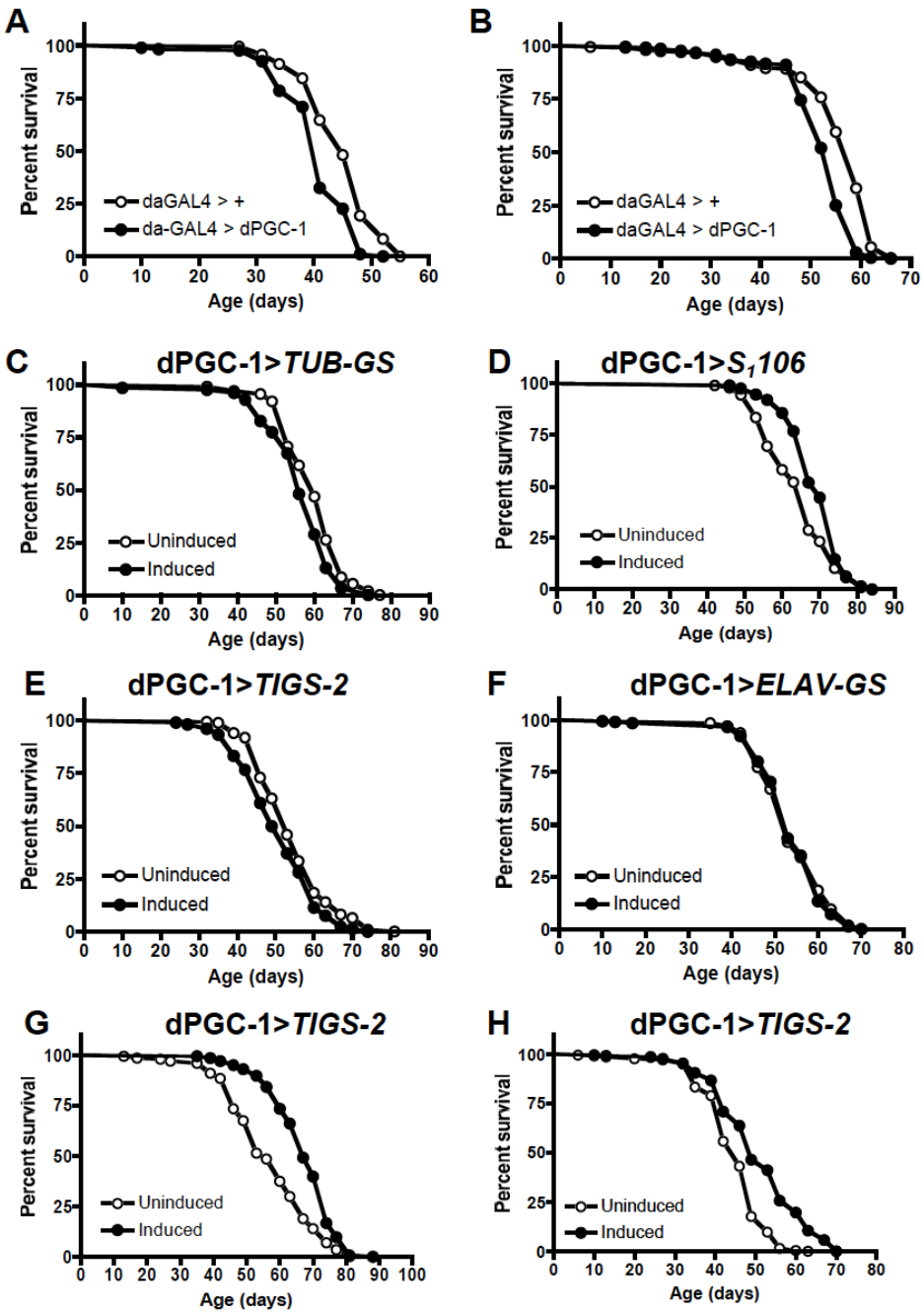

Figure S2-2. Effects of tissue-specific overexpression of *dPGC-1* on fly longevity.

(A, B) *UAS-dPGC-1* and isogenic control lines (w^{1118}) were crossed to the constitutive driver *da-GAL4*. *UAS-dPGC-1* confers a moderate decrease in survival (P=0.0001) in both male (A) and (B) female flies. n >170 flies. (C-F) Longevity effects in male flies. *UAS-dPGC-1* was crossed to Gene-Switch (GS) driver lines (C) the ubiquitous *Tubulin* (*tub*)-*GS* driver, (D) the abdominal fat

and digestive tract driver *S$_1$106*, (E) the digestive tract driver *TIGS-2* and (F) the pan-neuronal driver *ELAV-GS*, and lifespan curves are shown as induced (5 μg mL^{-1} RU486 during development and 25 μg mL^{-1} RU486 from the onset of adulthood (black circles) added on top of the food or uninduced (−RU486, open circles). (C) Lifespan curves of *UAS-dPGC-1*/*tub-GS* males. A moderate decrease in survival was observed in response to RU486 (P<0.0001). (D) Lifespan curves of *UAS-dPGC-1*/ *S$_1$106* males. A moderate increase in mean survival was observed in response to RU486 (*P* < 0.0001). (E) Lifespan curves of *UAS-dPGC-1*/ *TIGS-2* males. A moderate decrease in mean survival was observed in response to RU486 (P=0.0016). (F) Lifespan curves of *UAS-dPGC-1*/ *ELAV-GS* males. No impact on survival was observed in response to RU486 (*P* = 0.7445). n>200 flies. (G, H) Independent *UAS-dPGC-1* inserts promote longevity with *TIGS-2*. *UAS-dPGC-1* was crossed to the digestive tract driver *TIGS-2* and lifespan curves are shown as induced (1μg mL^{-1} RU486 during development and 5μg mL^{-1} RU486 from the onset of adulthood (black circles) added on top of the food or uninduced (−RU486, open circles). (G) Lifespan curves of *UAS-dPGC-1*/*TIGS-2* females. An 18% increase in mean survival was observed in response to RU486 (P<0.0001). (H) Lifespan curves of *UAS-dPGC-1*/*TIGS-2* females. A 14% increase in mean survival was observed in response to RU486 (P<0.0001). n>200 flies. The significance of the difference between survival curves was analyzed using log-rank statistical test. n>200 flies.

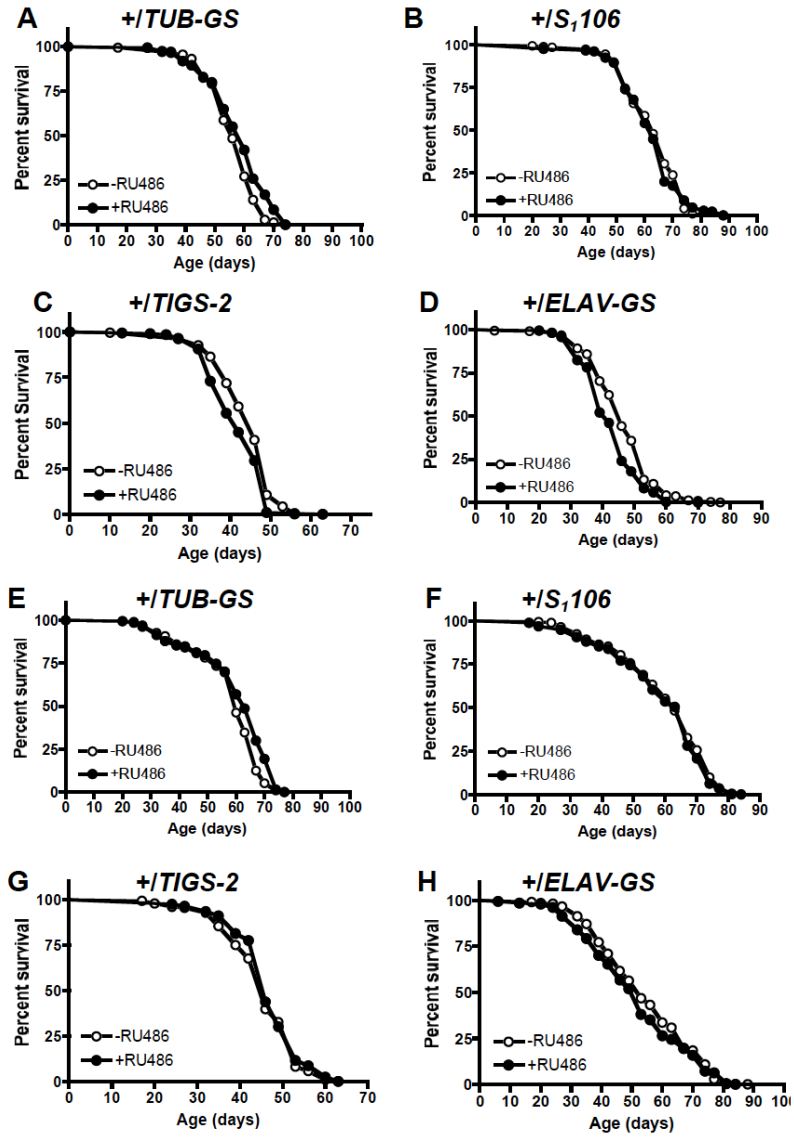

Figure S2-3. Effects of RU486 on longevity in control flies.

(A-D) Male flies. w^{1118} was crossed to Gene-Switch (GS) driver lines (A) the ubiquitous *Tubulin* (*tub*)-*GS* driver, (B) the abdominal fat and digestive tract driver *S1₁06*, (C) the digestive tract driver *TIGS-2* and (D) the pan-neuronal driver *ELAV-GS*, and lifespan curves are shown as induced (5 μg mL^{-1} RU486 during development and 25 μg mL^{-1} RU486 from the onset of adulthood (black circles) added on top of the food or uninduced (−RU486, open circles). (A) Lifespan curves of w^{1118}/*tub-GS* males. A moderate increase in survival was observed in

response to RU486 (P=0.0003). (B) Lifespan curves of w^{1118}/ S_1106 males. No impact on survival was observed in response to RU486 (P=0.7411). (C) Lifespan curves of w^{1118}/ *TIGS-2* males. A moderate decrease in mean survival was observed in response to RU486 ($P < 0.0001$). (D) Lifespan curves w^{1118}/ *ELAV-GS* males. A moderate decrease in mean survival was observed in response to RU486 ($P < 0.0001$). The significance of the difference between survival curves was analyzed using log-rank statistical test. n>200 flies. (E-H) Female Flies. w^{1118} was crossed to Gene-Switch (GS) driver lines (E) the ubiquitous *Tubulin* (*tub*)-*GS* driver, (F) the abdominal fat and digestive tract driver S_1106, (G) the digestive tract driver *TIGS-2* and (H) the pan-neuronal driver *ELAV-GS*, and lifespan curves are shown as induced (5 μg mL^{-1} RU486 during development and 25 μg mL^{-1} RU486 from the onset of adulthood (black circles) added on top of the food or uninduced (−RU486, open circles). (E) Lifespan curves of w^{1118}/*tub-GS* females. A moderate increase in survival was observed in response to RU486 (P=0.0003). (F) Lifespan curves of w^{1118}/ S_1106 females. No impact on survival was observed in response to RU486 (P=0.4941). (G) Lifespan curves of w^{1118}/ *TIGS-2* females. No impact on survival was observed in response to RU486 (P = 0.2204). (H) Lifespan curves w^{1118}/ *ELAV-GS* females. No impact on survival was observed in response to RU486 (P = 0.2559). The significance of the difference between survival curves was analyzed using log-rank statistical test. n>200 flies.

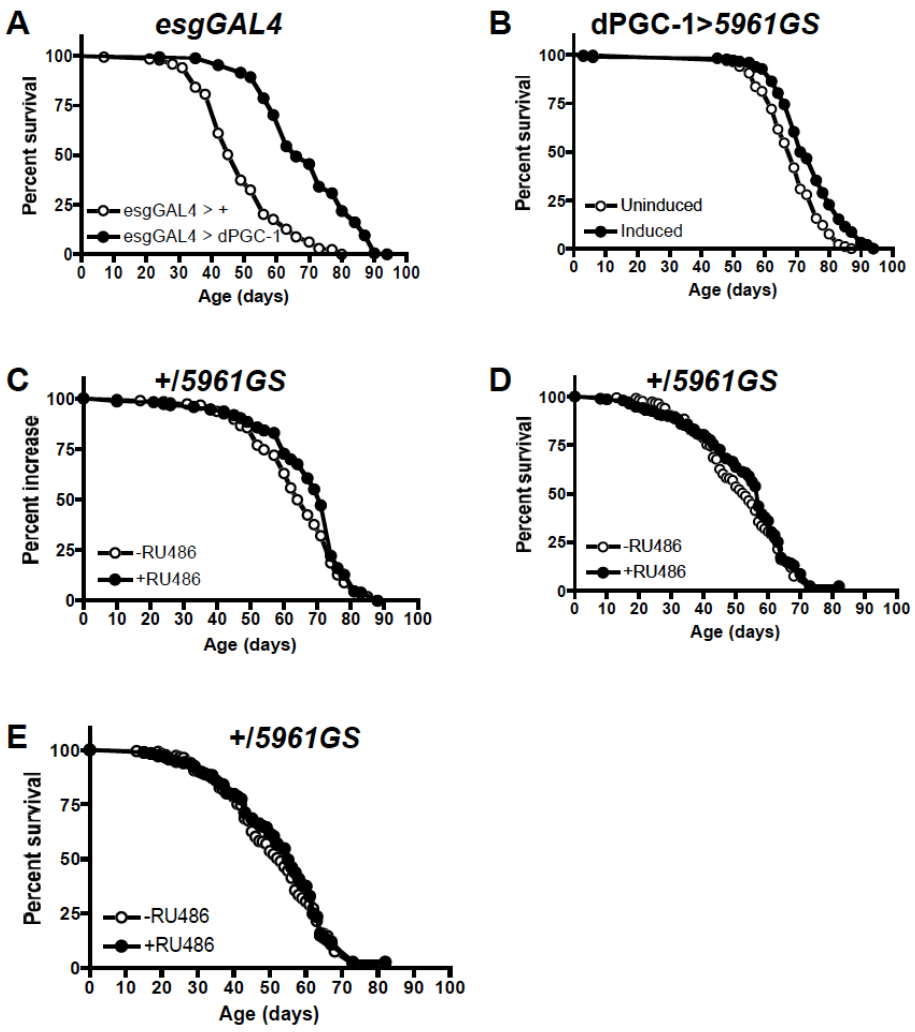

Figure S2-4. Overexpression of *dPGC-1* in intestinal stem and progenitor cells extends lifespan.

(A, B) Effects of *esgGAL4*- and *5961GS*-mediated expression of *dPGC-1* on male longevity. (A) Lifespan curves of *esgGAL4 > dPGC-1* males compared to isogenic controls. *UAS-dPGC-1* and the isogenic control strain (w^{1118}) were crossed to *esgGAL4*. A 41% increase in mean survival was observed in response to *dPGC-1* activation ($P < 0.0001$). (B) Lifespan curves of *UAS-dPGC-1*/ *5961GS* males. *UAS-dPGC-1* was crossed to the *5961GS* driver and lifespan curves are shown as induced (5 μg mL^{-1} RU486 during development and 25 μg mL^{-1} RU486 added on top of the food from the onset of adulthood (black circles) or uninduced (−RU486,

open circles). A 9% increase in mean survival was observed in response to RU486 ($P < 0.0001$). (C-E) Effects of RU486 on longevity in control flies crossed to *5961GS*. w^{1118} was crossed to the 5961Gene-Switch (GS) driver line and lifespan curves are shown as induced (black circles) or uninduced (−RU486, open circles). (C) Lifespan curves of w^{1118}/*5961GS* males. A moderate increase in survival was observed in response to 5μg mL^{-1} RU486 during development and 25 μg mL^{-1} RU486 from the onset of adulthood on top of the food (P= 0.0066). (D) Lifespan curves of w^{1118}/*5961GS* females. No impact on survival was observed in response to 1 μg mL^{-1} RU486 during development and 5 μg mL^{-1} RU486 from the onset of adulthood (P= 0.1909). (E) Lifespan curves of w^{1118}/*5961GS* females. No impact on survival was observed in response to 5 μg mL^{-1} RU486 from the onset of adulthood (P= 0.3513). The significance of the difference between survival curves was analyzed using log-rank statistical test. n >200 flies.

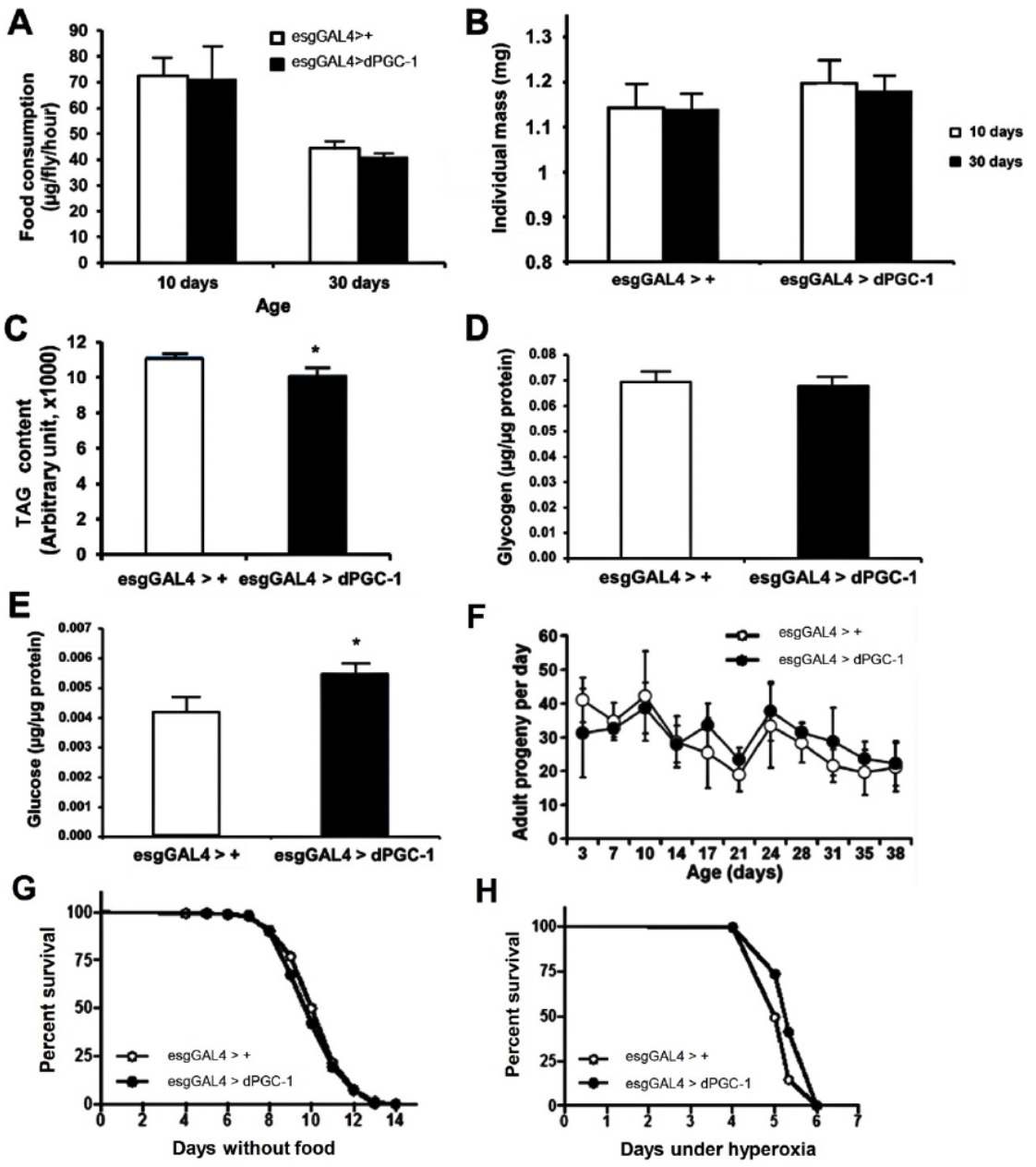

Figure S2-5. Physiological and behavioral characterization of long-lived *dPGC-1* overexpressing flies.

UAS-dPGC-1 and the isogenic control strain (w^{1118}) were crossed to *esgGAL4*.

(A) Food consumption. Quantification of food intake was based upon the uptake of a blue food dye (FD&C blue dye #1), see Experimental Procedures for details. Long-lived *dPGC-1*-expressing female flies display no obvious alterations in food consumption (n>7). (B) Mass.

Long-lived *dPGC-1*-expressing female flies display no major change in mass (n=6, 15 flies per replicate). (C) Triglyceride (TAG) content. Thin-layer chromatography and densitometry of female flies that overexpress *dPGC-1* shows a decrease in TAG content (*P< 0.05, *t*-test) relative to controls (n=3, 10 flies per replicate).(D) Glycogen content. A colorimetric glycogen assay of female flies that overexpress *dPGC-1* relative to controls. No difference was observed (n=3, 5 flies per replicate). (E) Glucose content. A colorimetric glucose assay of female flies that overexpress *dPGC-1* shows an increase in glucose content (*P< 0.05, *t*-test) relative to controls (n=3, 5 flies per replicate). (F) Fertility. Average number of progeny produced from crosses between five wild-type males and five *esgGAL4* > *dPGC-1* females or 5 isogenic control females. Long-lived *dPGC-1*-expressing flies display normal fertility compared to controls (*P* > 0.05; two-way Analysis of Variance). Error bars represent SEMs (n=4). (G) Starvation resistance. Long-lived *dPGC-1*-expressing female flies display normal survival in the absence of food (p=0.2727). (H) Survival under hyperoxia. Long-lived *dPGC-1*-expressing female flies display a moderate increase in resistance to hyperoxia (P<0.0001). The significance of the difference between survival curves was analyzed using log-rank statistical test (n>180 flies). All assays were carries out on 10 day-old flies unless stated otherwise. Data are represented as mean +/- SEM.

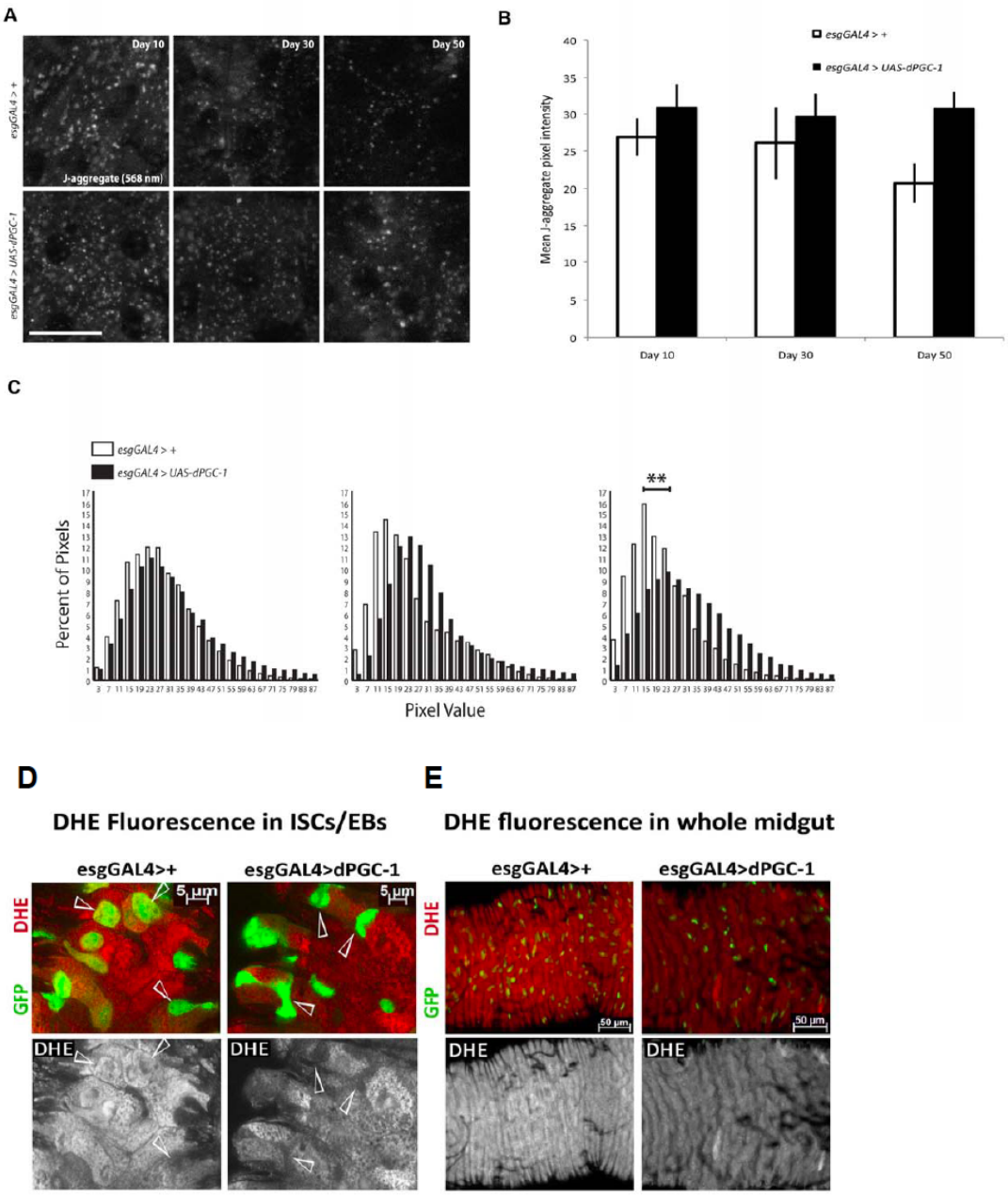

Figure S2-6. *dPGC-1* modulates mitochondrial membrane potential and ROS levels in the aged intestine.

UAS-dPGC-1 and the isogenic control strain (w^{1118}) were crossed to *esgGAL4*. (A) Visualization of enterocytes in the posterior midgut of 10, 30 and 50 day old control or *dPGC-1* overexpressing female flies. Unfixed midguts were stained with JC-1; J-aggregates (568 nm channel) were visualized to indicate mitochondria with high membrane potential. Scale bars

equal 20 μm. (B) Mean J-aggregate pixel intensity +/- SEM, or (C) compiled pixel intensity values for each treatment group are displayed. A Mann-Whitney U test was used to compare median J-aggregate intensity in *esgGAL4 > dPGC-1* flies and isogenic controls at day 10 (left), 30 (middle) and 50 (right); ** indicates significance at $P<0.01$ (n>7 guts per treatment). (D) DHE staining of intestines of *esgGAL4 > dPGC-1* flies and isogenic controls at 30 days of age. DHE channel is separated in grayscale in lower panels. Images are from single confocal sections. Arrowheads point to individual ISCs/EBs for orientation (basal location in the epithelium, isolated esg^+ cells). Mean DHE pixel intensity of ISCs/EBs (shown in Figure 5E) was quantified from Z-stacks obtained with a 63X objective. Brightness and contrast of the GFP channel was modified in order to determine cytoplasmic borders of morphologically defined ISC/EB clusters. All ISCs and EBs were then outlined in Image J, and the mean intensity in the DHE channel was taken from the unmodified image for each slice of the Z-stack. The intensities of each slice throughout the entire Z-stack were then averaged to obtain a value representing the mean intensity of the entire Z-stack per gut. Mean DHE intensity for each Z-stack/gut (n>18 guts/condition) was compared via unpaired, two-tailed Student's T-test. Representative images were arranged using Adobe Photoshop. (E) DHE staining of intestines of *esgGAL4 > dPGC-1* flies and isogenic controls at 30 days of age. DHE channel is separated in grayscale in lower panels. Images are from single confocal sections. Mean DHE pixel intensities for cells in the posterior midgut (shown in Figure 2-5F) were quantified from Z-stacks obtained with a 20X objective/normalized to gut area. The values obtained throughout each slice of the entire Z-stack were then averaged to obtain the mean intensity of the entire Z-stack per gut. Statistics were performed in the same manner as (A) with an n>10 guts/condition.

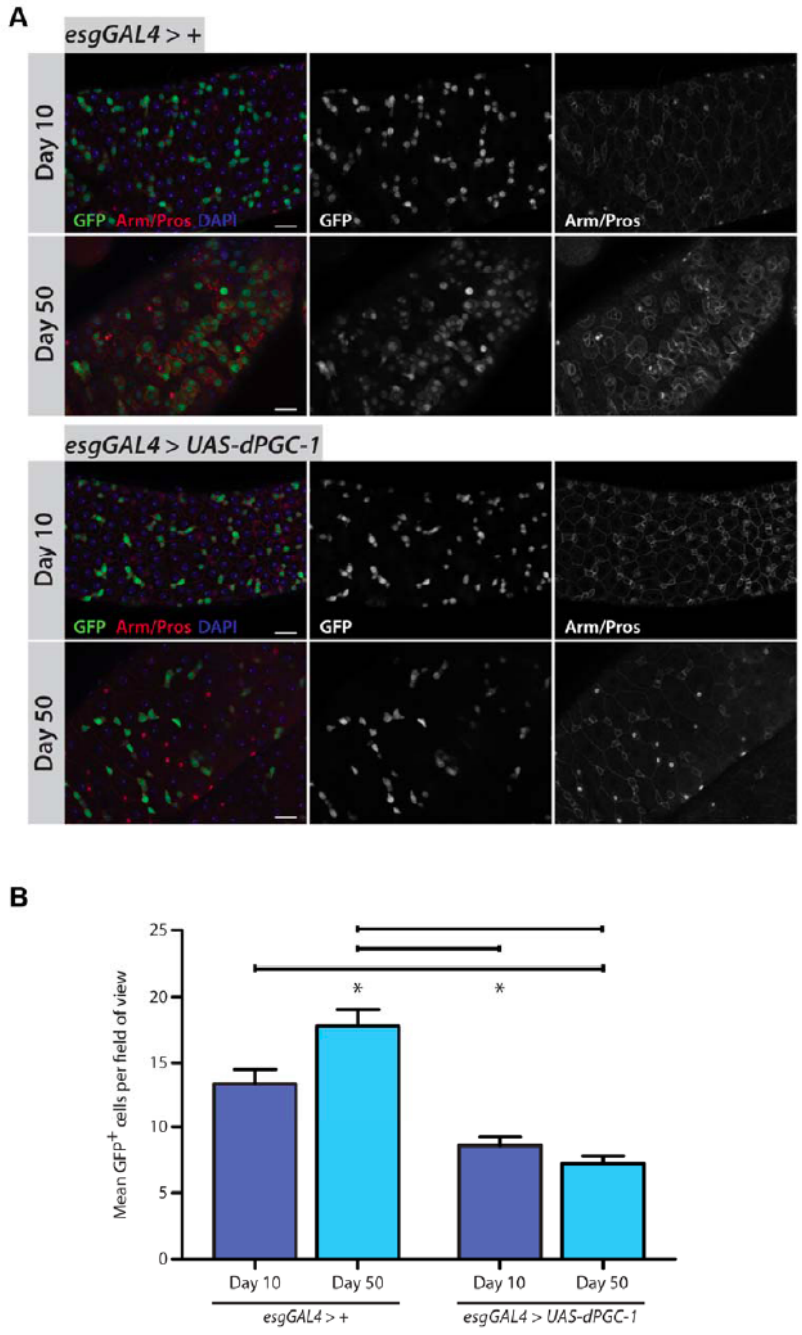

Figure S2-7. *dPGC-1* modulates tissue homeostasis in the aged intestine of male flies

UAS-dPGC-1 and the isogenic control strain (w^{1118}) were crossed to *esgGAL4*. (A) Immunofluorescence images evaluating intestinal homeostasis in male flies. Control and *dPGC-1* overexpressing flies were aged 10 or 50 days and assayed for Esg^+/GFP^+ cell counts. Scale bars, 20 μm. (B) Quantification of total number of GFP^+ cells per field of analysis. Error

bars represent SEMs with n>24 midguts per treatment. The mean number of GFP^+ cells increased significantly from 10 to 50 days in control but not *dPGC-1* overexpressing flies (One-way ANOVA with Tukey's HSD post hoc test - bars indicate $P<0.001$ and asterisks represent $P<0.01$ vs. 10 day control).

References:

1. Wallace, D.C., *A mitochondrial paradigm of metabolic and degenerative diseases, aging, and cancer: a dawn for evolutionary medicine.* Annu Rev Genet, 2005. **39**: p. 359-407.
2. McCarroll, S.A., et al., *Comparing genomic expression patterns across species identifies shared transcriptional profile in aging.* Nat Genet, 2004. **36**(2): p. 197-204.
3. Zahn, J.M., et al., *Transcriptional profiling of aging in human muscle reveals a common aging signature.* PLoS Genet, 2006. **2**(7): p. e115.
4. Guarente, L., *Mitochondria--a nexus for aging, calorie restriction, and sirtuins?* Cell, 2008. **132**(2): p. 171-6.
5. Bonawitz, N.D., et al., *Reduced TOR signaling extends chronological life span via increased respiration and upregulation of mitochondrial gene expression.* Cell Metab, 2007. **5**(4): p. 265-77.
6. Katic, M., et al., *Mitochondrial gene expression and increased oxidative metabolism: role in increased lifespan of fat-specific insulin receptor knock-out mice.* Aging Cell, 2007. **6**(6): p. 827-39.
7. Civitarese, A.E., et al., *Calorie restriction increases muscle mitochondrial biogenesis in healthy humans.* PLoS Med, 2007. **4**(3): p. e76.
8. Civitarese, A.E., S.R. Smith, and E. Ravussin, *Diet, energy metabolism and mitochondrial biogenesis.* Curr Opin Clin Nutr Metab Care, 2007. **10**(6): p. 679-87.
9. Lopez-Lluch, G., et al., *Calorie restriction induces mitochondrial biogenesis and bioenergetic efficiency.* Proc Natl Acad Sci U S A, 2006. **103**(6): p. 1768-73.
10. Nisoli, E., et al., *Calorie restriction promotes mitochondrial biogenesis by inducing the expression of eNOS.* Science, 2005. **310**(5746): p. 314-7.
11. Zid, B.M., et al., *4E-BP extends lifespan upon dietary restriction by enhancing mitochondrial activity in Drosophila.* Cell, 2009. **139**(1): p. 149-60.

12. Bishop, N.A. and L. Guarente, *Two neurons mediate diet-restriction-induced longevity in C. elegans.* Nature, 2007. **447**(7144): p. 545-9.

13. Lin, S.J., et al., *Calorie restriction extends Saccharomyces cerevisiae lifespan by increasing respiration.* Nature, 2002. **418**(6895): p. 344-8.

14. Bahadorani, S., et al., *Perturbation of mitochondrial complex V alters the response to dietary restriction in Drosophila.* Aging Cell, 2010. **9**(1): p. 100-3.

15. Lin, J., C. Handschin, and B.M. Spiegelman, *Metabolic control through the PGC-1 family of transcription coactivators.* Cell Metab, 2005. **1**(6): p. 361-70.

16. Scarpulla, R.C., *Transcriptional paradigms in mammalian mitochondrial biogenesis and function.* Physiol Rev, 2008. **88**(2): p. 611-38.

17. Puigserver, P. and B.M. Spiegelman, *Peroxisome proliferator-activated receptor-gamma coactivator 1 alpha (PGC-1 alpha): transcriptional coactivator and metabolic regulator.* Endocr Rev, 2003. **24**(1): p. 78-90.

18. Scarpulla, R.C., *Nuclear control of respiratory chain expression by nuclear respiratory factors and PGC-1-related coactivator.* Ann N Y Acad Sci, 2008. **1147**: p. 321-34.

19. Handschin, C., et al., *PGC-1alpha regulates the neuromuscular junction program and ameliorates Duchenne muscular dystrophy.* Genes Dev, 2007. **21**(7): p. 770-83.

20. Sandri, M., et al., *PGC-1alpha protects skeletal muscle from atrophy by suppressing FoxO3 action and atrophy-specific gene transcription.* Proc Natl Acad Sci U S A, 2006. **103**(44): p. 16260-5.

21. Wenz, T., et al., *Activation of the PPAR/PGC-1alpha pathway prevents a bioenergetic deficit and effectively improves a mitochondrial myopathy phenotype.* Cell Metab, 2008. **8**(3): p. 249-56.

22. Cui, L., et al., *Transcriptional repression of PGC-1alpha by mutant huntingtin leads to mitochondrial dysfunction and neurodegeneration.* Cell, 2006. **127**(1): p. 59-69.

23. Zheng, B., et al., *PGC-1alpha, a potential therapeutic target for early intervention in Parkinson's disease.* Sci Transl Med, 2010. **2**(52): p. 52ra73.

24. Wenz, T., et al., *Increased muscle PGC-1alpha expression protects from sarcopenia and metabolic disease during aging.* Proc Natl Acad Sci U S A, 2009. **106**(48): p. 20405-10.

25. Sahin, E., et al., *Telomere dysfunction induces metabolic and mitochondrial compromise.* Nature, 2011. **470**(7334): p. 359-65.

26. Cho, J., J.H. Hur, and D.W. Walker, *The role of mitochondria in Drosophila aging.* Exp Gerontol, 2011. **46**(5): p. 331-4.

27. Wang, L. and D.L. Jones, *The effects of aging on stem cell behavior in Drosophila.* Exp Gerontol, 2011. **46**(5): p. 340-4.

28. Gershman, B., et al., *High-resolution dynamics of the transcriptional response to nutrition in Drosophila: a key role for dFOXO.* Physiol Genomics, 2007. **29**(1): p. 24-34.

29. Tiefenbock, S.K., et al., *The Drosophila PGC-1 homologue Spargel coordinates mitochondrial activity to insulin signalling.* EMBO J, 2010. **29**(1): p. 171-83.

30. Brand, A.H. and N. Perrimon, *Targeted gene expression as a means of altering cell fates and generating dominant phenotypes.* Development, 1993. **118**(2): p. 401-15.

31. Herzig, S., et al., *CREB regulates hepatic gluconeogenesis through the coactivator PGC-1.* Nature, 2001. **413**(6852): p. 179-83.

32. Yoon, J.C., et al., *Control of hepatic gluconeogenesis through the transcriptional coactivator PGC-1.* Nature, 2001. **413**(6852): p. 131-8.

33. Zhang, Y., et al., *Peroxisome proliferator-activated receptor-gamma coactivator 1alpha (PGC-1alpha) regulates triglyceride metabolism by activation of the nuclear receptor FXR.* Genes Dev, 2004. **18**(2): p. 157-69.

34. Al-Anzi, B. and K. Zinn, *Colorimetric measurement of triglycerides cannot provide an accurate measure of stored fat content in Drosophila.* PLoS One, 2010. **5**(8): p. e12353.

35. Poirier, L., et al., *Characterization of the Drosophila gene-switch system in aging studies: a cautionary tale.* Aging Cell, 2008. **7**(5): p. 758-70.

36. Micchelli, C.A. and N. Perrimon, *Evidence that stem cells reside in the adult Drosophila midgut epithelium.* Nature, 2006. **439**(7075): p. 475-9.

37. Ohlstein, B. and A. Spradling, *The adult Drosophila posterior midgut is maintained by pluripotent stem cells.* Nature, 2006. **439**(7075): p. 470-4.

38. Biteau, B., et al., *Lifespan extension by preserving proliferative homeostasis in Drosophila.* PLoS Genet, 2010. **6**(10): p. e1001159.

39. Mathur, D., et al., *A transient niche regulates the specification of Drosophila intestinal stem cells.* Science, 2010. **327**(5962): p. 210-3.

40. Partridge, L., D. Gems, and D.J. Withers, *Sex and death: what is the connection?* Cell, 2005. **120**(4): p. 461-72.

41. Broughton, S.J., et al., *Longer lifespan, altered metabolism, and stress resistance in Drosophila from ablation of cells making insulin-like ligands.* Proc Natl Acad Sci U S A, 2005. **102**(8): p. 3105-10.

42. Clancy, D.J., et al., *Extension of life-span by loss of CHICO, a Drosophila insulin receptor substrate protein.* Science, 2001. **292**(5514): p. 104-6.

43. Lithgow, G.J. and G.A. Walker, *Stress resistance as a determinate of C. elegans lifespan.* Mech Ageing Dev, 2002. **123**(7): p. 765-71.

44. St-Pierre, J., et al., *Suppression of reactive oxygen species and neurodegeneration by the PGC-1 transcriptional coactivators.* Cell, 2006. **127**(2): p. 397-408.

45. Owusu-Ansah, E. and U. Banerjee, *Reactive oxygen species prime Drosophila haematopoietic progenitors for differentiation.* Nature, 2009. **461**(7263): p. 537-41.

46. Owusu-Ansah, E., et al., *Distinct mitochondrial retrograde signals control the G1-S cell cycle checkpoint.* Nat Genet, 2008. **40**(3): p. 356-61.

47. Biteau, B., C.E. Hochmuth, and H. Jasper, *JNK activity in somatic stem cells causes loss of tissue homeostasis in the aging Drosophila gut.* Cell Stem Cell, 2008. **3**(4): p. 442-55.

48. Choi, N.H., et al., *Age-related changes in Drosophila midgut are associated with PVF2, a PDGF/VEGF-like growth factor.* Aging Cell, 2008. **7**(3): p. 318-34.

49. Park, J.S., Y.S. Kim, and M.A. Yoo, *The role of p38b MAPK in age-related modulation of intestinal stem cell proliferation and differentiation in Drosophila.* Aging (Albany NY), 2009. **1**(7): p. 637-51.

50. Rando, T.A., *Stem cells, ageing and the quest for immortality.* Nature, 2006. **441**(7097): p. 1080-6.

51. Ito, K., et al., *Regulation of oxidative stress by ATM is required for self-renewal of haematopoietic stem cells.* Nature, 2004. **431**(7011): p. 997-1002.

52. Smith, J., et al., *Redox state is a central modulator of the balance between self-renewal and differentiation in a dividing glial precursor cell.* Proc Natl Acad Sci U S A, 2000. **97**(18): p. 10032-7.

53. Tothova, Z. and D.G. Gilliland, *FoxO transcription factors and stem cell homeostasis: insights from the hematopoietic system.* Cell Stem Cell, 2007. **1**(2): p. 140-52.

54. Hochmuth, C.E., et al., *Redox regulation by Keap1 and Nrf2 controls intestinal stem cell proliferation in Drosophila.* Cell Stem Cell, 2011. **8**(2): p. 188-99.

55. Boyle, M., et al., *Decline in self-renewal factors contributes to aging of the stem cell niche in the Drosophila testis.* Cell Stem Cell, 2007. **1**(4): p. 470-8.

Chapter 3: Enhanced mitochondrial complex I activity in *Drosophila* intestinal stem cell lineages prolongs lifespan while increasing food intake

Jae H. Hur, Sepehr Bahadorani, Jacqueline Graniel, Christopher L. Koehler, Matthew Ulgherait, Michael Rera, D. Leanne Jones, and David W. Walker

Summary

A functional decline in tissue stem cells and mitochondrial dysfunction have each been linked to aging and multiple aging-associated pathologies. However, the interplay between energy homeostasis, stem cells, and organismal aging remains poorly understood. Here, we report that expression of the single-subunit yeast alternative NADH dehydrogenase, *ndi1*, in *Drosophila* intestinal stem and progenitor cells delays the onset of multiple markers of intestinal aging. Improved intestinal homeostasis during aging, mediated by *ndi1*, is associated with increased lifespan at the organismal level. Remarkably, *ndi1* expression in adult intestinal stem cell lineages increases feeding behavior and results in organismal weight gain. In addition, flies expressing *ndi1* in the digestive tract display systemic alterations in metabolic signaling pathways including lower levels of AMPK activation and reduced expression of the insulin-responsive transcription factor dFOXO target genes. Together, these results demonstrate that *ndi1* expression in the intestinal epithelium is an effective strategy to delay tissue and organismal aging and that the processes of eating more and living longer are not mutually incompatible.

Introduction

Identifying the molecular and cellular mechanisms that underlie organismal aging represents an urgent biomedical challenge. Towards this goal, considerable attention has been focused on the progressive decline in stem cell functions [1] and, separately, mitochondrial activity [2] that occurs during aging. Fundamental questions remain, however, regarding the relationships among mitochondrial activity within stem cell populations, tissue homeostasis, and organismal aging. Nutrient intake is closely related to energy homeostasis, stem cell maintenance and lifespan determination [3, 4]. Indeed, moderate dietary restriction (DR) can delay the onset of pathology and extend lifespan in diverse species, from yeast to primates [5]. Similarly, many of the genetic mutations that have been reported to extend organismal lifespan are thought to decrease the activity of nutrient signaling pathways, such as the insulin/insulin-like growth factor signaling (IIS), and the target of rapamycin (TOR) signaling pathways [6-8]. Critically, however, interventions that increase nutrient intake, delay tissue aging, and extend lifespan have proven elusive.

The integrity of the intestinal epithelium is essential for maintaining barrier function, nutrient uptake, metabolic homeostasis, and hence, organismal health and survival [9]. In *Drosophila*, the midgut epithelium is maintained by multipotent intestinal stem cells (ISCs), which are distributed along the basement membrane [10, 11]. Division of an ISC gives rise to one daughter cell that retains stem cell fate and another daughter cell that becomes an enteroblast (EB). During aging, there is a dramatic increase in ISC proliferation which is accompanied by the accumulation of cells that express markers of both ISCs and terminally differentiated daughter cells [12-14]. In addition, loss of intestinal barrier function has been shown to accompany aging across a range of *Drosophila* genotypes and environmental conditions [15]. Moreover, the age-dependent loss of intestinal integrity is linked to multiple markers of organismal aging, including systemic metabolic dysfunction, increased expression of immunity-related genes, reduced spontaneous physical activity and, critically, is a harbinger of

death [15]. Recently, we have characterized the role of the *Drosophila* PGC-1 homolog (*dPGC-1*/*spargel*), a key regulator of mitochondrial energy metabolism, in the maintenance of ISC quiescence, intestinal integrity, and lifespan determination [16]. More specifically, up-regulation of *dPGC-1* in ISC/EBs delays the onset of markers of intestinal aging and confers increased longevity. However, given the diverse roles that PGC-1 plays in metabolism [17], the question of whether an increase in mitochondrial activity alone, in ISC lineages, is sufficient to confer these phenotypic outcomes remains to be determined.

The single subunit alternative internal NADH dehydrogenase (*ndi1*) from *Saccharomyces cerevisiae*, which lacks a conventional electron transport chain (ETC) complex I, can function in *Drosophila* mitochondria and is able to complement and supplement endogenous ETC complex I [18-21]. Here, we expressed *ndi1* in *Drosophila* somatic stem cell lineages and examined its impact on tissue and organismal aging. *ndi1* expression in ISCs/EBs improves tissue homeostasis in the aging intestine and confers increased longevity at the organismal level, demonstrating that increased NADH dehydrogenase activity alone is sufficient to produce these beneficial effects. Strikingly, we find that flies with ISC/EB-specific *ndi1* expression display increased feeding behavior and whole body alterations in metabolic signaling pathways. Consistent with an increase in nutrient intake, long-lived *ndi1* flies show a systemic reduction in the activity of AMP-activated protein kinase (AMPK), a key cellular energy sensor [22]. Our results reveal novel roles for *ndi1* in modulating stem cell behavior and intestinal homeostasis during aging. Moreover, we show that enhanced mitochondrial complex I activity in ISC lineages can simultaneously increase nutrient uptake in adult flies and prolong lifespan.

Results

Expression of *ndi1* in intestinal stem and progenitor cells extends lifespan.

The intestine is a critical target organ with respect to genetic manipulations that can extend longevity [23], as has been shown previously with *dPGC-1* upregulation [16]. To better understand the relationships among mitochondrial respiratory chain activity, intestinal

homeostasis, and lifespan determination, we expressed a previously described *UAS-ndi1* construct [18, 19] in the *Drosophila* intestine using the intestine-specific RU486-inducible Gene-Switch driver line *TIGS-2* [24]. Unlike the endogenous *Drosophila* ETC complex I which is sensitive to rotenone inhibition but insensitive to flavone, NDI1 is insensitive to rotenone but inhibited by flavone [25, 26]. Induced expression of *ndi1* in the adult intestine produced a robust rotenone-insensitive, flavone-sensitive NADH dehydrogenase activity in mitochondria isolated from intestines (Figure 3-1A). Isogenic control flies that were not provided RU486 did not show detectable levels of rotenone-insensitive, flavone-sensitive NADH dehydrogenase activity, supporting the fidelity of the Gene-Switch system [27, 28] and functionality of the *ndi1* transgene and NDI1 protein in the adult fly intestine.

We used this system to examine the impact of intestine-specific expression of *ndi1* on *Drosophila* lifespan. Induced expression of *ndi1* using the *TIGS-2* driver throughout the life of the fly resulted in a significant increase in lifespan in female flies (Figures 3-1B and S3-1A) and no major effect in male flies. RU486 produced no major effects on longevity in control flies (Figure S3-1B). To examine the impact of targeted expression of *ndi1* in intestinal stem cell lineages (ISCs and EBs), we first used the constitutive *esgGAL4* driver line and observed a significant extension of lifespan in both female (Figures 3-1C and S3-1C-D) and male flies (Figures S3-1E-F) compared to isogenic controls. *esgGal4* expression is restricted to ISCs and EBs in the intestine, however, it is also expressed in stem cells within malpighian tubules, germline and somatic stem cells in the testis, and in salivary glands [29]. Therefore, to validate and extend this finding we took advantage of the RU486-inducible *5961GS* driver which recapitulates the *esgGal4* expression pattern in the digestive tract (ISCs/EBs and malpighian tubule stem cells) [29, 30] but is not expressed in salivary glands [29] or testis (C.K. and L.J., unpublished data). Induced expression of *ndi1* during adulthood, via *5961GS*, resulted in a significant lifespan increase in females (Figures 3-1D and S3-1G-I) but not in males (Figures S3-1J-S3-1K). Expression of *ndi1* during adulthood using a Gene-Switch driver that is

expressed in EBs and post mitotic enterocytes (ECs) (*5966GS*, [30]) failed to increase lifespan (Figures S3-1L-M), implicating expression in ISCs as the major contributor to longevity. The largest and most consistent lifespan extension phenotypes using *ndi1* expression were observed with female flies. Therefore, unless noted otherwise, we focused our studies to mated female flies for the remainder of this report.

***ndi1* expression in ISCs/EBs improves markers of intestinal homeostasis during aging**

Homeostasis of the digestive tract in *Drosophila* has been shown to play a central role in lifespan determination [15, 16, 23, 29]. Therefore, we examined markers of intestinal homeostasis in flies that express *ndi1* in ISCs/EBs. First, we set out to determine whether *ndi1* could delay the onset of markers of ISC proliferation and the accumulation of misdifferentiated ISC daughter cells reported to occur in the aged midgut [12-14]. Consistent with improved intestinal tissue homeostasis, examination of aged flies that express *ndi1* in ISCs/EBs along with an *esg* reporter (*UAS-gfp*) revealed a significant decrease in the number of *esg* positive cells in the midgut relative to controls (Figure 3-2A-B). In addition, we also observed a delay in the precocious activation of ISC proliferation, as measured by phosphorylation of histone H3 (pHH3), a marker of cell cycle progression through mitosis. Female flies, 50 days post eclosion, expressing *ndi1* under the control of *esgGAL4* driver contained significantly fewer $pHH3^+$ cells, when compared to isogenic controls (Figure 3-2C). No difference in the number of $pHH3^+$ cells was observed in 10 day old flies, indicating that *ndi1* expression specifically delays the age-related increase in ISC proliferation.

An increase in reactive oxygen species (ROS) has been implicated in the loss of tissue homeostasis in the aged fly intestine [31, 32]. Previously, we reported that neuronal expression of *ndi1* can reduce ROS levels in the aged brain [18]. It is unclear, however, whether *ndi1* expression only in progenitor cells of a tissue is sufficient to cause such changes throughout the tissue. To test this idea, we examined the endogenous levels of ROS in the intestines of control

and *esgGAL4>ndi1* flies using dihydroethidium (DHE), a redox-sensitive dye that exhibits increased fluorescence intensity when oxidized [33, 34]. Targeted expression of *ndi1* in ISCs/EBs led to a reduction of DHE fluorescence in these cells and subsequently, throughout the aged intestine (Figures 3-2D-E, S3-2A). Loss of intestinal integrity can be assayed in living flies by monitoring the presence of non-absorbed dyes (e.g., FD&C blue No. 1) outside of the digestive tract post-feeding [15, 16]. To determine whether *ndi1* can delay the onset of intestinal barrier dysfunction, we examined flies of different ages fed FD&C blue No. 1 for evidence of this dye outside of the digestive tract. The proportion of aged flies with dye outside of the gut was significantly lower in flies with ISC/EB *ndi1* expression (Figure 3-2F). This was not a result of altered development, as adult only induction of *ndi1* in ISCs/EBs using the *5961GS* driver was sufficient to decrease the proportion of flies with dye outside of the digestive tract with age (Figure 3-2G and S3-2B). Both intestinal barrier dysfunction [15] and increased ROS in the gut [35] have been linked with increased systemic expression of anti-microbial peptides (AMPs). Hence, we assayed systemic expression levels of several AMP genes in *esgGAL4>ndi1* and control flies during aging. In line with decreased intestinal barrier dysfunction and ROS level phenotypes, flies that express *ndi1* in ISCs/EBs show significantly lower expression of multiple AMPs in whole bodies later in life (Figure 3-2H). Taken together, our findings show that ISC/EB-specific expression of *ndi1* leads to improved intestinal intestinal homeostasis during aging.

ndi1 expression in intestinal stem and progenitor cells does not affect fertility or physical activity but changes sensitivity to some stresses.

To gain further insight into intestinal *ndi1*-mediated longevity, we examined a number of physiological and behavioral parameters in long-lived *esgGAL4>ndi1* flies and controls. Although lifespan extending interventions are often associated with reproductive trade-offs [36], neither male nor female flies that express *ndi1* in ISC/EBs showed consistent alterations to

fertility (Figures S3-2C-G). Resistance to oxidative stress, assayed by survival under hyperoxia (80% O_2), was similarly unaffected (Figure S3-2H), suggesting that ROS levels in the intestinal epithelium are not limiting for survival under hyperoxia. Survival in elevated environmental temperatures (37°C) and water-only starvation showed considerable differences, with *ndi1* expressing flies showing significantly greater sensitivity to elevated temperatures (Figure S3-2I), and greater resistance to starvation (Figure S3-2J). These changes were not correlated with significant differences in either spontaneous locomotor activity per time of day (Figure S3-2K) or cumulative activity over 24-hour periods (Figure S3-2L). Together, these data indicate that intestinal *ndi1*-mediated longevity is not associated with a general increase in stress resistance or a decline in reproductive output.

***ndi1* expression in intestinal stem and progenitor cells stimulates feeding behavior**

A moderate reduction in food intake, commonly referred to as dietary restriction (DR), can extend lifespan in diverse organisms [5]. Therefore, upon identifying manipulations that increase lifespan, it is important to assay feeding behavior. Indeed, a number of genetic manipulations that increase longevity while reducing feeding have been reported in both worms [37] and flies [38]. To determine if a difference in food intake could play a role in *ndi1*-mediated longevity, we assayed feeding behavior in *esgGAL4>ndi1* flies and controls. Surprisingly, total food consumption, measured using a capillary feeding (CAFE) assay [39], revealed an overall increase in feeding in flies that express *ndi1* in ISCs/EBs at both young and aged time points (Figure 3-3A). An independent assay of feeding using a dye-tracking assay [40] was used to parse the feeding behavior into the proportion of flies that feed within the assay period and the meal size of flies that feed. Expression of *ndi1* in ISCs/EBs resulted in significant increases in both the proportion of flies that feed (Figure3- 3B) and their meal sizes (Figure 3-3C) in both young and aged flies. 24 hour activity profiles of *ndi1* expressing flies are similar to controls, suggesting that an altered activity at different times of day is not responsible for the increased

feeding during the assay period (Figure S3-2K). Moreover, adult-onset expression of *ndi1* for 10 days in ISCs/EBs using the *5961GS* driver was sufficient to confer an increase in total food consumption (Figure 3-3D) and meal size (Figure 3-3E). The presence of the inducing drug itself had no significant effect on total feeding (Figure S3-3B) or meal size (Figure S3-3C).

To determine whether increased feeding was associated with alterations in defecation, we examined the material excreted by ISC/EB *ndi1* expressing flies and controls. Although *ndi1* expressing flies ate significantly more than controls, excreta number were not significantly different than controls, at both young and aged time points (Figure S3-3 and 3-3D). Recent work has shown that qualitative analysis of excreta can provide insight into intestinal transit and fluid homeostasis [41]. Closer examination of excreta shape of young and aged flies expressing *ndi1* in ISC/EBs showed a significant reduction in the frequency of "reproductive oblong deposits" (RODs, Figures 3-3F and S3-3E) that have previously been linked to reduced fluid availability, concentrated intestinal contents, and slower intestinal transit [41]. Similarly, fecal pH analysis of flies maintained on bromophenol blue (BPB) containing diets showed less acidic fecal deposits in *ndi1* expressing flies (Figure 3-3G), consistent with a quicker transit through the intestinal tract. Together, these findings indicate that expression of *ndi1* in ISCs/EBs improves intestinal transit and fluid homeostasis.

Next, we set out to determine whether ISC/EB expression of *ndi1* flies show systemic physiological changes that are consistent with increased nutrient uptake. Whole body weight measurements indicated that *esgGAL4>ndi1* flies are heavier than controls, and maintain their weight during aging (Figure 3-3H). As with feeding behavior, adult-onset expression of *ndi1* for 10 days in ISCs/EBs using the *5961GS* driver was sufficient to confer an increase in body weight (Figure 3-3I), and this was not a result of the inducing drug itself (Figure S3-3F). Moreover, aged *esgGAL4>ndi1* flies display increased protein levels and triglyceride stores relative to controls at aged timepoints (Figures 3-3J-K, S3-3G). Unlike triglycerides, levels of glycogen declined similarly in both *ndi1* expressing flies and controls with age (Figure S3-3H).

***ndi1* expression in ISCs/EBs alters systemic metabolic signaling pathways.**

AMP-activated protein kinase (AMPK) is a crucial metabolic gauge that is activated by low cellular energy status [22]. Since expression of *ndi1* in ISCs/EBs stimulates feeding, we reasoned that these flies may show reduced systemic AMPK activity. Indeed, Western blots specific for phosphorylated AMPK revealed significantly decreased phosphorylation at Thr184 in whole bodies of *esgGAL4>ndi1* flies relative to controls (Figures 3-4A-B and S3-4A). AMPK activation has been shown to stimulate sirtuin1 (SIRT1) activity, which deacetylates FOXO and increases its transcriptional activity [42]. Consistent with this, systemic dFOXO transcriptional activity, assayed by measuring transcript levels of multiple direct downstream targets of dFOXO in whole bodies, was significantly decreased in *esgGAL4>ndi1* flies (Figure 3-4C). FOXO activity is independently regulated by a number of different signaling pathways, including the insulin/insulin-like growth factor signaling (IIS) pathway [43] To determine whether the observed decrease in dFOXO activity in *esgGAL4>ndi1* flies was associated with an increase in systemic IIS, we assayed the activation state of the direct mediator of FOXO activity in the IIS pathway, phosphoinositide-3-OH-kinase-dependent serine/threonine protein kinase (AKT). In whole bodies of *esgGAL4>ndi1* flies the phosphorylation of AKT was not significantly affected at either the IIS phosphorylation site (Thr423) or the TORC2 phosphorylation site (Ser505), nor was there a difference in total AKT protein levels (Figures 3-4D-E and S3-4B). Similarly, neither S6K phosphorylation at the TORC1 target residue (Thr398) nor total S6K levels were significantly changed in whole bodies of *ndi1* expressing flies (Figures S3-4C-D). Thus, the observed decrease in FOXO target gene expression in *esgGAL4>ndi1* flies is not associated with altered systemic IIS/TOR pathway activity.

Increased feeding, in ISC/EB *ndi* expressing flies, without a corresponding increase in AKT phosphorylation could result from defects upstream of AKT in the propagation of IIS. Therefore, we checked the expression levels of several *Drosophila* insulin-like peptides (*dilp*s)

to determine if head *dilp* levels in *esgGAL4>ndi1* flies were altered. Transcript levels in heads of *dilp2*, *dilp3* and *dilp5*, that are expressed in the insulin producing cells (IPCs) upon feeding, were significantly decreased in *esgGAL4>ndi1* flies (Figure 3-4F) while the transcript level of *dilp1*, which is not associated with expression in adult heads [44], was not altered significantly (Figure S3-4E). Direct quantification of DILP2 protein levels in IPCs by immunofluorescence showed a similar decrease in DILP2 fluorescence in IPCs of *esgGAL4>ndi1* flies (Figure 3-4G and 3-4H). Therefore, increased feeding in *esgGAL4>ndi1* is accompanied by lowered expression of *dilps* in heads and DILP2 levels in IPCs.

The *Drosophila* ortholog of mammalian neuropeptide Y, short neuropeptide F (sNPF), is expressed in the nervous system and regulates food intake [45]. Recently, it has been shown that *sNPF* and its cognate receptor, *sNPFR1,* regulate the expression of *dilps* in the fly brain [46]. To determine if decreased *dilp* transcription in heads of *esgGAL4>ndi1* flies is linked to altered sNPF/sNPFR1 expression, we measured transcript levels of *sNPF* and *sNPFR1* in heads. Interestingly, both *sNPF* and *sNPFR1* transcript levels were decreased in heads of *esgGAL4>ndi1* flies relative to controls (Figure 3-4I and 3-4J). One potential interpretation of these findings is that increased feeding in *ndi1* expressing flies results in decreased activation of this pro-feeding signaling pathway.

Discussion

A decline in mitochondrial activity has been implicated in multiple degenerative diseases of aging [2]. These findings raise the intriguing possibility that strategies to stimulate mitochondrial activity during aging may delay the onset of pathology and extend healthspan. In support of this idea, we recently reported that overexpression of the fly PGC-1 homolog, *dPGC-1,* in ISC lineages is sufficient to preserve intestinal homeostasis during aging and extend fly lifespan [16]. However, due to the extensive interactions that PGC-1 has with multiple aspects

of metabolism [17], the possibility persists that endogenous *dPGC-1* interactions, other than its role as a regulator of mitochondrial activity, play a role in the cellular and/or organismal phenotypes that we observed. Unlike *dPGC-1*, *ndi1* is exogenous, from a different kingdom, with no known homologs in animals, so any changes that result from *ndi1* expression can reasonably be expected to be from the function of *ndi1* itself and not from genetic interactions of *ndi1* with endogenous pathways. A previous study reported that ubiquitous expression of *ndi1* using a constitutive driver line can increase fly lifespan [20]. However, studies of the genetics of aging and lifespan determination are prone to confounding effects due to uncontrolled differences in genetic background between test and control lines [47, 48]. Using an inducible gene expression system, which eliminates this issue, we failed to observe lifespan extension upon ubiquitous expression, but instead observed that neuron-specific expression of *ndi1* can extend lifespan [18]. In the present study, we have extended this approach and show that expression of *ndi1* in adult intestinal stem and progenitor cells can delay the onset of intestinal barrier dysfunction and extend the lifespan of flies. Therefore, a major conclusion of this study is that an increase in mitochondial NADH dehydrogenase activity alone in somatic stem cell lineages can delay both tissue and organismal aging.

Numerous studies have reported that a moderate decrease in nutrient intake can delay aging and extend lifespan in diverse species including rodents, flies and worms [5] To our knowledge, however, this is the first report of a lifespan extending intervention in which the long-lived organisms consume more food than controls. Remarkably, long-lived flies expressing *ndi1* in ISCs/EBs have behavioral, physiological, and biochemical correlates of increased nutrition, showing increased feeding, weight, metabolic stores, and decreased systemic activation of AMPK. Moreover, both increased sensitivity to elevated temperatures, and resistance to starvation of the long-lived flies are wholly consistent with larger flies (with lower surface-to-mass ratios) and improved nutrient absorption and storage. Whether increased feeding is causally related to the extension of lifespan remains to be determined. However, one indication

that increased feeding may play a role in increasing lifespan is the improved ability of flies expressing *ndi1* in ISCs/EBs to maintain body weight and metabolic stores with age. A clue to why these flies eat more may lie with the regulation of DILP signaling (Figure S3-4F). DILPs have been shown to suppress feeding behavior and the decreased *dilp* transcripts in heads of *ndi1* flies may be consistent with decreased DILP2 signaling. Lowered DILP signaling regardless of the nutritional status of the fly, may contribute to the increased feeding behavior by maintaining a physiology permissive for feeding. Wild type flies that are well fed are characterized by high DILP signaling and increased IIS/TOR pathway activation, which in heads, decreases *sNPF*/*sNPFR1* transcription and signaling, leading to decreased feeding behavior [46, 49]. In contrast, *ndi1* flies, which show increased feeding, maintain low transcript levels of head *dilps*, failing to increase systemic IIS/TOR pathway activity. Therefore, *ndi1* expression in ISCs/EBs appears to uncouple DILP signaling from nutritional status. One interpretation of our findings is that feeding suppresses AMPK activity, leading to decreased FOXO activity and *sNPF*/*sNPFR1* transcript levels (Figure S3- 4F). Without a corresponding increase in DILP levels to inhibit feeding, however, the flies remain in a permissive state for feeding, and even with reduced sNPF/sNPFR1 signaling, eat more. Our work has focused on the head *dilps*, but compensatory *dilp* signaling from other tissues, such as *dilp6* from adipose tissues, may also play a role [50].

Forkhead Box-O (FOXO) transcription factors, inhibited by IIS, have been implicated in metabolic homeostasis and lifespan determination [51, 52]. Indeed, adult-onset and tissue-restricted overexpression of the single *Drosophila* FOXO ortholog (*dFOXO*) can increase longevity [53, 54]. Yet, the relationships between IIS, FOXO activity and organismal health are not straightforward. Reduced IIS in mammals results in diabetes, whose associated pathologies shorten lifespan [55] and, in *Drosophila*, dFOXO activation has been shown to contribute to infection-induced metabolic wasting and death [56]. Moreover, aged flies display markers of impaired IIS [15, 57], including dFOXO activation, which are predictive of impending death in

individual flies [15]. In the current study, we show that long-lived flies, expressing *ndi1* in ISCs/EBs, show reduced expression of multiple dFOXO target genes in whole bodies. However, reduced dFOXO activity was not associated with alterations in AKT activation indicating that systemic IIS activity is not altered. These findings are consistent with a model (Figure S4F) whereby ISC/EB-specific expression of *ndi1* confers increased feeding, nutrient uptake and, as a result, AMPK induced stimulation of dFOXO is reduced.

How do we reconcile our findings with previous work reporting that reduced IIS and/or FOXO activation prolongs lifespan in *Drosophila* [8, 53, 54, 58, 59]? Our observation that long-lived flies expressing *ndi1* in ISCs/EBs show reduced expression of *dilps* in heads and DILP2 levels in IPCs may provide some insight. Reduced expression of *dilp2* has been consistently associated with increased lifespan in multiple gentotypes in studies from different laboratories [44, 46, 50, 53, 60, 61]. Moreover, deletion of the neurosecretory cells that produce *dilp2*, *3*, and *5*, produces phenotypes that overlap with ISC/EB expression of *ndi1*, resistance to starvation stress, sensitivity to heat stress and increased lifespan [44]. Uncovering the mechanism by which *ndi1* expression in ISCs/EBs results in altered expression of *dilps* could provide important insights into the role of somatic stem cells in the regulation organismal lifespan, metabolism and behavior. Regardless of the underlying mechanisms, our findings demonstrate that providing exogenous NADH dehydrogenase activity in ISC lineages is an attractive strategy to delay markers of intestinal aging and prolong healthy lifespan in fruit flies. Given that *ndi1* can be functionally expressed in mammalian cells [62-64], and does not cause an immune response [65], expression of *ndi1* in mammalian stem cells may provide a strategy to similarly improve tissue homeostasis and delay the onset of aging in mammals.

Experimental Procedures

Fly lines, culture, and genotypes

UAS-ndi1 lines were constructed and backcrossed 10 times into a w^{1118} background. The *TIGS-2* line was provided by L. Seroude, *5961GS* was provided by H. Jasper, and *esgGAL4* was provided by A. Christiansen. Culturing of flies and measurements of lifespan were performed as previously described (Rera et al. 2011). Genotypes: *TIGS*>+: *+;+;TIGS-2/+, TIGS>ndi1*: *+;UAS-ndi1/+;TIGS-2/+, esgGAL4*>+: *+;esgGAL4,UAS-gfp/+;+, esgGAL4>ndi1*: *+;esgGAL4,UAS-gfp/UAS-ndi1;+, 5961GS*>+: *+;5961GS,UAS-gfp/+;+, 5961GS>ndi1*: *+;5961GS,UAS-gfp/UAS-ndi1;+, 5966GS*>+: *+;5966GS/+;+, 5966GS>ndi1*: *+;5966GS/UAS-ndi1;+*

NADH dehydrogenase activity assay

Fly guts were dissected on ice on ice-cold 1XPBS, and mitochondria were isolated and rotenone and/or flavone sensitive colorimetric NADH dehydrogenase assays were performed as previously described [19].

Feeding assays

Capillary feeding (CAFE) assays were performed as previously described [39]with modifications. Briefly, 10 flies were placed in vials with wet tissue paper as a water source and a capillary food source (5% sucrose, 5% yeast extract, 2.5% FD&C Blue No. 1 (SPS Alfachem, Lexington, MA, USA)). Feeding was monitored from approximately 3 hours after lights on until lights off, with capillaries being replaced and feeding amounts recorded every 2-3 hours.

Dye tracking assays were performed as described previously [40] with slight modifications. Approximately 30 flies were placed in vials with standard yeast-sugar-cornmeal medium (Lewis 1960) supplemented with 2.5% dye (FD&C Blue No. 1) from 3 hours after lights on until 5.5 hours after lights on at 25°C. Flies were frozen, decapitated, and homogenized separately in 200µl H_2O. Cell debris was pelleted via centrifugation, and absorbance (629nm) of a 1:2.5 dilution of the supernatant was used to determine whether the fly ate (A_{629nm} greater than 110% of the absorbance outside of the dye absorption range, at 800nm), and if so, the relative meal size (A_{629}-A_{800}).

qRT-PCR

RNA isolation, cDNA synthesis, and quantitative PCR were performed on whole flies or dissected body parts as previously described (Rera et al. 2012). *actin5c, drosomycin, diptericin, drosocin, InR, 4E-BP, ImpL2* primers from Rera et al. 2012, *l(2)efl*: CAGACGCGTTTATCCAAGTG, ATCCCACCAGTCACGGAAC, *dilp1*: GCTTTAATACGCTGCCAAGG, CGGATCCGTACAGATTGGTT, *dilp2*: ATCCCGTGATTCCACACAAG, GCGGTTCCGATATCGAGTTA, *dilp3*: AGAGAACTTTGGACCCCGTGA, TGAACCGAACTATCACTCAAC, *dilp5*: GCCTTGATGGACATGCTGA, TCATAATCGAATAGGGCCCAAG, *sNPF*: CCCGAAAACTTTTAGACTCA, TTTTCAAACATTTCCATCGT, *sNPFR1*: CTGGCCATATCGGACCTACT, GGCCAGTACTTGGACAGGAT.

Dihydroethidium (DHE) staining

ROS levels were detected in live tissue as previously described (Rera et al. 2011). Briefly, guts were dissected in ice-cold Schneider's medium (Caisson Labs, North Logan, UT, USA) and briefly fixed in 4% formaldehyde in Schneider's medium for 3 minutes at room temperature. Guts were washed twice in Schneider's medium for 30 seconds and stained in 50μM DHE (Life Technologies, Grand Island, NY, USA) in Schneider's medium for 7 minutes at room temperature in a light protected chamber. Samples were washed three times for 5 minutes in Schneider's medium at room temperature, mounted in Prolong Gold with DAPI (Life Technologies), and imaged immediately at 100X magnification.

Immunofluorescence and cell quantification

Fixation and staining of *Drosophila* midguts were carried out according to Rera *et al.* 2011. Midguts were co-labeled with chicken anti-GFP (1:5000, #GFP-1010, Aves Labs, Tigard, Oregon, USA) and rabbit anti-phospho-histone H3 (1:200, #06-570, EMD Millipore, Darmstadt, Germany) before mounting in Vectashield mounting medium (Vector Laboratories, Burlingame, CA, USA) containing 4',6-diamidino-2-phenylindole (DAPI). Images of the posterior midgut

(approximately 250 µm anterior to the pyloric ring) were acquired with a 20x objective on a Zeiss LSM 780 confocal microscope. Cells that stained for either GFP, phospho-histone H3 ($pHH3^+$), or DAPI were counted manually from at least 22 samples per treatment group. For GFP^+ counts, One-way ANOVA was used to determine statistical significance; means of each treatment were compared using Tukey's post hoc test. To determine significant differences in the median number of $pHH3^+$ cells per posterior midgut, a Kruskall-Wallis test was used followed by a Dunn's post hoc test.

Intestinal barrier dysfunction

Flies were tested in groups of approximately 30 per vial, as described in Rera *et al.* 2012.

Weight and metabolic stores

Flies were weighed as previously described in Cho *et al.* 2012, and metabolite contents, including triacylglycerides, glycogen, and protein, were measured as previously described in Rera *et al.* 2011.

Spontaneous activity, stress resistance, and fertility

Spontaneous activity and stress resistance were measured as previously described in Bahdorani *et al.* 2010a, and Cho *et al.* 2012, respectively. Fertility was measured 4 times per week over the entire lifespan by counting adult progeny from 10 flies, mated with w^{1118} flies, continuously or for a single day at day 3 of adulthood.

Fecal deposit number, shape, and pH

Excreta assays were performed as previously described in Cognigni *et al.* 2011 with modifications. Flies were maintained on standard yeast-sugar-cornmeal medium (Lewis 1960) supplemented with 0.5% bromophenol blue, sodium salt (BPB, Sigma-Aldrich, St. Louis, MO, USA) for 24 hours before the assay. Groups of 10 flies were maintained on 60X15mm petri

dishes with 2ml BPB medium for 72 hours, and the center of the lid was photographed and analyzed using ImageJ for fecal number, shape, and hue (Schneider et al. 2012).

Western blot

Western blot analyses were performed using standard procedures for Polyvinylidene difluoride (PVDF) membranes using the following antibodies and dilutions: phospho-AMPKα (Thr184) (1:1000, #2535, Cell Signaling Technology, Danvers, MA, USA), beta-Actin-peroxidase (1:5000, #a3854, Sigma-Aldrich), phospho-AKT (Ser505) (1:1000, #4060, Cell Signaling Technology), phospho-AKT (Thr423) (1:1000, #2965, Cell Signaling Technology), total AKT (1:1000, #4691, Cell Signaling Technology), phospho-S6K (Thr398) (1:500, #9209, Cell Signaling Technology), total S6K (1:750, #sc-230, Santa Cruz Biotechnology, Dallas, TX, USA), rabbit IgG-peroxidase (1:2000, #a6154, Sigma-Aldrich). Densitometry and quantification were performed using ImageJ (Schneider et al. 2012).

DILP2 Immunofluorescence

Dissected brains were fixed, stained, and mounted following published protocols (Géminard et al. 2009) with DILP2 antibodies provided by P. Leopold (1:800), rat IgG (#A11077, 1:250, Life Technologies, Grand Island, NY, USA), and phalloidin (#A12379, 1:100, Life Technologies). Approximately 10-20 images per brain were taken with a Zeiss CLS microscope and analyzed using ImageJ (Schneider et al. 2012) to measure total fluorescence of individual IPCs in slices with maximum nuclear area.

Statistical analyses

Unless otherwise indicated, significance was determined using a two-tailed, unpaired *t* test from at least three independent experiments and expressed as p values. All error bars reflect standard error of the mean.

Acknowledgments: We thank Jaehyoung Cho, Holly Vu, and Amna Khan for help with fly work and the M. Frye and D. Simmons labs for use of their equipment, H. Jasper, L. Seroude,A.

Christiansen and the Drosophila Stock Center (Bloomington) for fly stocks, and P. Léopold for DILP2 antibodies. DWW is supported by the National Institute on Aging (R01 AG037514, R01 AG040288) and the Ellison Medical Foundation. MU is supported by a Eureka fellowship. JG is funded by the National Institutes of Health/National Institute of General Medical Sciences (grant number NIH MARC T34 GM008563). DLJ is supported by the National Institute on Aging (R01 AG028092, R01 AG040288). CLK is supported by a National Science Foundation predoctoral training fellowship (DGE-1144087). D.W.W is an Ellison Medical Foundation New Scholar in Aging. The authors declare no conflict of interest.

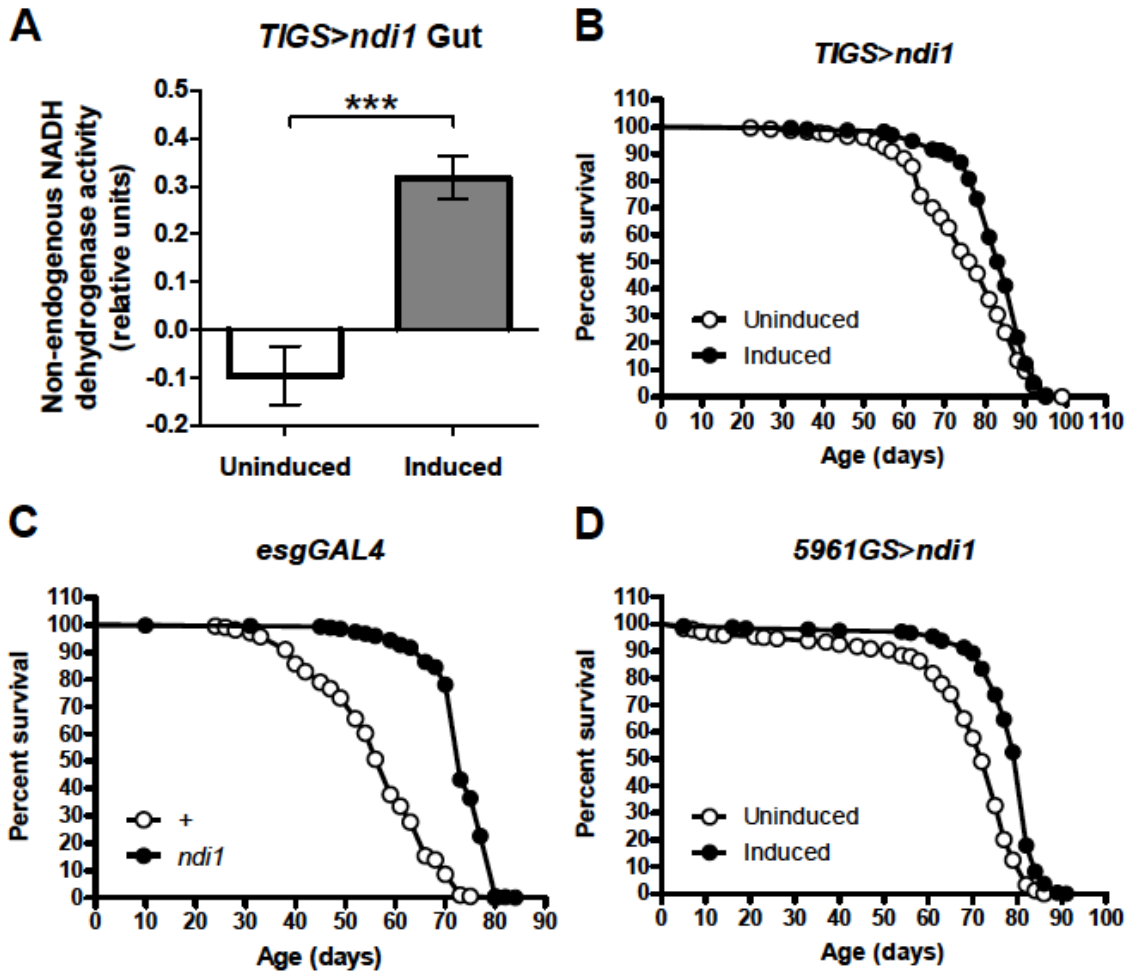

Figure 3-1. Intestine-specific expression of *ndi1* increases non-endogenous NADH dehydrogenase activity and lifespan.

(A) Expression of *ndi1* using a gut specific geneswitch driver, *TIGS-2* (*TIGS>ndi1*), is sufficient to confer flavone sensitive, rotenone insensitive NADH dehydrogenase activity to mitochondria isolated from guts of mated female flies 10 days post eclosion. *In vitro* colorimetric assays of flavone sensitive, rotenone insensitive NADH dehydrogenase activity show negligible activity in mitochondria isolated from guts of flies that were not provided the inducing drug, RU486 ("Uninduced", carrier ethanol only). Mitochondria isolated from flies that were provided RU486 ("Induced", 100mg/l) from day 1 of adulthood clearly show flavone sensitive, rotenone

insensitive NADH dehydrogenase activity. (***p<0.001, t test, 5 replicates per condition, mitochondria from 10 dissected guts per replicate).

(B) Induction of *ndi1* in guts of mated female flies throughout their life using the *TIGS-2* driver (*TIGS>ndi1*) in conjunction with RU486 ("Induced", 10mg/l during larval stages, 50mg/l during adulthood) is sufficient to increase lifespan relative to isogenic controls provided non-RU486 medium ("Uninduced", carrier ethanol only). (p<0.001, logrank test, 9.6% increase in mean, approximately 240 flies per condition).

(C) Expression of *ndi1* in intestinal stem cells (ISCs) and enteroblasts (EBs) using a constitutive driver, *esgGAL4* (*esgGAL4>ndi1*), is sufficient to increase lifespan in mated female flies relative to driver only controls (*esgGAL4>+*). (p<0.001, logrank test, 50% increase in mean, at least 200 flies per condition).

(D) Adulthood only induction of *ndi1* using an ISC/EB specific geneswitch driver, *5961GS* (*5961GS>ndi1*) in conjunction with RU486 ("Induced", 0.5mg/l) is sufficient to increase lifespan of mated female flies relative to isogenic controls provided non-RU486 medium ("Uninduced", carrier ethanol only). (p<0.001, logrank test, 14% increase in mean, approximately 240 flies per condition).

See also Figure S1.

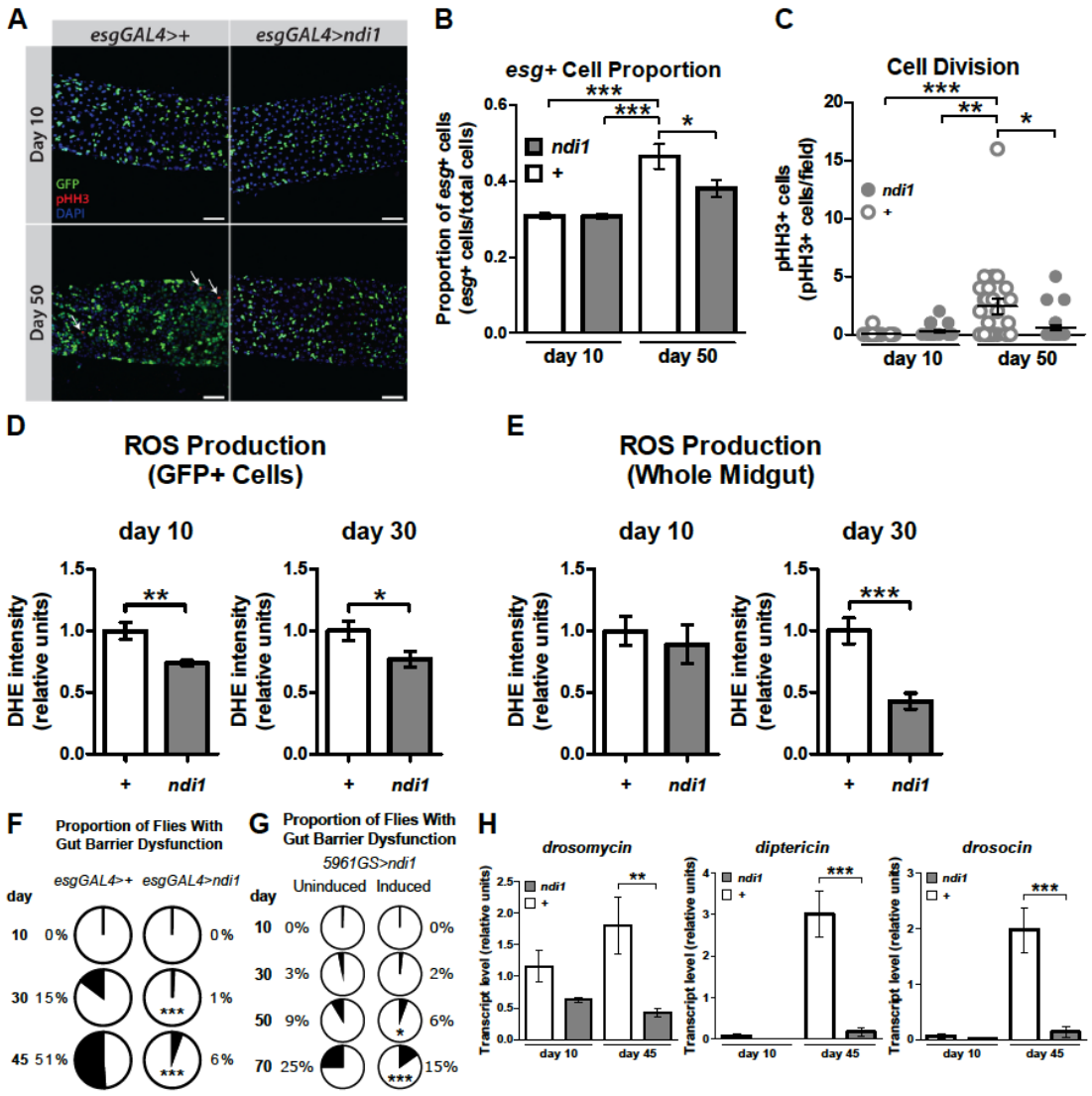

Figure 3-2. Expression of *ndi1* in ISCs/EBs leads to improved intestinal homeostasis during aging.

(A) Immunofluorescent images of the adult posterior midgut demonstrating age-associated changes in the tissue. Control flies ("*esgGAL4*>+", upper panel) or flies overexpressing *ndi1* in ISCs/EBs ("*esgGAL4>ndi1*", lower panel) 10 days and 50 days post eclosion were assayed for ISC mitoses ($pHH3^+$ stain, arrows) and *esg* expression (GFP stain). Scale=50μm.

(B) Induction of *ndi1* with the *esgGAL4* driver rescues the age-associated misexpression of *esg*. Total cell and esg^+ cell numbers were calculated from DAPI and GFP stains respectively.

The proportion of GFP^+ cells increased only in the aged controls. (*p<0.05, ***p<0.001, One-way ANOVA with Tukey's post hoc test, at least 22 flies per condition).

(C) The age-associated increase in ISC mitoses is rescued with *ndi1* expression via *esgGAL4*. The median number of mitotic events ($pHH3^+$ cells per field of view) in aged control flies (day 50, *esgGAL4*>+) was significantly higher than all other conditions. (*p<0.05, **p<0.01, ***p<0.001, Kruskal-Wallis test followed by Dunn's multiple comparisons, at least 22 flies per condition).

(D) Induction of *ndi1* expression with *esgGAL4* driver ("*ndi1*", *esgGAL4>ndi1*) decreases DHE fluorescence in esg^+ cells in both 10 and 30 day old intestines compared to driver only controls ("+", *esgGAL4*>+). DHE fluorescence intensity was measured within the borders of esg^+ cells (detected as gfp^+ cells, arrows in figure S2A) throughout the entire Z stack and averaged to obtain a value representing the mean intensity of all esg^+ cells per Z stack per gut (*p<0.05, **p<0.01, t test, at least 3 images per gut, 10 guts per condition).

(E) Induction of *ndi1* expression with *esgGAL4* driver ("*ndi1*", *esgGAL4>ndi1*) results in decreased DHE fluorescence throughout gut tissues relative to driver only controls ("+", *esgGAL4*>+) 30 days post eclosion. (***p<0.001, t test, at least 3 images per gut, 10 guts per condition).

(F) Mated female flies 10 days post eclosion do not show failure to sequester a non absorbed blue dye (FD&C blue dye #1) in the gastrointestinal (GI) tract. At later time points, flies that express *ndi1* under the control of the *esgGAL4* driver (*esgGAL4>ndi1*) show a significant improvement in gut sequestration of the blue dye relative to matched driver only controls (*esgGAL4*>+). (***p<0.001, binomial test, at least 190 flies per condition).

(G) Adulthood only induction of *ndi1* in ISCs/EBs in mated female flies using the *5961GS* geneswitch driver (*5961GS*>*ndi1*) in conjunction with RU486 ("Induced", 0.5mg/l) is sufficient to improve sequestration of GI luminal contents at older time points relative to matched isogenic

controls that were not provided RU486 (“Uninduced”, carrier ethanol only). (*p<0.05, ***p<0.001, binomial test, at least 140 flies per condition).

(H) Whole body transcript levels of *drosomycin*, *diptericin*, and *drosocin* are similar in mated female driver only control flies (*esgGAL4*>+) relative to those that express *ndi1* under the control of the *esgGAL4* driver (*esgGAL4>ndi1*) at day 10 of adulthood, but are significantly increased at day 45. (**p<0.01, ***p<0.001, t test, 5 replicates per condition, 5 flies per replicate).

See also Figure S2.

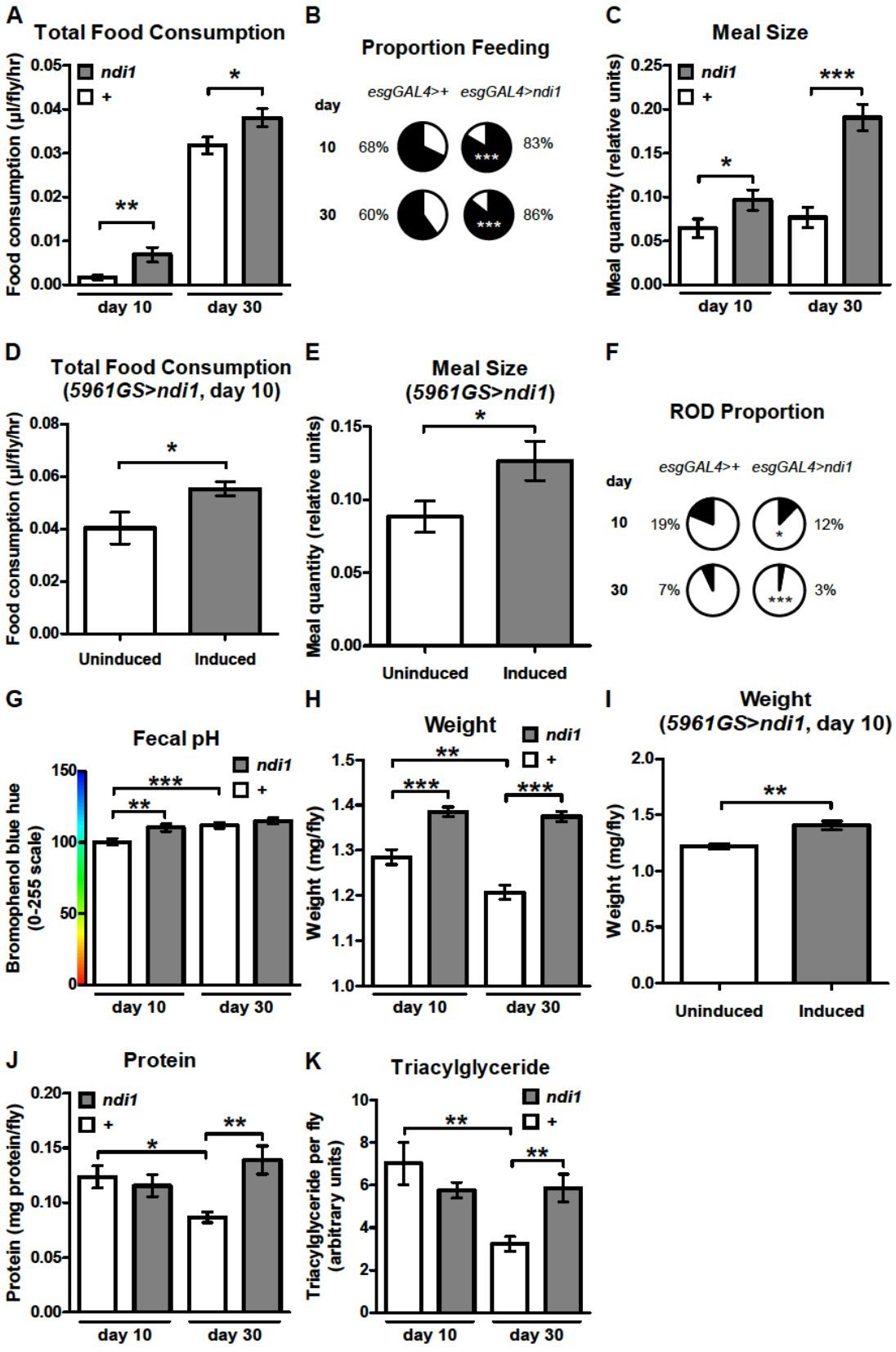
A
Total Food Consumption
Food consumption (µl/fly/hr)
ndi1
+
day 10
day 30
B
Proportion Feeding
esgGAL4>+
esgGAL4>ndi1
day
10
68%
83%
30
60%
86%
C
Meal Size
Meal quantity (relative units)
D
Total Food Consumption
(5961GS>ndi1, day 10)
Uninduced
Induced
E
Meal Size
(5961GS>ndi1)
F
ROD Proportion
19%
12%
7%
3%
G
Fecal pH
Bromophenol blue hue
(0-255 scale)
H
Weight
Weight (mg/fly)
I
Weight
(5961GS>ndi1, day 10)
J
Protein
Protein (mg protein/fly)
K
Triacylglyceride
Triacylglyceride per fly
(arbitrary units)

Figure 3-3. Expression of *ndi1* in ISCs/EBs stimulates feeding and confers weight gain.

(A) Total food consumption was measured using a capillary feeding (CAFE) assay. At 10 and 30 days post eclosion, mated female flies expressing *ndi1* under the control of the *esgGAL4* driver ("*ndi1*", *esgGAL4>ndi1*) consumed significantly more food relative to driver only control flies ("+", *esgGAL4*>+). (*p<0.05, **p<0.01, t test, 10 replicates per condition, 10 flies per replicate).

(B) A colorimetric dye-tracking assay was used to parse out feeding frequency and meal size. Mated female flies that express *ndi1* under the control of the *esgGAL4* driver (*esgGAL4>ndi1*) had a significantly greater proportion of flies that fed during the assay period, relative to matched driver only controls (*esgGAL4*>+) at both day 10 and day 30 of adulthood. (***p<0.001, binomial test, approximately 90 flies per condition).

(C) Of those flies that ate during the assay period in (B), meal size was significantly greater in mated female flies that express *ndi1* under the control of the *esgGAL4* driver ("*ndi1*", *esgGAL4>ndi1*) relative to matched driver only controls ("+", *esgGAL4*>+) at both day 10 and day 30 of adulthood. (*p<0.05, ***p<0.001, t test, 50-95 flies that ate from B per condition).

(D) By day 10 of adulthood, adulthood only expression of *ndi1* under the control of the *5961GS* driver (*5961GS>ndi1*) in conjunction with RU486 ("Induced", 0.5mg/l) is sufficient to increase total food consumption in mated female flies, as measured by a CAFE assay, relative to matched isogenic controls not provided RU486 ("Uninduced", carrier ethanol only). (*p<0.05, t test, 6 replicates per condition, 10 flies per replicate).

(E) Adulthood only expression of *ndi1* in ISCs/EBs under the control of the *5961GS* driver in conjunction with RU486 ("Induced", 0.5mg/l), in mated female flies 10 days post eclosion, is sufficient to increase meal size relative to matched isogenic controls ("Uninduced", carrier ethanol only). (*p<0.05, t test, approximately 85 flies that ate during the assay period in Figure S3A).

(F) The proportion of ROD-type deposits (Figure S3E, arrow) is significantly lower in deposits from mated female flies expressing *ndi1* under the control of the *esgGAL4* driver (*esgGAL4>ndi1*) relative to matched driver only controls (*esgGAL4*>+) at both day 10 and day 30 of adulthood. (*p<0.05, ***p<0.001, binomial test, at least 180 deposits per condition).

(G) Fecal pH was measured by hue analysis of fecal deposits from mated female flies cultured on BPB medium. Flies expressing *ndi1* under the control of the *esgGAL4* driver ("*ndi1*", *esgGAL4>ndi1*) had more basic excreta relative to matched driver only controls ("+", *esgGAL4*>+) at day 10 of adulthood and this pH is maintained at day 30. Fecal deposits from controls are similarly basic at day 30. (**p<0.01, ***p<0.001, t test, at least 180 deposits per condition).

(H) Mated female flies that express *ndi1* in ISCs/EBs under the control of the *esgGAL4* driver (*esgGAL4>ndi1*) are heavier at day 10 of adulthood and maintain their weight through day 30 of adulthood better than matched driver only controls (*esgGAL4*>+), which show significant weight loss with age. (**p<0.01, **p<0.01, ***p<0.001, t test, 12 replicates per condition, 5 flies per replicate).

(I) By day 10 of adulthood, adulthood only expression of *ndi1* under the control of the *5961GS* driver (*5961GS>ndi1*) in conjunction with RU486 ("Induced", 0.5mg/l) is sufficient to significantly increase weight of mated female flies relative to matched isogenic controls ("Uninduced", carrier ethanol only). (**p<0.01, t test, 6 replicates per condition, 10 flies per replicate).

(J) Protein content of mated female flies expressing *ndi1* under the control of the *esgGAL4* driver ("*ndi1*", *esgGAL4>ndi1*) is similar to matched driver only controls ("+", *esgGAL4*>+) at day 10 of adulthood and is maintained through 30 days of adulthood. In contrast, controls show a significant loss of protein content by day 30 of adulthood. (*p<0.05, **p<0.01, t test, 4 replicates per condition, 5 flies per replicate).

(K) Densitometric quantification of thin layer chromatography for triacylglyceride content (Figure S3G) of mated female flies that express *ndi1* under the control of the *esgGAL4* driver

(*esgGAL4>ndi1*) is similar to matched driver only controls (*esgGAL4*>+) at day 10 of adulthood and is maintained at day 30, whereas controls show a significant loss of triacylglyceride stores by day 30. (**p<0.01, t test, 5 replicates per condition, 5 flies per replicate).

See also Figure S3.

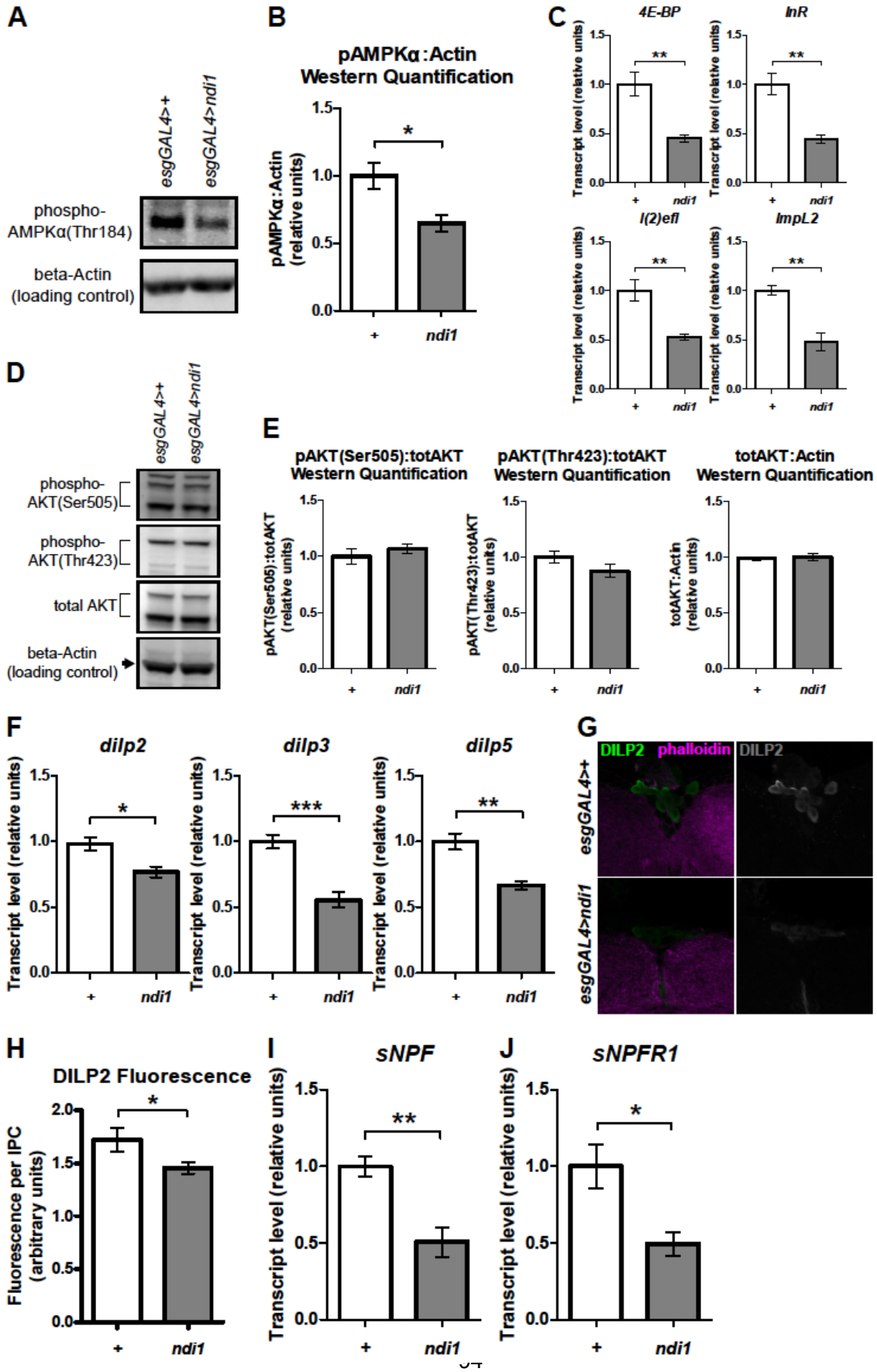
A
esgGAL4>+
esgGAL4>ndi1
phospho-AMPKα(Thr184)
beta-Actin (loading control)
B
pAMPKα:Actin Western Quantification
pAMPKα:Actin (relative units)
ndi1
C
4E-BP
InR
I(2)efl
ImpL2
Transcript level (relative units)
D
phospho-AKT(Ser505)
phospho-AKT(Thr423)
total AKT
beta-Actin (loading control)
E
pAKT(Ser505):totAKT Western Quantification
pAKT(Thr423):totAKT Western Quantification
totAKT:Actin Western Quantification
F
dilp2
dilp3
dilp5
G
DILP2
phalloidin
H
DILP2 Fluorescence
Fluorescence per IPC (arbitrary units)
I
sNPF
J
sNPFR1

Figure 3-4. Expression of *ndi1* in ISCs/EBs leads to alterations in systemic metabolic signaling pathways.

(A-B) Western blot (A, Figure S4A) and densitometric analysis (B) of AMPKα phosphorylation at Thr184 normalized to a loading control, beta-Actin, shows a significant decrease in AMPKα phosphorylation in mated female flies 10 days post eclosion that express *ndi1* under the control of the *esgGAL4* driver ("*ndi1*", *esgGAL4>ndi1*), relative to matched driver only controls ("+", *esgAL4>+*). (*p<0.05, t test, 5 replicates per condition, 15 flies per replicate).

(C) Transcript levels of multiple downstream targets of FOXO, *4E-BP*, *InR*, *l(2)efl*, and *ImpL2* are significantly decreased in mated female flies 10 days post eclosion that express *ndi1* under the control of the *esgGAL4* driver ("*ndi1*", *esgGAL4>ndi1*) relative to matched driver only controls ("+", *esgGAL4>+*). (**p<0.01, t test, 5 replicates per condition, 5 flies per replicate).

(D-E) Western blot (D, Figure S4B) and densitometric analysis (E) of AKT phosphorylation at Ser505 or Thr423, normalized to total AKT, do not show a significant difference in AKT phosphorylation of either residue in mated female flies that express *ndi1* under the control of the *esgGAL4* driver ("*ndi1*", *esgGAL4>ndi1*), relative to matched driver only controls ("+", *esgGAL4>+*) at 10 days post eclosion. Total AKT levels, relative to a loading control (beta-Actin) are similarly unchanged. (n.s., t test, 5 replicates per condition, 5 flies per replicate).

(F) Transcript levels of *dilp2*, *dilp3*, and *dilp5* from heads of mated female flies 10 days post eclosion that express *ndi1* under the control of the *esgGAL4* driver ("*ndi1*", *esgGAL4>ndi1*) are significantly lower than those from heads of matched driver only controls ("+", *esgGAL4>+*). (*p<0.05, **p<0.01, ***p<0.001, t test, 5 replicates per condition, 30 heads per replicate).

(G-H) Immunofluorescence staining (G) and fluorescence analysis (H) of dissected brains from mated female flies 10 days post eclosion that express *ndi1* under the control of the *esgGAL4* driver ("*ndi1*", *esgGAL4>ndi1*) show significantly lower DILP2 fluorescence in insulin producing cells (IPCs) compared those of matched driver only controls ("+", *esgGAL4>+*). (*p<0.05, t test, at least 170 IPCs from 12 different brains).

(I-J) Transcript levels of *sNPF* (I) and its cognate receptor, *sNPFR1* (J) from heads of mated female flies 10 days post eclosion that express *ndi1* under the control of the *esgGAL4* driver ("*ndi1*", *esgGAL4>ndi1*) are significantly lower than those from heads of matched driver only controls ("+", *esgGAL4*>+). (*p<0.05, **p<0.01, t test, 4-5 replicates per condition, 30 heads per replicate).

See also Figure S4

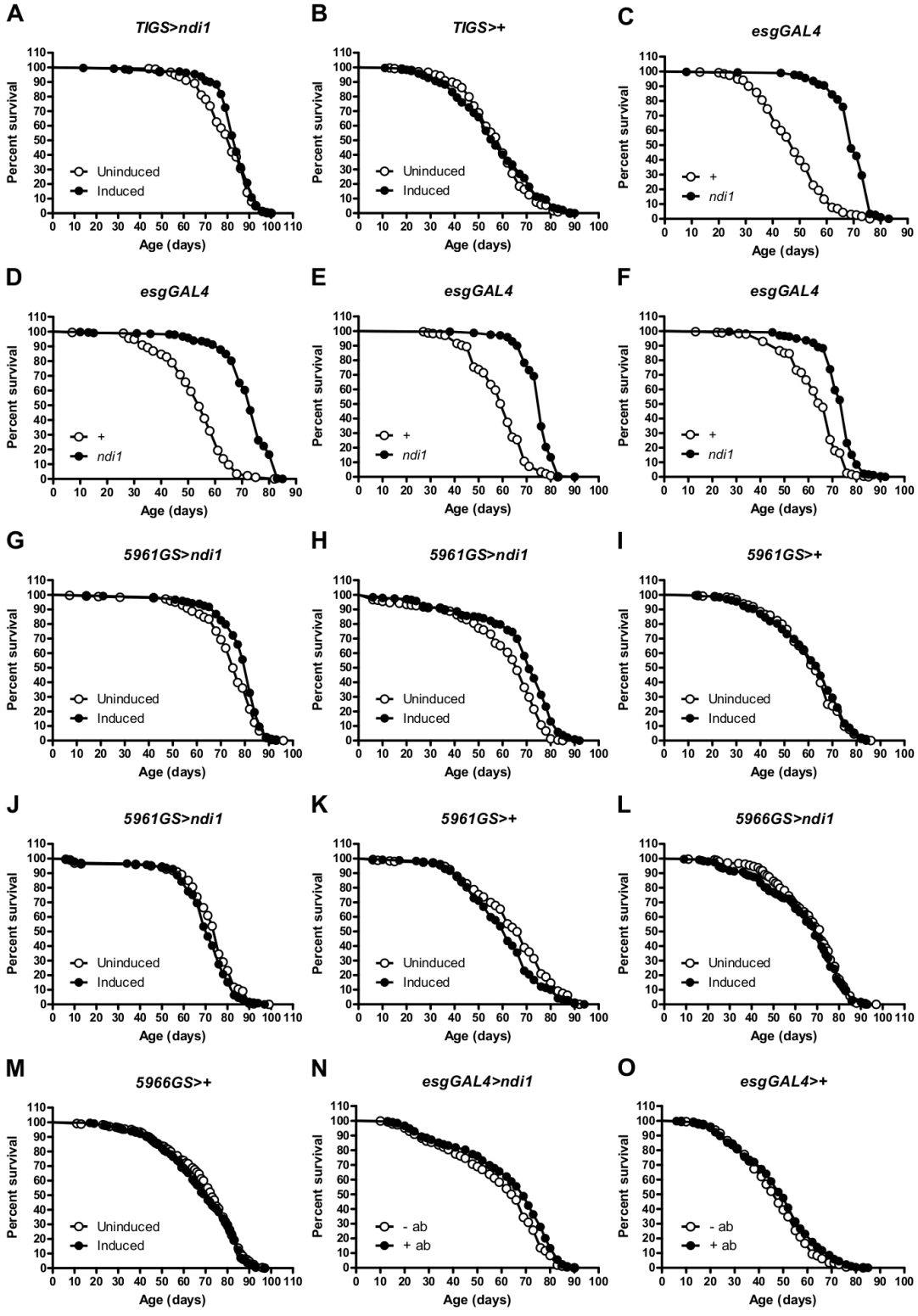
A
TIGS>ndi1
B
TIGS>+
C
esgGAL4
D
esgGAL4
E
esgGAL4
F
esgGAL4
G
5961GS>ndi1
H
5961GS>ndi1
I
5961GS>+
J
5961GS>ndi1
K
5961GS>+
L
5966GS>ndi1
M
5966GS>+
N
esgGAL4>ndi1
O
esgGAL4>+
Percent survival
Age (days)
Uninduced
Induced
+
ndi1
- ab
+ ab

Figure S3-1. Replicate lifespans of tissue specific *ndi1* expression. Related to Figure 3-1.

(A) Induction of *ndi1* in guts of mated female flies throughout their life using the *TIGS-2* driver (*TIGS>ndi1*) in conjunction with RU486 ("Induced", 10mg/l during larval stages, 50mg/l during adulthood) is sufficient to increase lifespan relative to isogenic controls provided non-RU486 medium ("Uninduced", carrier ethanol only). ($p<0.001$, logrank test, 4.2% increase in mean, approximately 240 flies per condition).

(B) The presence of the inducing drug RU486 (same conditions as Figure 1B and S1A) in media of mated female *TIGS-2* driver only controls (*TIGS>+*) does not extend lifespan. (n.s., logrank test, approximately 240 flies per condition).

(C-D) Expression of *ndi1* using a constitutive driver for ISCs/EBs, *esgGAL4* ("*ndi1*", *esgGAL4>ndi1*), is sufficient to increase lifespan in mated female flies relative to driver only controls ("+", *esgGAL4>+*). ($p<0.001$, logrank test, 46% (C) and 35% (D) increase in mean, at least 170 flies per condition).

(E-F) Expression of *ndi1* using a constitutive driver for ISCs/EBs, *esgGAL4* ("*ndi1*", *esgGAL4>ndi1*), is sufficient to increase lifespan in mated male flies relative to driver only controls ("+", *esgGAL4>+*). ($p<0.001$, logrank test, 27% (E) and 16% (F) increase in mean, approximately 240 flies per condition).

(G-H) Adulthood only induction of *ndi1* in mated female flies using an ISC/EB specific geneswitch driver, *5961GS* (*5961GS>ndi1*) in conjunction with RU486 ("Induced", 0.5mg/l) is sufficient to increase lifespan relative to isogenic controls provided non-RU486 medium ("Uninduced", carrier ethanol only). ($p<0.001$, logrank test, 5.6% (G) and 10.5% (H) increase in mean, approximately 240 flies per condition).

(I) The presence of RU486 (same conditions as Figure S1G and S1H) in media of mated female *5961GS* driver only control flies (*5961GS>+*) does not alter lifespan. (n.s., logrank test, approximately 240 flies per condition).

(J) Adulthood only induction of *ndi1* in mated male flies using an ISC/EB specific geneswitch driver, *5961GS* (*5961GS>ndi1*) in conjunction with RU486 ("Induced", 0.5mg/l) results in a mild decrease in lifespan relative to isogenic controls provided non-RU486 medium ("Uninduced", carrier ethanol only). ($p<0.01$, logrank test, 2% decrease in mean, approximately 240 flies per condition).

(K) The presence of RU486 (same conditions as Figure S1J) in media of mated male *5961GS* driver only control flies (*5961GS>+*) decreases lifespan. ($p<0.01$, logrank test, 6% decrease in mean, approximately 240 flies per condition).

(L) Adulthood only induction of *ndi1* in mated female flies using a geneswitch driver for EBs and ECs, *5966GS* (*5966GS>ndi1*) in conjunction with RU486 ("Induced", 0.5mg/l) did not increase lifespan relative to isogenic controls provided non-RU486 medium ("Uninduced", carrier ethanol only). (n.s., logrank test, approximately 240 flies per condition).

(M) The presence of RU486 in (same conditions as Figure S1L) in media of mated female *5966GS* driver only control flies (*5966GS>+*) does not alter lifespan. (n.s., logrank test, approximately 240 flies per condition).

(N) Supplementation of antibiotics in the medium ("+ ab") of mated female flies expressing *ndi1* in ISCs/EBs (*esgGAL4>ndi1*) from day 10 of adulthood results in a further increase in lifespan relative to isogenic controls not provided with antibiotics ("-ab"). ($p<0.001$, logrank test, 6.3% increase in mean).

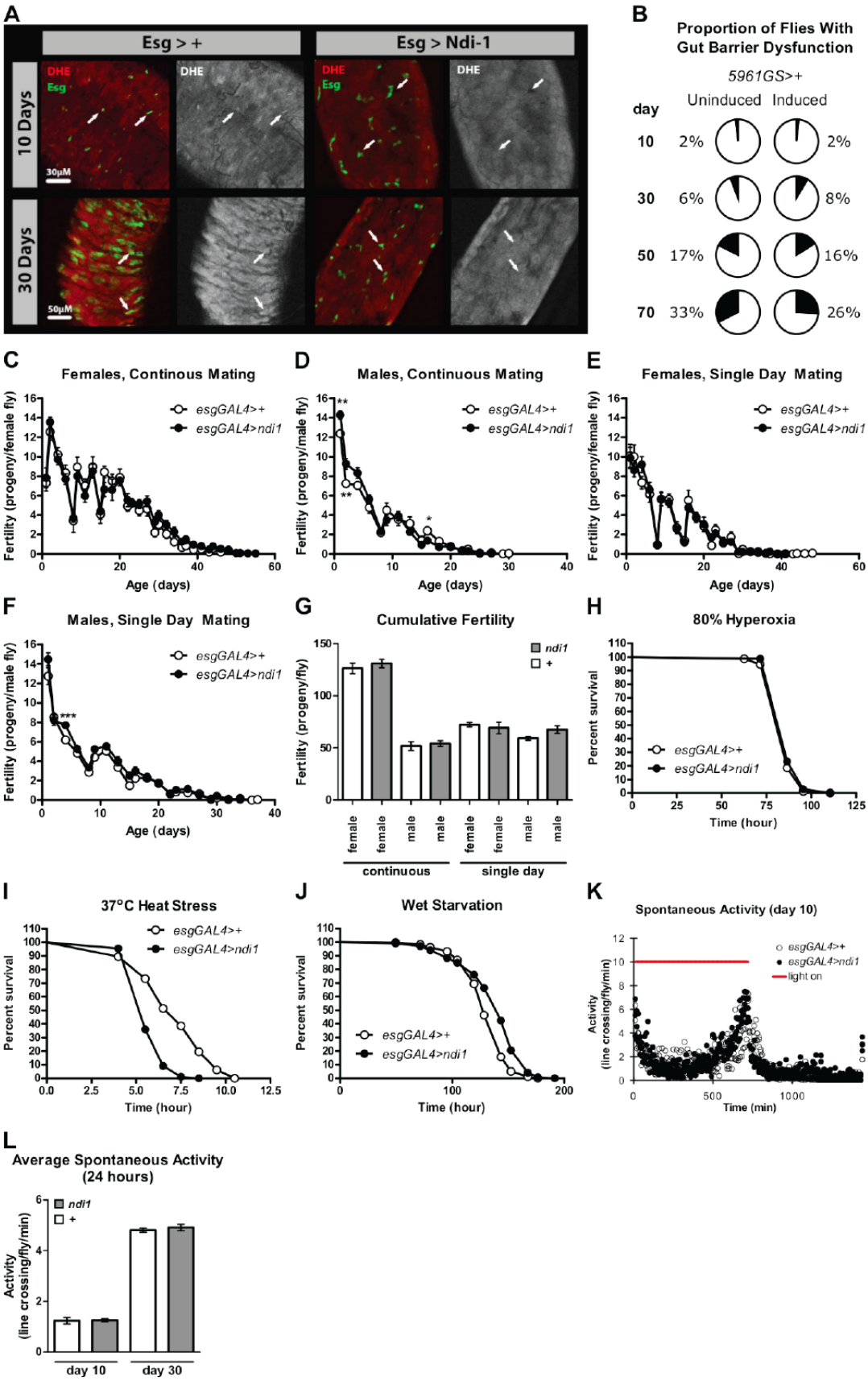
A
Esg > +
Esg > Ndi-1
10 Days
30 Days
DHE
Esg
30μM
50μM
B
Proportion of Flies With
Gut Barrier Dysfunction
5961GS>+
Uninduced Induced
day
10 2% 2%
30 6% 8%
50 17% 16%
70 33% 26%
C
Females, Continous Mating
Fertility (progeny/female fly)
Age (days)
esgGAL4>+
esgGAL4>ndi1
D
Males, Continuous Mating
Fertility (progeny/male fly)
Age (days)
E
Females, Single Day Mating
F
Males, Single Day Mating
G
Cumulative Fertility
Fertility (progeny/fly)
ndi1
+
female female male male female female male male
continuous
single day
H
80% Hyperoxia
Percent survival
Time (hour)
I
37°C Heat Stress
J
Wet Starvation
K
Spontaneous Activity (day 10)
Activity
(line crossing/fly/min)
Time (min)
light on
L
Average Spontaneous Activity
(24 hours)
day 10
day 30

Figure S3-2. Gut barrier dysfunction is not altered by RU486, and *ndi1* expression does not alter activity or fertility, but affects susceptibility to some stresses. Related to Figure 3-2.

(A) Representative single confocal section images of DHE stained midguts (200–500 μm anterior to the pylorus) of *esgGAL4>ndi1* flies and driver only controls (*esgGAL4*>+), 10 and 30 days post eclosion, show age associated changes in ROS levels. (arrows=esg^+ cells).

(B) Mated female *5961GS* driver only control flies (*5961GS*>+) do not show significant differences in ability to sequester GI luminal contents regardless of RU486 presence at all time points (same conditions as Figure 2G). (n.s., binomial test, at least 120 flies per condition).

(C-D) Neither continuously mated female (B) nor male (C) flies that express *ndi1* under the control of the *esgGAL4* driver (*esgGAL4>ndi1*) show consistent and significant differences in timing of reproductive output, compared to matched driver only controls (*esgGAL4*>+). (**p<0.01, *p<0.05, t test, 7-8 replicates per condition, 10 male and 10 female flies per replicate).

(E-F) After mating for a single day, neither female (D) nor male (E) flies that express *ndi1* under the control of the *esgGAL4* driver (*esgGAL4>ndi1*) show consistent and significant differences in timing of reproductive output, compared to matched driver only controls (*esgGAL4*>+). (***p<0.001, t test, 7-8 replicates per condition, 10 female flies that were mated to 10 male flies per replicate).

(G) Total lifetime reproductive output of flies (as profiled in Figure S2C-F) that express *ndi1* under the control of the *esgGAL4* driver ("*ndi1*", *esgGAL4>ndi1*) do not differ significantly, relative to matched driver only controls ("+", *esgGAL4*>+). (n.s., t test, 7-8 replicates per condition, as described in Figure S2C-F).

(H) Survival under hyperoxic conditions (80% O_2) is not altered by an appreciable extent in mated female flies 10 days post eclosion that express *ndi1* under the control of the *esgGAL4*

driver (*esgGAL4>ndi1*), relative to matched driver only controls (*esgGAL4*>+). ($p<0.05$, logrank test, 1.6% increase in mean, approximately 240 flies per condition).

(I) Mated female flies 10 days post eclosion that express *ndi1* under the control of the *esgGAL4* driver (*esgGAL4>ndi1*) are more sensitive to elevated temperatures (37°C) relative to matched driver only controls (*esgGAL4*>+). ($p<0.001$, logrank test, 18% decrease in mean, approximately 180 flies per condition).

(J) Mated female flies 10 days post eclosion that express *ndi1* under the control of the *esgGAL4* driver (*esgGAL4>ndi1*) survive longer under water-only starvation conditions relative to matched driver only controls (*esgGAL4*>+). ($p<0.001$, logrank test, 6% increase in mean, approximately 240 flies per condition).

(K) Mated female flies 10 days post eclosion that express *ndi1* under the control of the *esgGAL4* driver (*esgGAL4>ndi1*) have similar spontaneous activity profiles to matched driver only controls (*esgGAL4*>+). (3 replicates per condition, approximately 30 flies per replicate).

(L) Average spontaneous activities, measured over a 24 hour period, do not show significant differences between mated female flies that express *ndi1* under the control of the *esgGAL4* driver ("*ndi1*", *esgGAL4>ndi1*) and matched driver only controls ("+", *esgGAL4*>+) at 10 and 30 days post eclosion. (n.s., t test, 3 replicates per condition, approximately 30 flies per replicate).

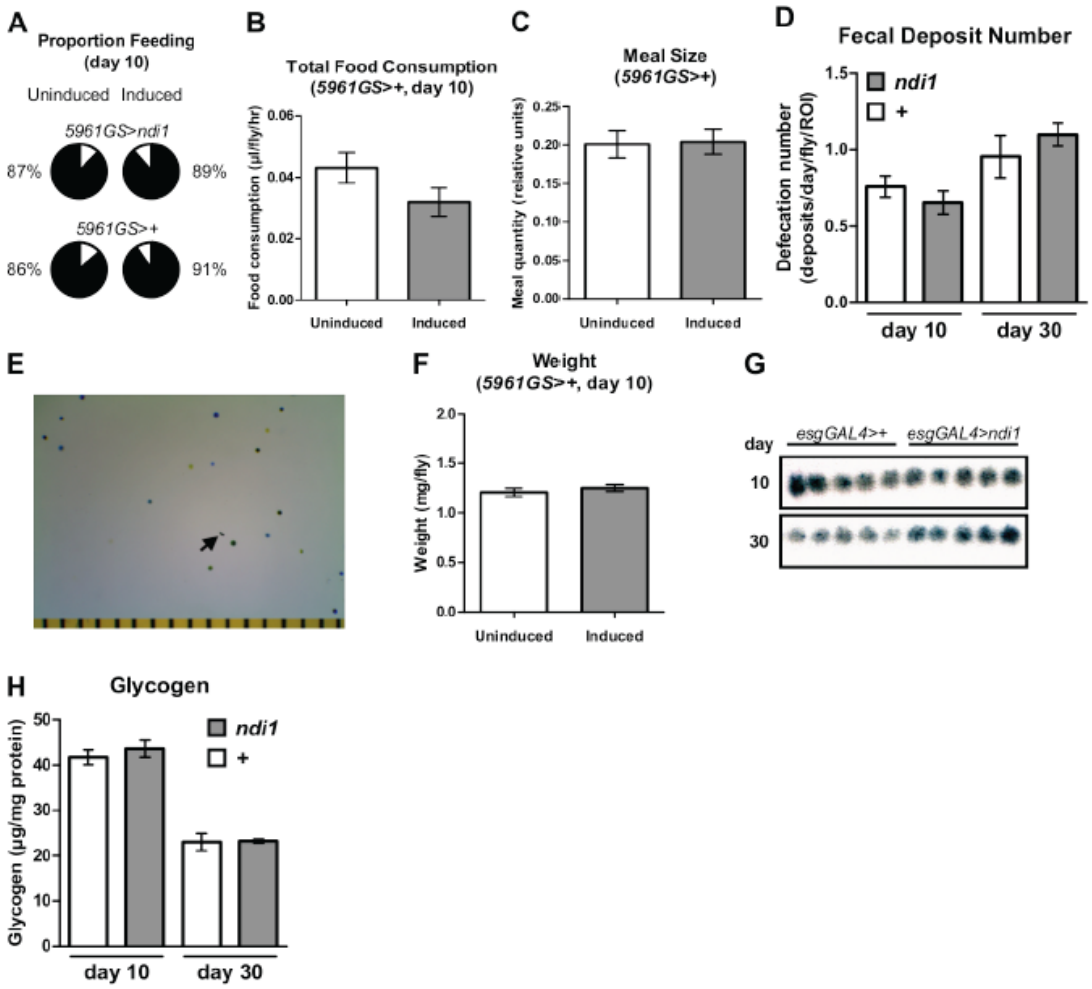

Figure S3-3. Feeding behavior and weight are not affected by RU486, and *ndi1* expression does not alter fecal deposit number or glycogen content. Related to Figure 3-3.

(A) A dye-tracking assay at 10 days post eclosion shows that feeding frequencies do not differ significantly between mated female flies with adulthood only induced expression of *ndi1* under the control of the *5961GS* driver ("*5961GS>ndi1* Induced", 0.5mg/l) and uninduced matched isogenic controls ("*5961GS>ndi1* Uninduced", carrier ethanol only). The presence of RU486 does not affect feeding frequency in matched driver only control flies ("*5961GS*>+ Induced" and "*5961GS*>+ Uninduced"). (n.s., binomial test, 96 flies per condition).

(B) Mated female *5961GS* driver only control flies (*5961GS*>+) 10 days post eclosion do not show significant differences in total feeding, as measured by CAFE assay, regardless of RU486 presence (same conditions as Figure 3D). (n.s., t test, 6 replicates per condition, 10 flies per replicate).

(C) Meal sizes of *5961GS* driver only control flies (*5961GS*>+) that fed during the assay period in (A) do not show significant differences, regardless of RU486 presence. (n.s., t test, approximately 85 flies that ate during the assay period in (A)).

(D) *ndi1* expression under the control of the *esgGAL4* driver in mated female flies ("*ndi1*", *esgGAL4>ndi1*) does not alter total number of fecal deposits per fly relative to matched driver only controls ("+", *esgGAL4*>+). (n.s., t test, 9-10 replicates per condition, 10 flies per replicate).

(E) Sample image of fecal deposits from flies cultured on BPB medium, used for fecal deposit number (Figure S3D), shape (Figure 3F), and pH analysis (Figure 3G). (Tick marks=1mm, arrow=ROD).

(F) Weights of mated female *5961GS* driver only control flies (*5961GS*>+) 10 days post eclosion do not show significant differences, regardless of RU486 presence (same conditions as Figure 3I). (n.s., t test, 6 replicates per condition, 10 flies per replicate).

(G) Thin layer chromatography of mated female flies that express *ndi1* under the control of the *esgGAL4* driver (*esgGAL4>ndi1*) and matched driver only controls (*esgGAL4*>+) used for densitometric quantification (Figure 3K). (5 flies per lane).

(H) Glycogen content is not altered in mated female flies that express *ndi1* under the control of *esgGAL4* driver ("*ndi1*", *esgGAL4>ndi1*) relative to matched driver only controls ("+", *esgGAL4*>+) 10 and 30 days post eclosion. (n.s., t test, 5 replicates per condition, 5 decapitated flies per replicate).

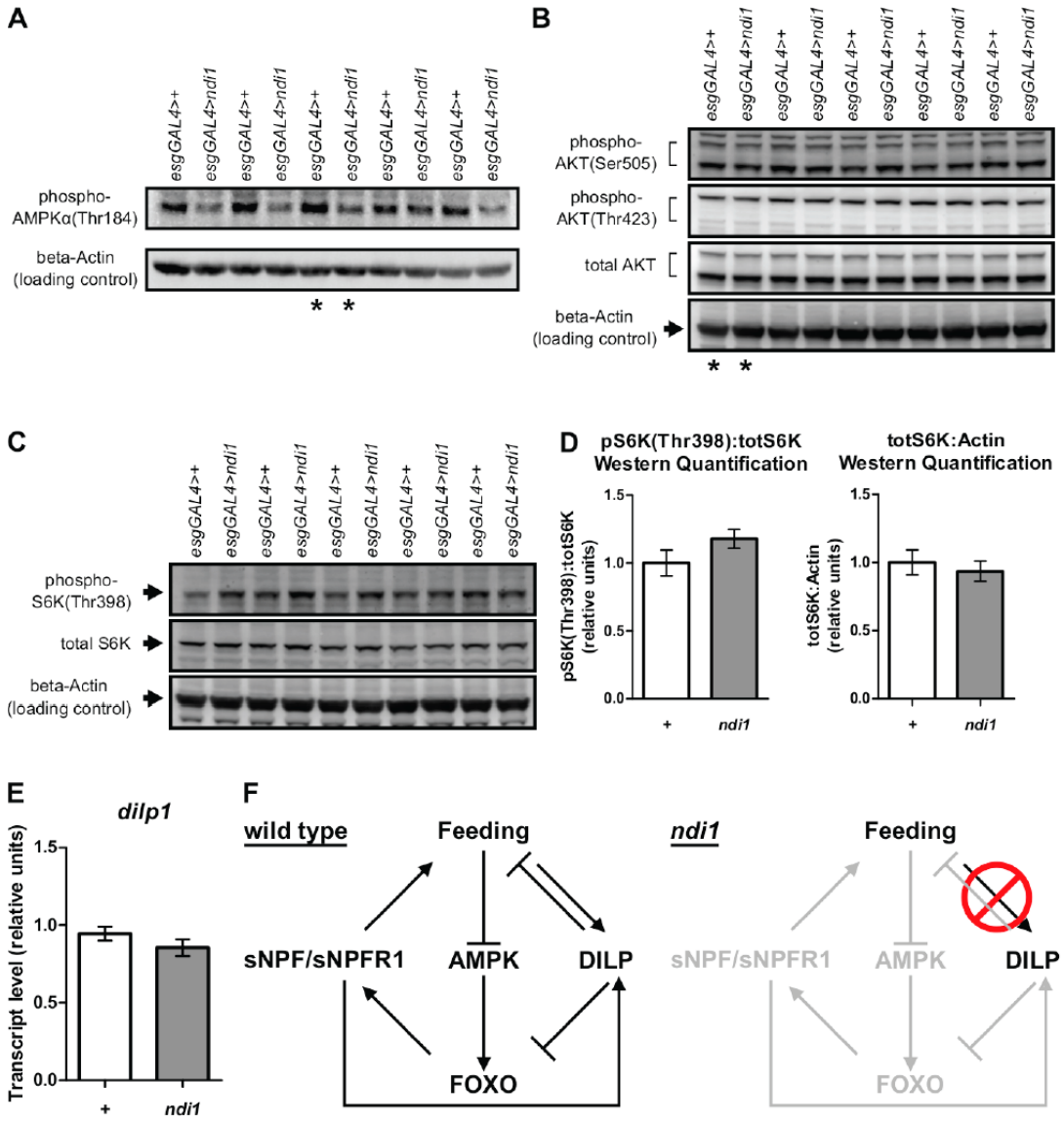

Figure S3-4. Western blots of *ndi1* expressing flies, transcript level of a control *dilp* that is not expressed in adult IPCs, and a model for overfeeding. Related to Figure 3-4.

(A) Phosphoryated AMPKa (Thr184) and beta-Actin Western blot of mated female flies 10 days post eclosion that express *ndi1* under the control of the *esgGAL4* driver (*esgGAL4>ndi1*) and matched driver only controls (*esgGAL4*>+) used for densitometric analysis (Figure 4B) and representative images (lanes marked *, Figure 4A) . (15 flies per lane).

(B) Phosphorylated AKT(Ser505), phosphorylated AKT(Thr423), total AKT, and beta-Actin Western blot of mated female flies 10 days post eclosion that express *ndi1* under the control of the *esgGAL4* driver (*esgGAL4>ndi1*) and matched driver only controls (*esgGAL4*>+) used for densitometric analysis (Figure 4D) and representative images (lanes marked *, Figure 4C). (5 flies per lane).

(C) Phosphorylated S6K(Thr398), total S6K, and beta-Actin Western blot of mated female flies 10 days post eclosion that express ndi1 under the control of the *esgGAL4* driver (*esgGAL4>ndi1*) and matched driver only controls (*esgGAL4*>+) used for densitometric analysis (Figure S4D). (5 flies per lane).

(D) Densitometric analysis of S6K phosphorylation at Thr398, normalized to total S6K does not show a significant difference in S6K phosphorylation in mated female flies that express *ndi1* under the control of the *esgGAL4* driver ("*ndi1*", *esgGAL4>ndi1*), relative to matched driver only controls ("+", *esgGAL4*>+) at 10 days post eclosion. Total S6K levels, relative to a loading control (beta-Actin) are similarly unchanged. (n.s., t test, 5 replicates per condition, 5 flies per replicate).

(E) Transcript level of *dilp1* from heads of mated female flies 10 days post eclosion that express *ndi1* under the control of the *esgGAL4* driver ("*ndi1*", *esgGAL4>ndi1*) are similar to those from heads of matched driver only controls ("+", *esgGAL4*>+). (n.s., t test, 5 replicates per condition, 30 heads per replicate).

(F) A model for the feeding behavior exhibited by control and *ndi1* expressing flies in this study. In control flies ("wild type"), feeding both inhibits AMPK to reduce FOXO activation, and triggers DILP release to inhibit feeding and FOXO activity, with the end result of active FOXO inhibition and suppression of sNPF/sNPFR1 pro-feeding signaling. In flies with ISC/EB *ndi1* expression ("*ndi1*"), feeding induces proper AMPK inhibition but fails to increase DILP release to actively inhibit feeding. Without suppression of feeding by DILPs, flies remain in a permissive state for feeding and eat more, even with reduced stimulation of feeding by sNPF/sNPFR1 signaling.

References

1. Jones, D.L. and T.A. Rando, *Emerging models and paradigms for stem cell ageing.* Nat Cell Biol, 2011. **13**(5): p. 506-12.
2. Green, D.R., L. Galluzzi, and G. Kroemer, *Mitochondria and the autophagy-inflammation-cell death axis in organismal aging.* Science, 2011. **333**(6046): p. 1109-12.
3. Guarente, L., *Mitochondria--a nexus for aging, calorie restriction, and sirtuins?* Cell, 2008. **132**(2): p. 171-6.
4. Jasper, H. and D.L. Jones, *Metabolic regulation of stem cell behavior and implications for aging.* Cell Metab, 2010. **12**(6): p. 561-5.
5. Piper, M.D. and A. Bartke, *Diet and aging.* Cell Metab, 2008. **8**(2): p. 99-104.
6. Kenyon, C.J., *The genetics of ageing.* Nature, 2010. **464**(7288): p. 504-12.
7. Fontana, L., L. Partridge, and V.D. Longo, *Extending healthy life span--from yeast to humans.* Science, 2010. **328**(5976): p. 321-6.
8. Alic, N. and L. Partridge, *Death and dessert: nutrient signalling pathways and ageing.* Curr Opin Cell Biol, 2011. **23**(6): p. 738-43.
9. Marchiando, A.M., W.V. Graham, and J.R. Turner, *Epithelial barriers in homeostasis and disease.* Annu Rev Pathol, 2010. **5**: p. 119-44.
10. Micchelli, C.A. and N. Perrimon, *Evidence that stem cells reside in the adult Drosophila midgut epithelium.* Nature, 2006. **439**(7075): p. 475-9.
11. Ohlstein, B. and A. Spradling, *The adult Drosophila posterior midgut is maintained by pluripotent stem cells.* Nature, 2006. **439**(7075): p. 470-4.
12. Biteau, B., C.E. Hochmuth, and H. Jasper, *JNK activity in somatic stem cells causes loss of tissue homeostasis in the aging Drosophila gut.* Cell Stem Cell, 2008. **3**(4): p. 442-55.
13. Choi, N.H., et al., *Age-related changes in Drosophila midgut are associated with PVF2, a PDGF/VEGF-like growth factor.* Aging Cell, 2008. **7**(3): p. 318-34.

14. Park, J.S., Y.S. Kim, and M.A. Yoo, *The role of p38b MAPK in age-related modulation of intestinal stem cell proliferation and differentiation in Drosophila.* Aging (Albany NY), 2009. **1**(7): p. 637-51.

15. Rera, M., R.I. Clark, and D.W. Walker, *Intestinal barrier dysfunction links metabolic and inflammatory markers of aging to death in Drosophila.* Proc Natl Acad Sci U S A, 2012. **109**(52): p. 21528-33.

16. Rera, M., et al., *Modulation of longevity and tissue homeostasis by the Drosophila PGC-1 homolog.* Cell Metab, 2011. **14**(5): p. 623-34.

17. Lin, J., C. Handschin, and B.M. Spiegelman, *Metabolic control through the PGC-1 family of transcription coactivators.* Cell Metab, 2005. **1**(6): p. 361-70.

18. Bahadorani, S., et al., *Neuronal expression of a single-subunit yeast NADH-ubiquinone oxidoreductase (Ndi1) extends Drosophila lifespan.* Aging Cell, 2010. **9**(2): p. 191-202.

19. Cho, J., et al., *Expression of yeast NDI1 rescues a Drosophila complex I assembly defect.* PLoS One, 2012. **7**(11): p. e50644.

20. Sanz, A., et al., *Expression of the yeast NADH dehydrogenase Ndi1 in Drosophila confers increased lifespan independently of dietary restriction.* Proc Natl Acad Sci U S A, 2010. **107**(20): p. 9105-10.

21. Vilain, S., et al., *The yeast complex I equivalent NADH dehydrogenase rescues pink1 mutants.* PLoS Genet, 2012. **8**(1): p. e1002456.

22. Hardie, D.G., F.A. Ross, and S.A. Hawley, *AMPK: a nutrient and energy sensor that maintains energy homeostasis.* Nat Rev Mol Cell Biol, 2012. **13**(4): p. 251-62.

23. Rera, M., M.J. Azizi, and D.W. Walker, *Organ-specific mediation of lifespan extension: More than a gut feeling?* Ageing Res Rev, 2013. **12**(1): p. 436-44.

24. Poirier, L., et al., *Characterization of the Drosophila gene-switch system in aging studies: a cautionary tale.* Aging Cell, 2008. **7**(5): p. 758-70.

25. Marres, C.A., S. de Vries, and L.A. Grivell, *Isolation and inactivation of the nuclear gene encoding the rotenone-insensitive internal NADH: ubiquinone oxidoreductase of mitochondria from Saccharomyces cerevisiae.* Eur J Biochem, 1991. **195**(3): p. 857-62.

26. de Vries, S. and L.A. Grivell, *Purification and characterization of a rotenone-insensitive NADH:Q6 oxidoreductase from mitochondria of Saccharomyces cerevisiae.* Eur J Biochem, 1988. **176**(2): p. 377-84.

27. Osterwalder, T., et al., *A conditional tissue-specific transgene expression system using inducible GAL4.* Proc Natl Acad Sci U S A, 2001. **98**(22): p. 12596-601.

28. Roman, G., et al., *P[Switch], a system for spatial and temporal control of gene expression in Drosophila melanogaster.* Proc Natl Acad Sci U S A, 2001. **98**(22): p. 12602-7.

29. Biteau, B., et al., *Lifespan extension by preserving proliferative homeostasis in Drosophila.* PLoS Genet, 2010. **6**(10): p. e1001159.

30. Mathur, D., et al., *A transient niche regulates the specification of Drosophila intestinal stem cells.* Science, 2010. **327**(5962): p. 210-3.

31. Biteau, B., C.E. Hochmuth, and H. Jasper, *Maintaining tissue homeostasis: dynamic control of somatic stem cell activity.* Cell Stem Cell, 2011. **9**(5): p. 402-11.

32. Hochmuth, C.E., et al., *Redox regulation by Keap1 and Nrf2 controls intestinal stem cell proliferation in Drosophila.* Cell Stem Cell, 2011. **8**(2): p. 188-99.

33. Owusu-Ansah, E. and U. Banerjee, *Reactive oxygen species prime Drosophila haematopoietic progenitors for differentiation.* Nature, 2009. **461**(7263): p. 537-41.

34. Owusu-Ansah, E., et al., *Distinct mitochondrial retrograde signals control the G1-S cell cycle checkpoint.* Nat Genet, 2008. **40**(3): p. 356-61.

35. Wu, S.C., et al., *Infection-induced intestinal oxidative stress triggers organ-to-organ immunological communication in Drosophila.* Cell Host Microbe, 2012. **11**(4): p. 410-7.

36. Partridge, L., D. Gems, and D.J. Withers, *Sex and death: what is the connection?* Cell, 2005. **120**(4): p. 461-72.

37. Lakowski, B. and S. Hekimi, *The genetics of caloric restriction in Caenorhabditis elegans.* Proc Natl Acad Sci U S A, 1998. **95**(22): p. 13091-6.

38. Demontis, F. and N. Perrimon, *FOXO/4E-BP signaling in Drosophila muscles regulates organism-wide proteostasis during aging.* Cell, 2010. **143**(5): p. 813-25.

39. Ja, W.W., et al., *Prandiology of Drosophila and the CAFE assay.* Proc Natl Acad Sci U S A, 2007. **104**(20): p. 8253-6.

40. Wong, R., et al., *Quantification of food intake in Drosophila.* PLoS One, 2009. **4**(6): p. e6063.

41. Cognigni, P., A.P. Bailey, and I. Miguel-Aliaga, *Enteric neurons and systemic signals couple nutritional and reproductive status with intestinal homeostasis.* Cell Metab, 2011. **13**(1): p. 92-104.

42. Canto, C., et al., *AMPK regulates energy expenditure by modulating NAD+ metabolism and SIRT1 activity.* Nature, 2009. **458**(7241): p. 1056-60.

43. Samuel, V.T. and G.I. Shulman, *Mechanisms for insulin resistance: common threads and missing links.* Cell, 2012. **148**(5): p. 852-71.

44. Broughton, S.J., et al., *Longer lifespan, altered metabolism, and stress resistance in Drosophila from ablation of cells making insulin-like ligands.* Proc Natl Acad Sci U S A, 2005. **102**(8): p. 3105-10.

45. Lee, K.S., et al., *Drosophila short neuropeptide F regulates food intake and body size.* J Biol Chem, 2004. **279**(49): p. 50781-9.

46. Lee, K.S., et al., *Drosophila short neuropeptide F signalling regulates growth by ERK-mediated insulin signalling.* Nat Cell Biol, 2008. **10**(4): p. 468-75.

47. Partridge, L. and D. Gems, *Benchmarks for ageing studies.* Nature, 2007. **450**(7167): p. 165-7.

48. Lombard, D.B., et al., *Ageing: longevity hits a roadblock.* Nature, 2011. **477**(7365): p. 410-1.

49. Hong, S.H., et al., *Minibrain/Dyrk1a regulates food intake through the Sir2-FOXO-sNPF/NPY pathway in Drosophila and mammals.* PLoS Genet, 2012. **8**(8): p. e1002857.

50. Bai, H., P. Kang, and M. Tatar, *Drosophila insulin-like peptide-6 (dilp6) expression from fat body extends lifespan and represses secretion of Drosophila insulin-like peptide-2 from the brain.* Aging Cell, 2012. **11**(6): p. 978-85.

51. Russell, S.J. and C.R. Kahn, *Endocrine regulation of ageing.* Nat Rev Mol Cell Biol, 2007. **8**(9): p. 681-91.

52. Piper, M.D., et al., *Separating cause from effect: how does insulin/IGF signalling control lifespan in worms, flies and mice?* J Intern Med, 2008. **263**(2): p. 179-91.

53. Hwangbo, D.S., et al., *Drosophila dFOXO controls lifespan and regulates insulin signalling in brain and fat body.* Nature, 2004. **429**(6991): p. 562-6.

54. Giannakou, M.E., et al., *Long-lived Drosophila with overexpressed dFOXO in adult fat body.* Science, 2004. **305**(5682): p. 361.

55. Johnson, A.M. and J.M. Olefsky, *The origins and drivers of insulin resistance.* Cell, 2013. **152**(4): p. 673-84.

56. Dionne, M.S., et al., *Akt and FOXO dysregulation contribute to infection-induced wasting in Drosophila.* Curr Biol, 2006. **16**(20): p. 1977-85.

57. Morris, S.N., et al., *Development of diet-induced insulin resistance in adult Drosophila melanogaster.* Biochim Biophys Acta, 2012. **1822**(8): p. 1230-1237.

58. Tatar, M., et al., *A mutant Drosophila insulin receptor homolog that extends life-span and impairs neuroendocrine function.* Science, 2001. **292**(5514): p. 107-10.

59. Clancy, D.J., et al., *Extension of life-span by loss of CHICO, a Drosophila insulin receptor substrate protein.* Science, 2001. **292**(5514): p. 104-6.

60. Wang, M.C., D. Bohmann, and H. Jasper, *JNK extends life span and limits growth by antagonizing cellular and organism-wide responses to insulin signaling.* Cell, 2005. **121**(1): p. 115-25.

61. Gronke, S., et al., *Molecular evolution and functional characterization of Drosophila insulin-like peptides.* PLoS Genet, 2010. **6**(2): p. e1000857.

62. Seo, B.B., et al., *Use of the NADH-quinone oxidoreductase (NDI1) gene of Saccharomyces cerevisiae as a possible cure for complex I defects in human cells.* J Biol Chem, 2000. **275**(48): p. 37774-8.

63. Seo, B.B., et al., *Molecular remedy of complex I defects: rotenone-insensitive internal NADH-quinone oxidoreductase of Saccharomyces cerevisiae mitochondria restores the NADH oxidase activity of complex I-deficient mammalian cells.* Proc Natl Acad Sci U S A, 1998. **95**(16): p. 9167-71.

64. Santidrian, A.F., et al., *Mitochondrial complex I activity and NAD+/NADH balance regulate breast cancer progression.* J Clin Invest, 2013. **123**(3): p. 1068-81.

65. Marella, M., et al., *No immune responses by the expression of the yeast Ndi1 protein in rats.* PLoS One, 2011. **6**(10): p. e25910.

Chapter 4: Pink1 and Parkin regulate *Drosophila* intestinal stem cell proliferation during stress and aging.

Christopher L. Koehler, Guy A. Perkins, Mark H. Ellisman, and D. Leanne Jones

Abstract

Similar to the mammalian intestine, intestinal stem cells (ISCs) maintain the midgut epithelium in *Drosophila*. Proper cellular turnover and tissue function rely on tightly regulated rates of ISC division and appropriate differentiation of daughter cells. However, aging and epithelial injury cause elevated ISC proliferation and decreased capacity for terminal differentiation of daughter enteroblasts (EBs). The exact mechanisms causing functional decline of stem cells with age remain elusive; however, recent findings indicate stem cell metabolism may play an important role in the regulation of stem cell activity. The homeostasis and quality of a mitochondrial network is, in part, regulated by the fission, fusion, and movement of mitochondria within the network, cumulatively referred to as mitochondrial dynamics. Here, we investigate how alterations in the mitochondrial network regulate stem cell behavior *in vivo* via RNAi-mediated knockdown of factors involved in mitochondrial dynamics. ISC/EB-specific knockdown of the mitophagy-related genes Pink1 or Parkin suppresses the age-related loss of tissue homeostasis, despite dramatic changes in mitochondrial ultrastructure and mitochondrial damage in ISC/EBs. Furthermore, progenitor specific depletion of Pink1 or Parkin limits age and stress associated proliferation of ISCs, possibly through induction of ISC senescence. Our results indicate an uncoupling of cellular, tissue, and organismal aging through inhibition of ISC proliferation and provide insight into strategies employed by stem cells to maintain tissue homeostasis despite severe damage to organelles.

Introduction

Tissue homeostasis in many adult metazoans is maintained via the activity of resident somatic stem cells. Through asymmetric, mitotic divisions, adult stem cells can self-renew to maintain the stem cell population and, simultaneously, give rise to daughter cells that can differentiate along a given lineage to replace lost or damaged cells. The long-term regenerative capacity of a tissue, therefore, relies heavily on the careful balance between stem cell self-renewal and the initiation of differentiation. Deregulation of stem cell function can lead to altered organ function that is detrimental to overall organismal health and lifespan [1].

Intestinal stem cells (ISCs) maintain the midgut epithelium in *Drosophila*, in a manner similar to their mammalian counterparts. Genetic tractability, a simple cell lineage, and conserved pathways that regulate ISC behavior combine to make the *Drosophila* midgut epithelium a powerful model system for the study of stem cell regulation and tissue homeostasis. Regional differences exist along the length of the midgut, although ISCs are involved in maintaining homeostasis throughout [2, 3]. The ISCs of the posterior midgut reside adjacent to the basement membrane and undergo asymmetric division in order to maintain turnover of differentiated epithelial cells [4, 5] or symmetric division to increase ISC numbers in response to nutritional cues [6]. Asymmetric ISC division leads to generation of a new stem cell and a daughter cell, called an enteroblast (EB). Delta/Notch signaling between the ISC/EB dictates whether an EB will differentiate into an absorptive enterocyte (EC) or a secretory enteroendocrine (EE) cell [7-10], though data have indicated that EEs can also derive directly from ISCs [11-13].

Under normal, homeostatic conditions, the *Drosophila* midgut epithelium undergoes slow turnover [4, 5], yet ISCs respond to a number of intrinsic and extrinsic stimuli that regulate proliferation [14-25]. Importantly, ISC proliferation rates increase

significantly in response to chemical induced damage or pathogenic bacterial infection. While adaptive ISC divisions can maintain tissue homeostasis through the replenishment of lost or damaged cells, uncontrolled ISC division and altered differentiation programs can lead to loss of tissue function.

In the *Drosophila* midgut, aging results in the consistent manifestation of several ISC-related phenotypes, including an increase in ISC proliferation and a block in terminal differentiation of ISC progeny, as reflected by the accumulation of polyploid cells that express the ISC/EB marker Escargot (Esg). Consequently, this leads to alterations in localization of cell-cell junctional complexes, loss of the typical apical-basal organization of the epithelial monolayer, and a decline in intestinal barrier function.

The ISCs are relatively long-lived cells with very few mitochondria (Fig 4-1A-C). Throughout the lifetime of a fly, the ISC must give rise to numerous differentiated cells, which require extensive mitochondrial biogenesis to expand the mitochondrial mass in order to cope with increased energy demands. We recently demonstrated that ISC/EB-specific overexpression of *spargel (srl*), the *Drosophila* homologue of *PGC1α* – a master regulator of mitochondrial biogenesis, delays age-related changes to ISCs and the loss of intestinal homeostasis, leading to a dramatic increase in lifespan in both sexes [26]. This suggested that stem cell metabolism is important in the regulation of ISC behavior, midgut homeostasis, and longevity; however, little is known about the role of mitochondrial quality control plays in regulating stem cell function under homeostatic conditions, in response to damage, and with age.

In order to avoid passage of damaged mitochondria or mtDNA mutations to differentiating daughter cells, we hypothesized ISCs would have a stringent mechanism for the removal of damaged mitochondria. Isolation and degradation of damaged mitochondria via selective autophagy (mitophagy) relies largely on two genes associated with autosomal recessive juvenile parkinsonism (AR-JP): *parkin*, an E3 ubiquitin ligase

and *pink1*, phosphatase and tensin homolog-induced putative kinase 1, a mitochondria-targeted serine/threonine kinase. In *Drosophila*, both *pink1* and *parkin* mutants exhibit male sterility, loss of normal mitochondrial morphology, and muscle degeneration [27, 28]. Pink1 acts upstream of Parkin and is stabilized on the outer mitochondrial membrane (OMM) with collapsed membrane potentials (depolarized mitochondria). Stabilization of Pink1 on the OMM leads to the recruitment of Parkin which, in turn, ubiquitinates a number of proteins on the OMM. Ubiquitinated proteins can be recognized by Ref(2)P, the *Drosophila* homolog of p62. Acting as an adaptor, Ref(2)P links the ubiquitinated cargo to the lipidated form of Atg8 (the *Drosophila* homolog of LC3) on a phagophore, ultimately leading to mitophagic degradation [29-32]. However, mitochondrial quality control is also achieved through constant remodeling of the mitochondrial network through fission and fusion [33-37] reviewed in [38, 39]. To determine what mechanisms could be utilized by ISCs to maintain a healthy pool of mitochondria, we conducted an RNAi screen to deplete factors required for mitochondrial dynamics and examined the effects on the mitochondria, stem cell function, tissue homeostasis, and longevity. This approach revealed that depletion of Pink1 and Parkin in ISCs results in changes in ISC behavior, consistent with the onset of senescence.

Results and Discussion

ISC/EB-specific knockdown of Pink1 or Parkin alters mitochondrial morphology and density

In order to determine whether genes involved in mitochondrial dynamics (fission, fusion, movement, turnover) play a role in ISC function, we used the ISC/EB-specific, RU486-inducible 5961-Gal4^{GeneSwitch} (5961^{GS}) "driver" to direct expression of a number of *UAS*-RNAi lines in ISC/EBs in the adult midgut (Supp Table 4-1). Overexpression of *srl*

lead to a decrease in intestinal dysplasia, as previously reported (Rera et al., 2011). However, in contrast to our expectations, RNAi-mediated depletion of Pink1 or Parkin (two mitophagy-related gene products) resulted in drastic improvement in intestinal homeostasis in aged flies (Supp Table 4-1). Manipulation of other factors tested had no effect on the ISC maintenance or tissue homeostasus during the time points assayed (10, 30, and 50 days post-eclosion) (Supp Table 4-1).

Mutations in the mitochondrial-associated proteins Pink1 and Parkin are among the causative factors in familial forms of Parkinson's disease (PD) (reviewed in [40]. In *Drosophila*, loss of function mutations in *pink1* or *parkin* result in a number of mitochondrial phenotypes, including defects in mitochondrial function and cristae morphology [28]. To determine if RNAi-mediated depletion of Pink1 or Parkin showed similar mitochondrial phenotypes in ISCs, we used transmission electron microscopy (TEM) to examine ISCs in posterior midguts from young (Day 10) versus old (Day 55) flies (Fig 4-1A-F). In young flies, $pink1^{RNAi}$ and $parkin^{RNAi}$ caused altered cristae structure and increased electron density in the mitochondrial matrix (Fig 4-1A'-C'). In aged, ISC controls, the mitochondria have a slightly varied morphology (Fig 4-1D'); however, knockdown of Pink1 or Parkin in aged samples resulted in swollen mitochondria with altered cristae shape, accumulation of multilamellar bodies, and the appearance of electron-dense granules (Fig 4-1E'-F'). Importantly, the alterations in mitochondrial morphology were restricted to the ISCs, as mitochondria in adjacent ECs exhibited wild type morphology (Supp Fig 4-1A-B). Furthermore, knockdown of Pink1 or Parkin in the ECs via the $5966\text{-}Gal4^{GS}$ driver did not cause a decrease in age-associated phenotypes in the midgut (Supp Fig 4-1C-F); this indicates that the observed phenotype is not due to perdurance of the RNAi into the progeny of the ISC/EBs.

A number of studies have demonstrated a relationship between mitochondrial ultrastructure and energetic state of the mitochondria [41, 42]. Specifically, mitochondria

tend to exist in two major forms *in vivo*: orthodox and condensed. Larger matrix volumes and inner boundary membranes that are closely opposed to the outer mitochondrial membrane are characteristics of orthodox mitochondria, which correlate with low respiratory activity. Conversely, in periods of high respiratory activity, a mitochondrion can adopt the condensed configuration, in which the matrix volume is drastically decreased and the cristae become enlarged and often irregular with expanded cristae junctions [42]. We conducted detailed, 3-dimensional electron tomographic reconstructions to ascertain whether the observed changes in mitochondrial morphology upon knockdown of Pink1 or Parkin represented an orthodox to condensed transition (Fig 4-1G-J'). In unperturbed ISCs, the mitochondria tended to adopt an orthodox morphology, indicating that mitochondria of normal ISCs had low respiratory output (Fig 4-1G-G'). Conversely, many mitochondria within the Pink1 or Parkin depleted progenitor cells adopted an ultracondensed structure with enlarged intracristal space accompanied by reduced matrix volume (Fig 4-1H-J'). This indicates that reduction of the mitophagy-associated proteins Pink1 or Parkin in ISC/EBs causes changes in mitochondria associated with higher respiratory output.

Proper function of Pink1 and Parkin are essential for the efficient elimination of damaged mitochondria via mitophagy; therefore, in addition to altered mitochondrial substructure, loss of Pink1 or Parkin function could affect mitochondrial abundance and network formation. We examined the effect of Pink1/Parkin depletion on the mitochondrial network of ISC/EBs via STimulated Emission Depletion (STED) microscopy. The mitochondrial networks appeared much more fused upon progenitor-specific depletion of Pink1 or Parkin (Fig 1L-M and O-P), in comparison to controls. Since Pink1/Parkin activity results in Mfn ubiquitination and degradation, the increasingly fused mitochondrial networks may be the result of decreased Mfn turnover. In contrast, aging resulted in the accumulation of more punctate mitochondria in the ISCs of control

flies but not in ISCs depleted of Pink1 or Parkin (Fig 4-1K compared to 4-1N-P, arrows). Collectively, these data demonstrate that progenitor-specific RNAi-mediated depletion of Pink1 or Parkin disrupts normal mitochondrial structure in the ISC/EBs.

Progenitor-specific knockdown of Pink1 or Parkin delays tissue level aging phenotypes in the posterior midgut

Recent reports indicate that changes in metabolism-associated factors such as altered nutrient availability, mitochondrial abundance, or electron transport chain (ETC) function can impact ISC behavior and tissue homeostasis in the *Drosophila* midgut [6, 26, 43, 44]. Given the influence of Pink1 and Parkin on cellular metabolism via their roles in mitophagy, we investigated the effect of progenitor-specific loss of Pink1 or Parkin on tissue homeostasis in the posterior midgut. In order to assay tissue homeostasis, we performed a number of assays for phenotypes that consistently manifest as a consequence of aging in the fly including: increased ISC mitoses ($pHH3^+$ cells), expanded expression of the ISC/EB marker Esg, and loss of the epithelial monolayer.

In order to test whether midgut homeostasis is affected by loss of Pink1 or Parkin in the progenitor cells, we utilized an inducible *esg*-mediated "flip out" (*esg* F/O) system [23] to generate clones in which all ISC/EBs and their progeny express a UAS-RNAi construct of interest, as well UAS-*gfp*. After rearing flies at 18°C, transgene expression was induced 1 to 2 days after eclosion (hatching) by culturing flies at 29°C. Clonal expansion was assayed after 7 or 25 days (Fig 4-2A-C'). Interestingly, while the number of cells per clone is the same across all groups after 7 days of transgene induction (Fig 4-2D, left panel), loss of Pink1 or Parkin significantly reduced the average number of cells per clone after 25 days (Fig 4-2D, right panel). Furthermore, loss of Pink1 or

Parkin resulted in significantly smaller clonal area at 7 and 25 days after clone induction (Fig 4-2E).

As the '*esg* F/O' system is engineered to label the progenitor cells and their progeny, we expected many of the flip out clones to include large, differentiated ECs under normal conditions. Indeed, in the control groups, the average area of each clone increases with time (Fig 4-2E), which included large, polyploid ECs (Fig 4-2A-A'). However, clones expressing either *pink1*^{RNAi} or *parkin*^{RNAi} demonstrated a noticeable lack of ECs even 25 days after clone induction (Fig 4-2B-C'). The lack of differentiated cells and smaller clone sizes could be the result of either a lack of ISC mitotic divisions or induction of cell death upon differentiation in Pink1/Parkin knockdown clones. To test the first possibility, we measured ISC proliferation in guts from '*esg* F/O' flies 7 or 25 days after induction of transgene expression. We found that basal proliferation rates of ISCs in the young, male midgut were low enough as to be undetectable by pHH3 staining in either control (*mCherry*^{RNAi}) or test (*pink1*^{RNAi} or *parkin*^{RNAi}) groups (Fig 4-2F), but an increase in ISC proliferation was detected in guts from older control males. Interestingly, the previously described age-associated increase in ISC mitoses was almost completely abrogated in the Pink1/Parkin knockdowns (Fig 4-2F). These data indicate that the reduced clone size and clone cell numbers observed upon RNAi-mediated knockdown of Pink1 or Parkin are due to reduced ISC proliferation during aging.

The '*esg* F/O' system induces expression of transgenes in the midgut progenitor cells, as well as any resulting progeny; therefore, the effects of Pink1/Parkin loss on ISC behavior could result from cell non-autonomous activity caused by knockdown in differentiated progenitor cells. In order to determine if depletion of Pink1 or Parkin specifically in ISCs or EBs was sufficient to reduce ISC proliferation and gut turnover, we directed expression of *UAS-pink1*^{RNAi} or *UAS-parkin*^{RNAi} to ISCs, EBs, or both cell types.

Using an *esg-Gal4* driver under the control of the temperature-sensitive *tub-Gal80^{ts}* transgene (referred to as *esg^{ts}*), expression was restricted to ISC/EBs of the adult midgut for 25 days, by shifting the flies to 29ºC. In contrast to controls, the previously reported, age-associated misexpression of *esg* was significantly reduced upon Pink1 or Parkin depletion (Supp Fig 4-2A-A''). Furthermore, ISC-specific expression of *pink1* or *parkin* RNAi along with a *UAS-2X-yfp* reporter (ISC-Gal4) [45] also revealed a reduction in ISC number 25 days after induction of the RNAi transgenes (Fig 4-2G, Supp Fig 4-2C-C''). In addition, ISC-specific depletion of Pink1 or Parkin was sufficient to cause a significant reduction in ISC proliferation (Fig 4-2H). Similarly, specific knockdown of Pink1 or Parkin in EBs using a temperature sensitive version of the *Su(H)Gal4* driver (EB-Gal4) [46] resulted in fewer EBs 25 days after induction of the RNAi (Fig 4-2I, Supp Fig 4-2D-D''). Interestingly, EB-directed knockdown of Pink1 or Parkin also resulted in a non-cell autonomous reduction in ISC proliferation (Fig 4-2J). These data indicate that either Pink1 or Parkin can act independently in either ISCs or EBs to inhibit the age-associated increase in ISC proliferation.

Because increased ISC proliferation and Esg misexpression are intimately linked with age, it is important to test whether the different fly lines being compared have similar lifespans to avoid misinterpretation of the data based on different rates of aging. We preformed lifespan assays using the *5961^{GeneSwitch}* (*5961^{GS}*) driver; this allowed drug inducible expression of the RNAi transgenes in order to avoid any differences that could be attributed to different genetic backgrounds. In addition, we crossed the *5961^{GS}* driver to *UAS-mCherry^{RNAi}* to validate its use as a control in other assays. In all cases, our data indicate that progenitor specific knockdown of mCherry (Control), Pink1, or Parkin had no effect on lifespan (Supp Fig 4-4 A-C).

Progenitor-specific depletion of Pink1 or Parkin limits the normal proliferative response to stress in the young midgut

Our findings indicate that progenitor-specific loss of Pink1 or Parkin results in a reduction in ISC proliferation and suppression of *esg* misexpression with age, which accompany severe alterations in mitochondrial morphology. However, it was not apparent whether suppression of ISC proliferation was restricted to aging or whether loss of Pink1/Parkin would suppress induction of ISC proliferation as a result of other stimuli. To test for any proliferative defects upon Pink1/Parkin loss in the young gut, we induced a stress response by feeding the flies the DNA damaging agent bleomycin. When fed to flies, bleomycin induces an increase in ISC division without affecting the fate of the progeny [14]. We employed the esg^{ts} driver to selectively deplete Pink1 or Parkin in the progenitor cells of the gut for 7 days prior to bleomycin feeding. Under homeostatic conditions, the *Drosophila* midgut is largely quiescent; evidence of proliferation via pHH3 staining is elusive in young (7 day old) male midguts (Fig 4-2F). In bleomycin-fed controls, a significant increase in ISC proliferation was observed (Fig 4-3A-A' & D). However, the increase in ISC proliferation in response to chemical induced damage was significantly attenuated upon knockdown of either Pink1 or Parkin (Fig 4-3B-C' & D), indicating that depletion of Pink1 or Parkin was sufficient to block ISC proliferation in response to age and damage. Similar results were obtained using 5961^{GS} to drive expression of additional *UAS-pink1RNAi* and *UAS-parkinRNAi* lines (Supp Fig 3I). We confirmed that bleomycin caused similar levels of DNA damage across the treatment groups by staining for the phospho-histone 2A variant D (H2AvD) – a histone variant that accumulates in response to DNA damage [14, 47] in flies expressing RNAi transgenes in the ISC/EBs for 10 days prior to bleomycin feeding. Nuclear intensity of H2AvD in the ECs increased dramatically upon bleomycin feeding (Fig 4-3 E-G' & H) in all samples, indicating significant damage across genotypes.

Knockdown of Pink1, but not Parkin, also significantly inhibited the stress-induced expansion of the *esg-gfp* reporter, although Parkin knockdown samples showed a strong trend for reduced *esg-gfp* expansion (Fig 4-3I). The effect of Pink1/Parkin depletion on stress-induced expansion of esg^{+} cells was further confirmed using several additional RNAi lines against Pink1 and Parkin, all of which demonstrated either a significant reduction or downward trend in expansion of *esg* (Supp Fig 4-3J). We speculated that the increased severity of the DNA damage in the Parkin depleted samples (Fig 4-3H) resulted in an elevated stress stimulus, thus overcoming the proliferative inhibition of the ISCs. Importantly, in uninduced controls in which 5961^{GS} is not active, neither the UAS-*pink1RNAi* nor UAS-*parkinRNAi* transgene limited expansion of *esg-gfp* reporter expression or demonstrated an increase in H2AvD intensity upon bleomycin feeding, when compared to controls (Fig Supp 4-3A-B, right panels).

As the age-associated increase in ISC proliferation was alleviated upon ISC- or EB-specific knockdown of Pink1 or Parkin (Fig 4-2 G-J), we wanted to determine if cell type specific knockdown had similar results in young flies fed bleomycin. We once again employed the ISC-Gal4 and EB-Gal drivers to deplete Pink1 or Parkin in the ISCs or EBs, respectively. ISC-specific loss of Pink1 or Parkin inhibited the bleomycin-induced increase in ISC number and inhibited the increase in $pHH3^{+}$ cells (Fig 4-3J & K, Supp Fig 4-3C-E'). Alternatively, EB-specific knockdown of Pink1 or Parkin limited the expansion of EBs caused by bleomycin feeding but did not inhibit ISC proliferation (Fig 4-3L & M, Supp Fig 4-3F-H'), as expected. Therefore, EB-specific knockdown affected ISC proliferation differently in aged versus bleomycin stressed midguts (compare Fig 4-2I and Fig 4-3M). This discrepancy may be due to the EC-specific damage caused by bleomycin, which results in elevated Upd3 signaling from the damaged ECs to ISCs that still express Pink1 and Parkin.

Pink1 or Parkin depletion results in elevated ROS in the intestinal progenitor cells of the young or aged midgut

As Pink1 and Parkin function is critical for the identification and elimination of depolarized mitochondria, loss of function mutations in either gene can result in increased basal ROS production [48]. To determine whether depletion of Pink1/Parkin in the intestinal progenitors has a functional effect on the mitochondrial network, we assayed endogenous ROS production in the midgut upon ISC/EB-specific knockdown of Pink1 or Parkin. As an indirect measure for ROS production, we employed a GFP reporter for the antioxidant gene *gstD1* [49]. In young flies with relatively quiescent ISCs, we found that *gstD1* reporter expression in ISC/EBs was lower than the surrounding ECs (Fig 4-4A-A''). Upon knockdown of either Pink1 or Parkin, the expression of gstD1 is elevated in the ISC/EBs, when compared to controls (Fig 4-4B-C''). In order to account for variations between immunofluorescent stains, we quantified the ratio of GFP signal within progenitor cells versus the ECs immediately adjacent to the ISC/EBs (Fig 4-4D).

A previous report demonstrated that the shift from a quiescent ISC to a proliferative state upon aging or exposure to mitogenic conditions is due to KEAP1/CncC mediated elevation in ROS levels [50]. Interestingly, our data indicate that, despite increased ROS levels in the ISCs of Pink1/Parkin knockdown samples, the stem cells did not proliferate. This suggests that loss of Pink1/Parkin in the midgut progenitor cells inhibits proliferation despite displaying an intrinsic pro-proliferative phenotype.

To determine if the changes to ROS levels persisted when ISCs divide more rapidly, we employed live imaging of aged guts (50 days old) stained with dihydroethidium (DHE), a dye whose fluorescent intensity increases upon oxidation. Similar to the *gstD1* reporter expression in the young guts, we find that ROS levels were lower in cells positive for *esg* (Fig4-4E-E'' & H). In contrast, ISC/EBs depleted of Pink1

or Parkin exhibited elevated levels of ROS, when compared to the surrounding ECs (Fig 4-4F-G'' & H). These data indicate that the functional effect of loss of the mitophagic machinery exhibits effects as early as day 10 and persist throughout the life of the fly, resulting in elevated ROS levels in the progenitor cells throughout life.

Progenitor-specific depletion of Pink1/Parkin results in upregulation of senescence-associated markers and continued proliferation defects after RNAi repression

In mammals, oncogene expression can lead to cellular senescence via increased ROS levels [51]. That invertebrates also demonstrate a ROS-dependent cellular senescence phenotype has only recently been revealed. In the *Drosophila* imaginal epithelium, compromised mitochondrial function in conjunction with oncogenic Ras expression can lead to cellular senescence [52]. Since we observed increased ROS levels in the ISC/EBs of young and aged flies and a decrease in ISC proliferation, we investigated the possibility that ISCs depleted of Pink1 or Parkin adopted a senescence-like phenotype and, therefore, were uncapable of dividing. We first tested the midguts for markers of cellular senescence, such as senescence-assocaiated β-galactosidase (SA-β-gal) and HP-1 [52]. Knockdown of Pink1 or Parkin, mediated by the *5961^{GS}* driver, caused elevated senescence-associated β-galactosidase (SA-β-gal) activity in many of the diploid cells of the posterior midgut (Fig 4-5A-C'). Furthermore, Pink1/Parkin depletion resulted in elevated HP-1 levels in the *esg*$^{+}$ cells of the posterior midgut (Fig 4-5D-F, arrows indicate *esg*$^{+}$ cells, ISC/EBs, and asterisks indicate polyploid, *esg*$^{-}$ cells, ECs). These data indicate that several hallmarks of cellular senescence are elevated in the intestinal progenitor cells in response to knockdown of Pink1/Parkin in the ISC/EBs.

Since knockdown of Pink1 or Parkin resulted in proliferative defects in the ISCs and several senescence-associated markers were expressed in ISCs upon Pink1/Parkin

depletion, we next sought to determine if the ISCs are truly senescent upon ISC/EB-specific knockdown of Pink1 or Parkin and unable to re-enter the cell cycle. In order to test for functional senescence, we employed the temperature-inducible *esg* flip-out approach described above. The esg F/O flies were crossed to *UAS-mCherry*^{RNAi} (control), *UAS-pink1*^{RNAi}, or *UAS-parkin*^{RNAi} at 18°C to repress RNAi expression during development. Upon eclosion, adult flies were moved to 29°C to induce expression of the RNAi constructs for seven days. After seven days of knockdown, the flies were returned to 18°C to once again repress the RNAi expression and allow the ISC/EBs to recover for another seven days. At this point, flies were assayed for gut proliferation (Fed samples), fed 5% sucrose for 48 hours (Sucrose), or fed 5 µg/ml bleomycin in 5% sucrose for 48 hours (Bleomycin) to stimulate ISC division (Fig 4-5G). All samples in the Fed and Sucrose conditions showed very little or no ISC proliferation (Fig 4-5H, left and middle panels). Interestingly, however, midguts that had been pulsed with *parkin*^{RNAi} in the ISC/EBs had significantly fewer dividing ISCs upon bleomycin feeding, while a *pink1*^{RNAi} pulse resulted in a tendency to have fewer pHH3-positive ISCs (Fig 4-5H, far right section). These data indicate that the proliferative defect in ISCs upon Parkin depletion is largely irreversible. This, together with the expression of several senescence-associated factors upon Pink1/Parkin knockdown, indicates that loss of Pink1 or Parkin in the midgut progenitor cells results in cellular senescence.

Cellular senescence is a potent tumor suppressive mechanism, yet numerous recent studies have indicated that the presence of senescent cells can contribute to age-related tissue degeneration through the induction of a senescence-associated secretory phenotype (SASP) [53] and elevated levels of ROS [54]. Here, we demonstrate that a block in mitochondrial turnover via mitophagy results in hallmarks of senescence in *Drosophila* ISCs. Specifically, we show that ISC/EB-specific reduction of Pink1 and Parkin leads to significant intracellular damage and alterations to mitochondrial

morphology (Fig. 4-1, Supp. Fig. 4-1A, B). These changes in mitochondrial ultrastructure correlate with a block in the uncontrolled ISC proliferation normally present in aged animals and induced in response to acute intestinal damage (Figs. 4-2, 4-3; Supp. Fig. 4-2). The block in ISC proliferation occurs in the presence of high levels of ROS accumulation in PINK and Parkin depleted ISCs (Fig. 4-4). Finally, we show that several hallmarks of senescence are elevated in ISCs upon depletion of Pink1 or Parkin and that ISCs are functionally senescent, as stress-induced proliferation remains limited even after RNAi repression is relieved (Fig. 4-5). Taken together, our results indicate that progenitor-specific mitochondrial dysfunction uncouples cellular and tissue aging, in part, through induction of ISC senescence and suggest that ISCs utilize mitophagy as one strategy to maintain a healthy complement of mitochondria. The role of mitochondria in enhancing the onset of senescence has been recently reported in mammals [55], and our data reveal a similar relationship is present in invertebrates.

Acknowledgements

We thank Drs. H. Jasper, B. Edgar, L. Cooley, S. Hou, the Bloomington stock center, the Vienna Drosophila Resource center, and the TRiP at Harvard Medical School (NIH/NIGMS R01-GM084947) for providing transgenic RNAi fly stocks and/or plasmid vectors used in this study and Dr. D. Walker and the Jones lab for helpful discussions. In addition, we thank Dr. Yong Wu and Dr. Enrico Stefani for the use of their custom STED microscope. This work was supported by the Eli and Edythe Broad Center of Regenerative Medicine and Stem Cell Research at the University of California- Los Angeles (D.L.J), the NIH: AG028092 and AG040288 (D.L.J.) and 5P41GM103412-28 (M.H.E.); and a graduate student fellowship from the National Science Foundation DGE-1144087 (C.L.K.)

Materials and methods

Fly food and husbandry

Flies were cultured in vials containing standard cornmeal medium (in w/v, 1% agar, 3% brewer's yeast, 1.9% sucrose, 3.8% dextrose, and 9.1% cornmeal). Flies carrying the drug inducible Gal4/UAS system, GeneSwitch [56, 57], were cultured at 25°C, and trasngene induction was carried out by supplementing the food with 25 µg/ml of the steroid hormone mifepristone (RU486, Sigma M8046). Flies carrying the temperature inducible Gal4/UAS system, TARGET [58], were crossed at 18°C to repress transgene expression. Upon eclosion, flies were cultured at 29°C to induce Gal4-dependent expression. In all cases, flies were flipped to fresh media every 2-3 days. Male flies were used in all assays described.

Drosophila strains

The following TRiP (Transgenic RNAi Project – Harvard Medical School) RNAi lines were obtained from the Bloomington Stock Center: UAS-Pink1^{RNAi} (BL#31170), UAS-Pink1^{RNAi} (BL#31262), UAS-Pink1^{RNAi} (BL#38262), UAS-Parkin^{RNAi} (BL#31259), UAS-Parkin^{RNAi} (37509), UAS-Luciferase^{RNAi} (BL#31603), and UAS-mCherry^{RNAi} (BL#35785). An addition UAS-Parkin^{RNAi} line was obtained from the VDRC (v104363). RU486-inducible 5961^{GS} and 5966^{GS} drivers were described previously [59] and provided by H. Jasper. The *esg-GFP* enhancer trap line (P01986) was obtained from Lynn Cooley as part of the FlyTrap collection. The reporter lines UAS-GFP^{mito} (BL#8443) and UAS-LacZ^{nls} (BL#3956) were acquired from Bloomington.

w;esg-Gal4,UAS-GFP,tubGal80^{TS}/CyO; UAS-flp,act>CD2>Gal4/Tm6b (*escargot* F/O) line was obtained from B. Edgar. *Su(H)Gal4,*UAS-*GFP^{CD8}/CyO;tubGal80^{TS}/MKRS* (EB-

Gal4), and *esgGal4,UAS-2xYFP/CyO;Su(H)Gal80, tubGal80^{TS}/TM3, Sb* (ISC-Gal4) (gifts from S. Hou).

Bleomycin feeding experiments

For experiments with Gal80^{ts}-dependent induction, flies were collected 1-2 days after eclosion and shifted to 29°C on standard cornmeal/molasses medium for 7 days before being transferred to treatment vials. In experiments with GeneSwitch-based induction, flies were collected 1-2 days after eclosion and reared on standard medium for 10 days at 25°C before being transferred to treatment vials. Treatment vials consisted of empty vials containing a folded KimWipe saturated with 750 µl of: *Uninduced Control*- 0.25% v/v ethanol in 5% sucrose, *Induced Control*- 25 µg/ml RU486 in 5% sucrose, *Uninduced Treatment*- 0.25% v/v ethanol and 5 µg/ml bleomycin in 5% sucrose, and *Induced Treatment*- 25 µg/ml RU486 and 5 µg/ml bleomycin in 5% sucrose.

Survivorship

All progeny from parental crosses were collected within 24 hours of eclosion and allowed to mate for two days before sorting for the appropriate genotypes using light CO_2 anesthesia. Flies were housed in a 25°C incubator kept on a 12-hour light/dark cycle. For standard lifespan experiments, the flies were housed at a density of 20 flies per vial and flipped to new vials with standard cornmeal/molasses medium containing either ethanol (0.25% v/v as vehicle for uninduced GeneSwitch controls) or RU486 (25 µg/ml) every 2-3 days. For bleomycin survivorship experiments, flies were collected as before but aged to 10 days on standard food containing either RU486 (25 µg/ml) or ethanol (0.25% v/v) before being transferred to treatment vials described above.

Immunostaining and microscopy

The *Drosophila* gastrointestinal tract was dissected into 4% paraformaldehyde in PLP buffer and fixed for one hour at room temperature. The tissue washes were carried out with PBT (1X PBS, 0.1% Triton X-100). Antibody incubations were carried out in PBT supplemented with 3% BSA and 0.02% sodium azide. Primary antibodies incubated at room temperature for at least four hours or overnight at 4°C; secondary antibody incubations were two hours at room temperature. Fixed and stained tissue was whole mounted in Vectashield mounting medium containing 4′,6-diamidino-2-phenylindole (DAPI) from Vector Laboratories. Primary antibodies used in this study included: rabbit α-GFP (1:5000) from Molecular Probes (A11122), mouse α-GFP (1:200) from Molecular Probes (A11120), chicken α-GFP (1:1000) from Aves Labs Inc., rabbit α-βGal (1:2000) from Cappel, rabbit α-phospho Histone-H3 (1:200) from Millipore (06-570), rabbit α-H2AvD pS137 (1:200) from Rockland (600-401-914), and mouse α-βGal (1:20) (40-1a), mouse α-Armadillo (1:20) (N2 7A1), mouse α-HP1 (C1A9), and mouse α-Prospero (1:100) (MR1A) from the Developmental Studies Hybridoma Bank (DSHB).

Super resolution images were obtained from a custom build Stimulated Emission Depletion (STED) super resolution microscope currently reaching a resolution of about 30-40nm. The STED system was built in the Dept of Anesthesiology, UCLA. Supported an NIH grant from the National Heart, Lung, and Blood Institute BRG R01 HL088640.

Image analysis

For quantification of ISCs/EBs, clone number and size, H2AvD intensity, or pHH3 in the posterior midgut, images were acquired using a 40X objective on either a Zeiss LSM 780 confocal microscope or a Zeiss Axio Observer.Z1 fitted with an ApoTome. In order to image the entire posterior midgut, three to five images were taken to cover the area from the pylorus to the posterior aspect of the iron/copper region, corresponding to the P3-P4 region of the *Drosophila* midgut [3]. Each image was acquired as a 3-plane Z-stack

spaced at 0.75 μm. Raw images were converted to max intensity projections using ImageJ. Image features were quantified with CellProfiler.

Electron Microscopy

The gastrointestinal tract was dissected into 2% EM-grade glutaraldehyde in PBS then fixed for 1 hour at room temperature then two hours on ice. Samples were washed in PBS before embedding in soft agar. Tissues underwent secondary fixation in 1% osmium tetroxide plus 0.3% potassium ferricyanide. Guts were then en bloc stained with 2% uranyl acetate, dehydarated in ethanol, and embedded in EPON epoxy resin. For standard TEM, thin sections were mounted on slot grids and stained with uranyl acetate and lead citrate. Images were acquired using a Zeiss Libra 120 PLUS EF-TEM transmission electron microscope or a JEOL 100CX transmission electron microscope. For tomographic studies, thick sections were embedded with gold particles and imaged using a FEI Titan 80-300 (CTWIN) IVEM/STEM. Tomographic reconstructions and 3-D models of mitochondria were generated with IMOD.

Senescence associated β-galactosidase assay

Full, intact midguts were stained for senescent cells using the Senescence Cells Histochemical Staining Kit (Sigma, CS0030). Briefly, ten-day-old flies were anesthetized by covering the culture vial with ice until the flies fell to the bottom of the vial. Flies were immediately dissected into 1x PBS. Dissection of flies from all of the genotypes to be analyzed would take place in a 15-minute window after which the remainder of the staining protocol would be carried out as follows. Guts were washed twice with 1 x PBS before being lightly fixed for 6 minutes at room temperature in 1 x Fixation Buffer. Guts were washed 3 times in 1 x PBS before being incubated in 1 x Staining Mixture (mixed as per kit instructions) at 37°C for 30 minutes. After staining, the midguts were washed in 1 x PBS, and mounted in 1 x PBS on Superfrost® Plus micro slides (VWR 48311-

703). The guts were images immediately on a Zeiss Axio Imager A2 microscope using Zen imaging software by Zeiss.

Statistical analysis

When data sets followed a normal distribution, significance was determined via one-way ANOVA followed by a Dunnett's multiple comparison test. When data were non-normally distributed (typically pHH3 count data), a non-parametric Kruskal-Wallis analysis was used followed by a Dunn's multiple comparison test. Any deviations from this standard are noted in the text.

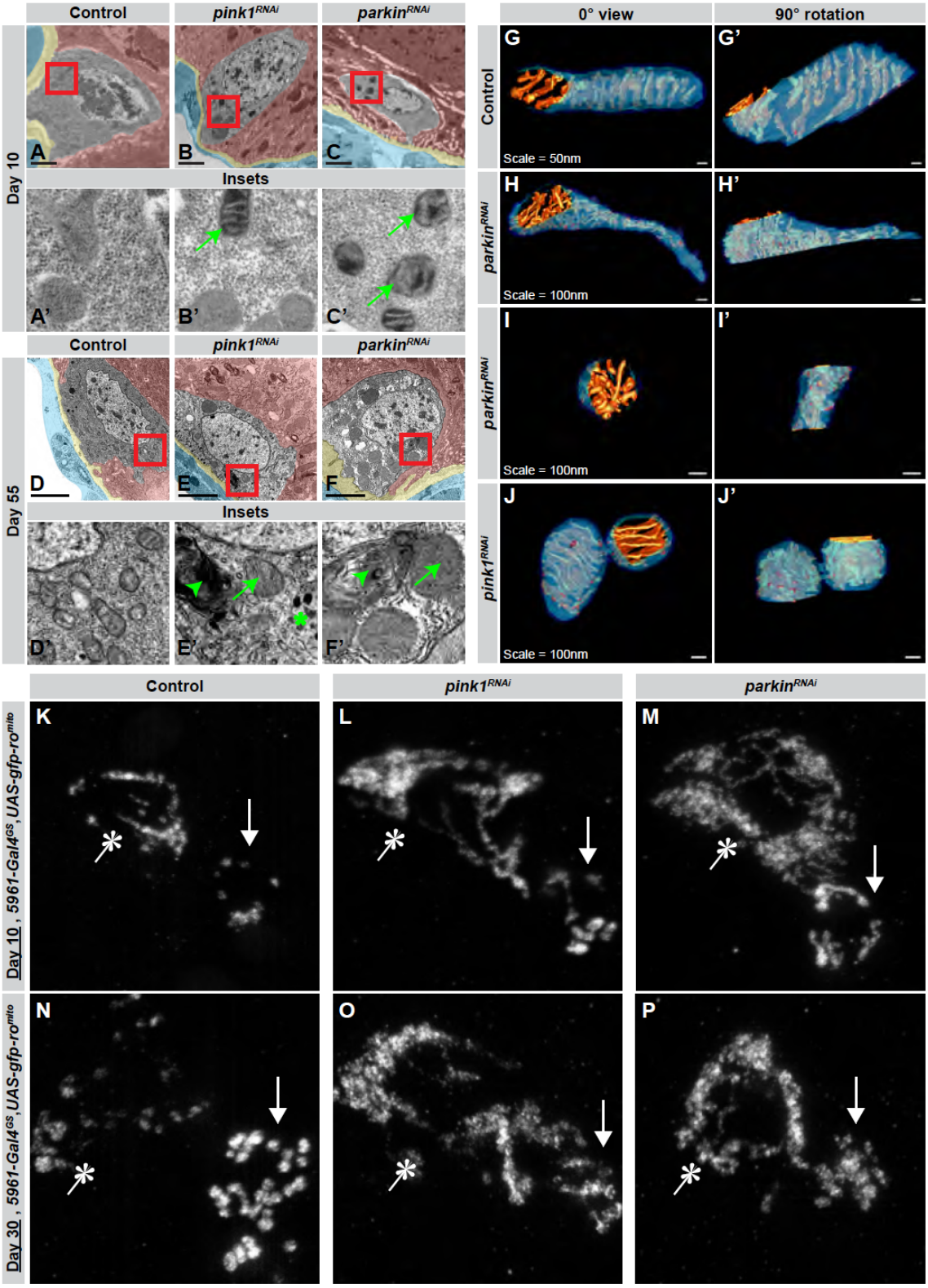

Figure 4-1: ISC/EB-specific knockdown of Pink1 or Parkin alters mitochondrial morphology and density. **A**-**F**, transmission electron micrographs (TEM) of midgut

progenitor cells in the posterior midgut of 10- or 55-day-old Control, *Su(H)LacZ*;*esg-gfp*,*5961-Gal4^{GS}*/+;*UAS-mCherry^{RNAi}*/+ (**A** & **D**), Pink1 knockdown, *Su(H)LacZ*;*esg-gfp*,*5961-Gal4^{GS}*/*UAS-pink1^{RNAi}* (**B** & **E**), or Parkin knockdown, *Su(H)LacZ*;*esg-gfp*,*5961-Gal4^{GS}*/*UAS-parkin^{RNAi}* (**C** & **F**) adult flies. Visceral muscle (blue), basement membrane (yellow), and enterocytes (red) are labeled via pseudo color. Scale bars = 1 μm. **A'**-**F'**, magnified regions outlined in **A**-**F**. Arrows indicate swollen or condensed mitochondria, arrowheads show multilamellar bodies (MLBs), and an asterisk denotes electron dense granule accumulation. **G**-**J'**, reconstructed, segmented, and surface-rendered mitochondria from electron tomography of midgut progenitors in 55-day-old Control, Pink1 knockdown, or Parkin knockdown posterior midguts. Outer mitochondrial membrane (OMM, dark blue), inner boundary membrane (IBM, light blue), and cristae (orange) are shown; the intersections of cristae with the IBM represent cristae junctions. **K**-**P**, stimulation emission depletion (STED) microscopy images of mitochondria in the ISC/EBs from 10-day-old (**K**-**M**) or 30-day-old (**N**-**P**) flies. Arrows point to ISCs and asterisks indicate EBs.

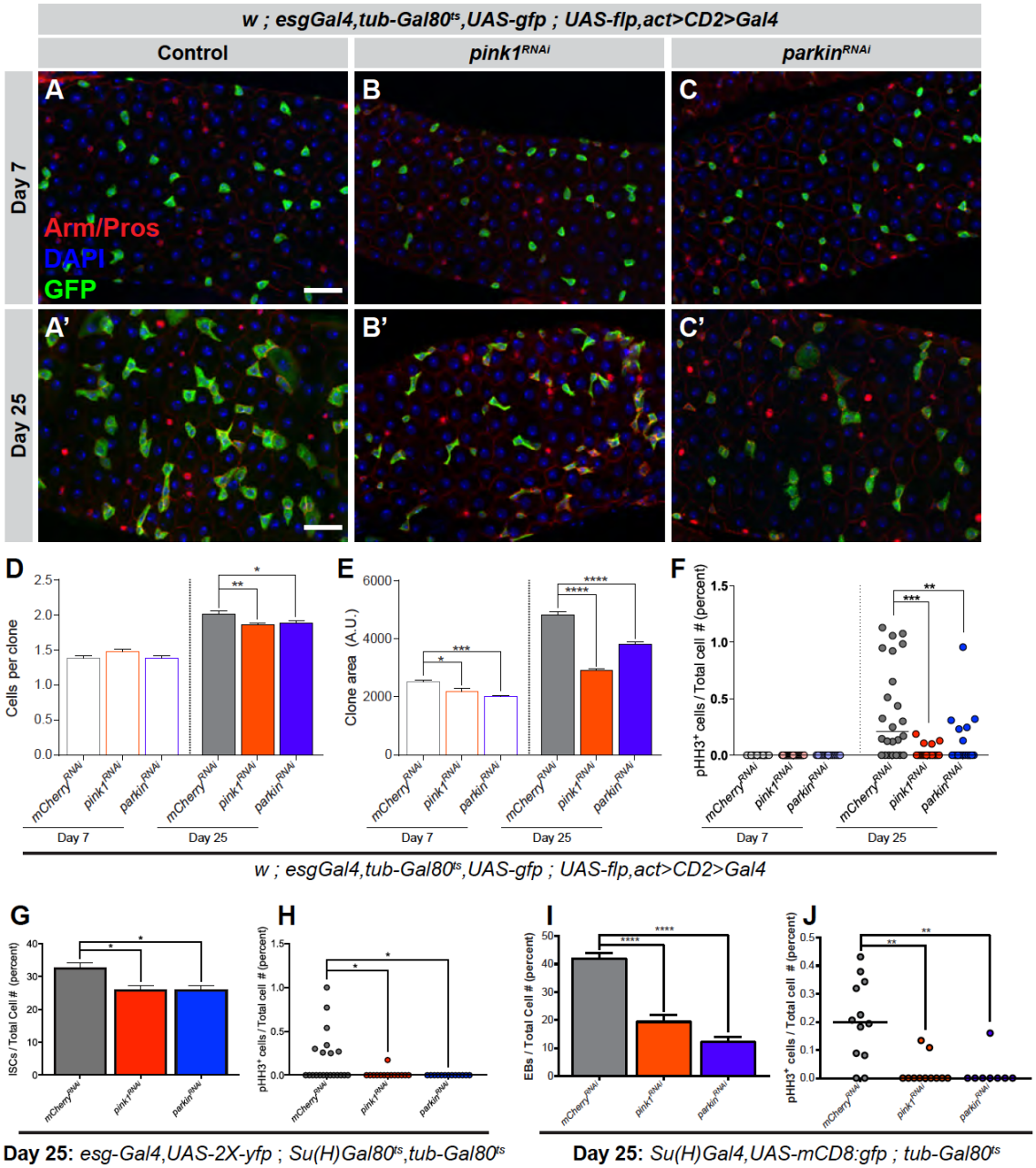

Figure 4-2: Progenitor-specific knockdown of Pink1 or Parkin delays tissue level aging phenotypes in the posterior midgut. **A-C'**, representative immunofluorescence images of the posterior midgut of 7- or 25-day-old Control (*esg-Gal4*, *tub-GAL80^{ts}*, *UAS-gfp* /+ ; *UAS-flp*, *act*>CD2>Gal4/UAS-*mCherry^{RNAi}*), Pink1 knockdown (*esg-Gal4*, *tub-GAL80^{ts}*, *UAS-gfp* /*UAS-pink1^{RNAi}* ; *UAS-flp*, *act*>CD2>Gal4/+), or Parkin knockdown (*esg-Gal4*, *tub-GAL80^{ts}*, *UAS-gfp* /*UAS-parkin^{RNAi}* ; *UAS-flp*, *act*>CD2>Gal4/+) flies aged

at 29°C. Scale bar = 20 μm. **D**, quantification of the number of cells comprising each *esg F/O* clone from **A-C'**. **E**, groups of contiguous GFP-positive cells were classified as individual *esg F/O* clones. The average area of all clones per treatment group is represented. **F**, quantification of actively dividing ($pHH3^+$ cells) from **A-C'**. Quantification of the proportion of ISCs in the posterior midgut (**G**) or mitotic ISCs (**H**) upon ISC-specific knockdown of mCherry, Pink1, or Parkin in 25-day-old-flies. Quantification of the proportion of EBs in the posterior midgut (**I**) or mitotic ISCs (**J**) upon EB-specific knockdown of mCherry, Pink1, or Parkin. Data sets **D**, **E**, **G**, and **I** were analyzed using One-way ANOVA followed by a Dunnet's post test to determine significant differences in means. For data sets F, H, and J, each age group was analyzed independently using a Kruskal-Wallis test for nonparametric data followed by a Dunn's post test for multiple comparisons to determine significantly different median values. * $P<0.05$, ** $P<0.01$, *** $P<0.001$, **** $P<0.0001$.

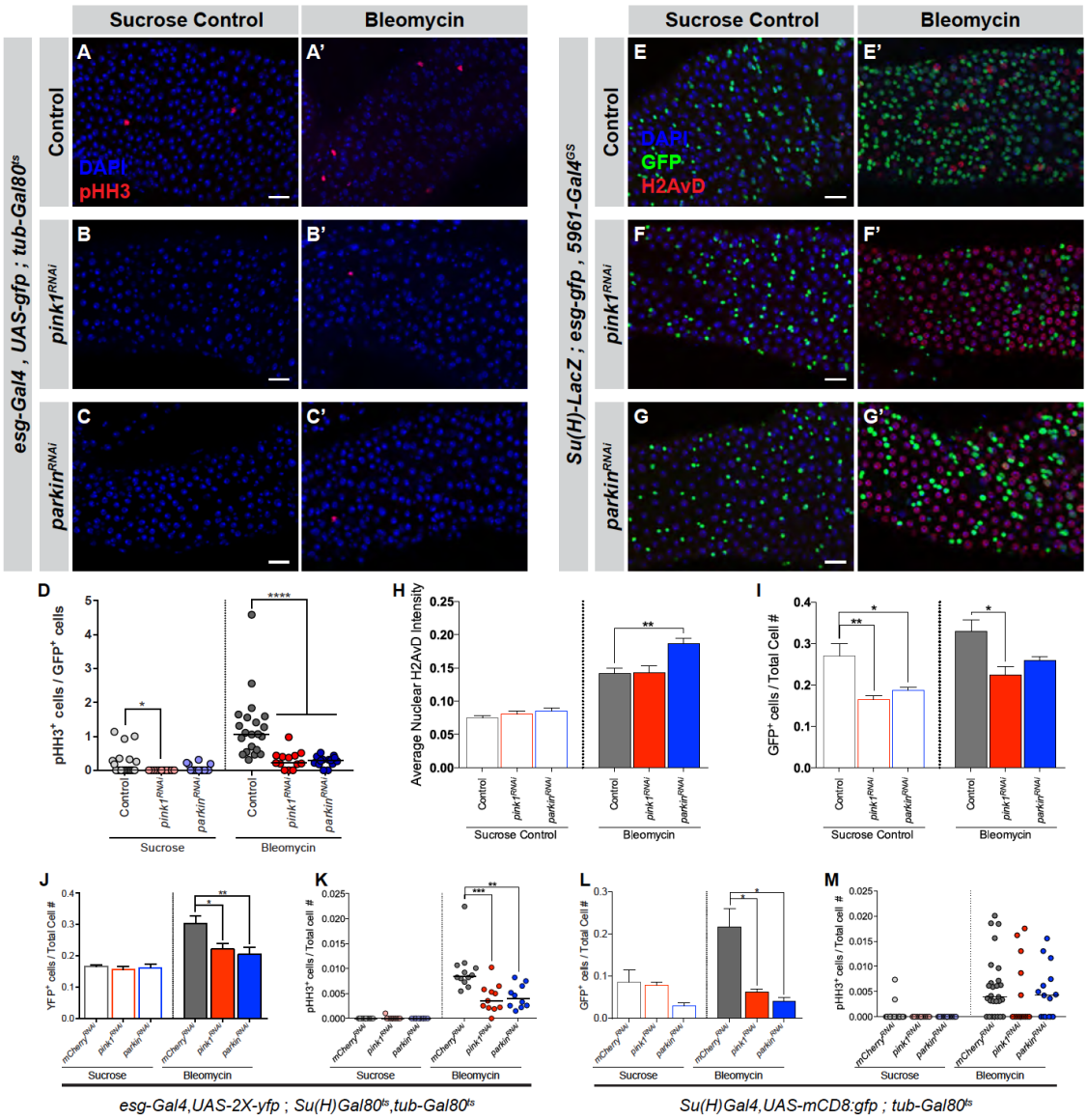

Figure 4-3: Progenitor-specific depletion of Pink1 or Parkin limits the normal proliferative response to stress in the young midgut. **A-C'**, representative immunofluorescence images of the posterior midgut of 10-day-old flies treated for 48 hours with sucrose control (5% sucrose) or bleomycin (5 µg/ml in 5% sucrose) at 29°C. **D**, quantification of mitotic cells in the posterior midgut of flies from **A-C'** in response to bleomycin-induced stress. Significance determined via Kruskal-Wallis test with a Dunn's post test for multiple comparisons. **E-G'**, immunofluorescence images of the posterior midgut of 10-day-old flies housed at 25 °C on standard cornmeal/molasses medium

supplemented with 25 µg/ml RU486 to induce transgene expression prior to 48 hour exposure to either sucrose control (5% sucrose) or bleomycin (5 µg/ml bleomycin in 5% sucrose) medium. **H**, quantification of H2AvD stain intensity in the nuclei of GFP-negative cells from **E**-**G'**. **I**, quantification of *esg-gfp* reporter activity in the posterior midgut of flies from **E**-**G'**. Each group of conditions was analyzed independently with one-way ANOVA followed by Dunnett's post test. Quantification of the proportion of ISCs in the posterior midgut (**J**) or mitotic ISCs (**K**) upon ISC-specific knockdown of mCherry, Pink1, or Parkin in 10-day-old flies treated with bleomycin. Quantification of the proportion of EBs in the posterior midgut (L) or mitotic ISCs (**M**) upon EB-specific knockdown of mCherry, Pink1, or Parkin in flies stimulated with beomycin at 10 days of age. Data sets **J** and **L** were analyzed using One-way ANOVA followed by a Dunnet's post test to determine significant differences in means. For data sets **K** and **M**, sucrose control versus bleomycin groups were analyzed independently using a Kruskal-Wallis test for nonparametric data followed by a Dunn's post test for multiple comparisons to determine significantly different median values. * $P<0.05$, ** $P<0.01$, *** $P<0.001$.

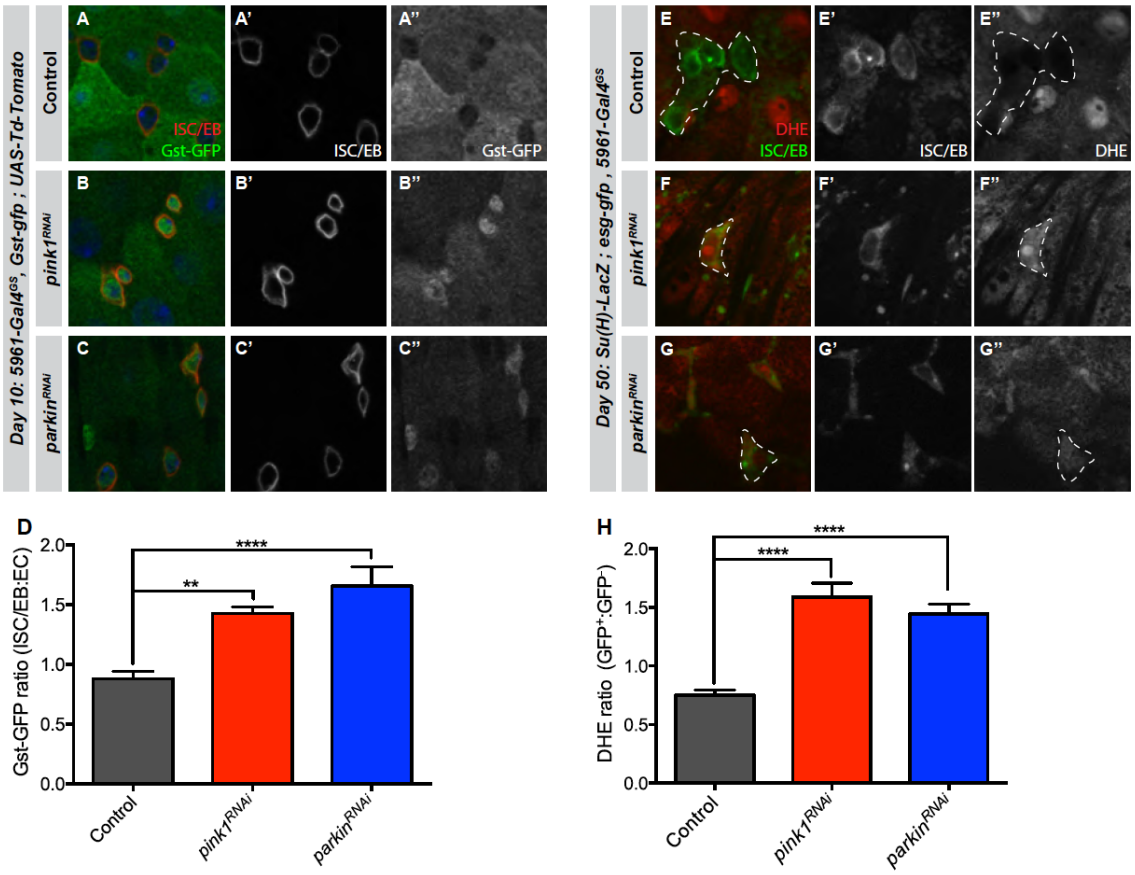

Figure 4-4: Pink1 or Parkin depletion results in elevated ROS in the intestinal progenitor cells of the young or aged midgut. A-C'' representative immunoflourescence images of the posterior midguts of ten day old flies bearing a GstD-GFP reporter construct. Expression of *UAS-Td-Tomato* along with **A**, *mCherry*^{RNAi} (Control), **B**, *pink1*^{RNAi}, or **C**, *parkin*^{RNAi} was accomplished with the *5961-Gal4*^{GS} driver. *Gal4*^{GS} activity was stimulated by supplementing 25 µg/ml RU486 throughout adulthood. **D** quantification of GstD:GFP signal from **A-C** reported as a ratio of GFP within the boundary of the ISC/EBs versus the adjacent ECs. **E-G''** Example images from live-mounted posterior midguts stained with DHE from 50 day old flies. RNAi construct expression was induced by feeding 25 µg/ml RU486 throughout adulthood to flies carrying the *5961-Gal4*^{GS} driver and **E**, *mCherry*^{RNAi} (Control), **F**, *pink1*^{RNAi}, or **G**, *parkin*^{RNAi}. Dotted lines mark ISC/EBs as indicated by *esg-gfp* reporter expression (**E'-**

G'). **H** quantification of the ratio of DHE within the ISC/EBs to adjescent ECs. Data sets were analyzed by One-way ANOVA and a Dunnet's post test. ** P<0.01, **** P<0.0001.

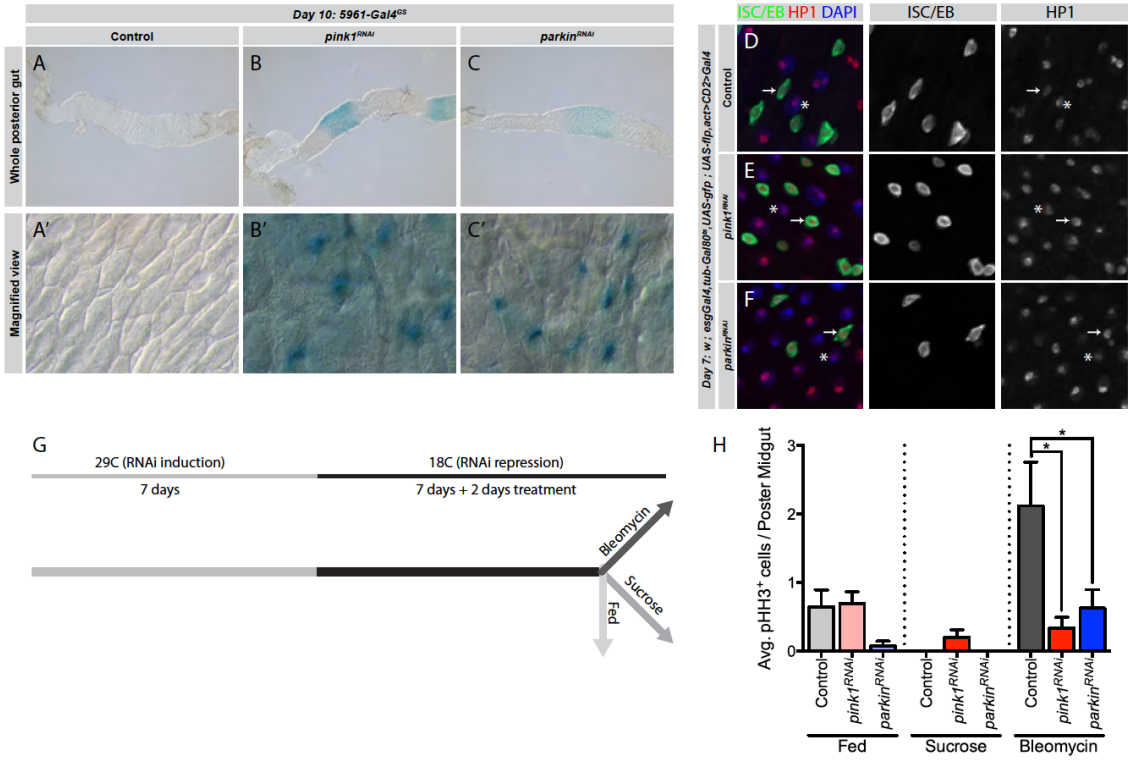

Figure 4-5: Progenitor-specific depletion of Pink1/Parkin results in upregulation of senescence-associated markers and continued proliferation defects after RNAi repression. **A-C'** representative senescence-associated β-galactosidase activity in the P3/P4 region of the posterior midgut. Progenitor-specific knockdown of Pink1 (**B**) or Parkin (**C**) results in a faint band of SA-β-gal activity in the posterior midgut with strong expression in some of the small, diploid cells (**B'-C'**). **D-F** example immunoflourescent images showing HP1 stain in the posterior midgut of 7-day-old flies upon expression of **D**, *mCherry*^{RNAi} (Control), **E**, *pink1*^{RNAi}, or **F,** *parkin*^{RNAi}. Arrows denote ISC nuclei, and asterisks mark the nuclei of differentiated midgut cells. **G**, model of experimental design to test functional senescence upon recovery from Pink1 or Parkin depletion in the midgut progenitor cells. **H**, quantification of the number of actively dividing cells in the posterior midgut as outlined by the experiment in **G**.

Transgene	Mitochondrial morphology	Gut morphology	ISC proliferation
UAS-dPGC-1*	Normal	Delayed aging	Decreased with age
UAS-dPGC-1^{RNAi}	Normal	Advanced aging	Increased with age
UAS-drp:HA	Normal	Normal	No change
UAS-drpRNAi	Highly fused / clustered	Normal	No change
UAS-opa1RNAi	Normal	Normal	No change
UAS-marfRNAi	Punctate / spheroid	Normal	No change
UAS-tamasRNAi	Normal	Normal	No change
UAS-miltonRNAi	Normal	Normal	No change
UAS-miroRNAi	Normal	Normal	No change
UAS-ralaRNAi	Normal	Normal	No change
UAS-pink1RNAi	Slightly fused	Delayed aging	Decreased with age
UAS-parkinRNAi	Slightly fused	Delayed aging	Decreased with age

* Rera *et al*. 2011a

Supplementary Table 4-1: RNAi screen for mitochondria-related genes affecting tissue homeostasis and ISC proliferation. The indicated transgenic lines were crossed to *5961-Gal4^{GS}/UAS-gfp^{mito}* flies, and the progeny were aged at 25°C for 10, 30, or 50 days. Tissue homeostasis was assayed by tissue morphology, GFP expression, ISC proliferation, and mitochondrial morphology. Similar to previous findings, overexpression of dPGC1 resulted in a delayed aging phenotype and decreased ISC proliferation [26]. Similar to the effects of dPGC1 overexpression, RNAi-mediated knockdown of either Pink1 or Parkin resulted in decreased ISC proliferation and delayed the loss of the epithelial monolayer morphology.

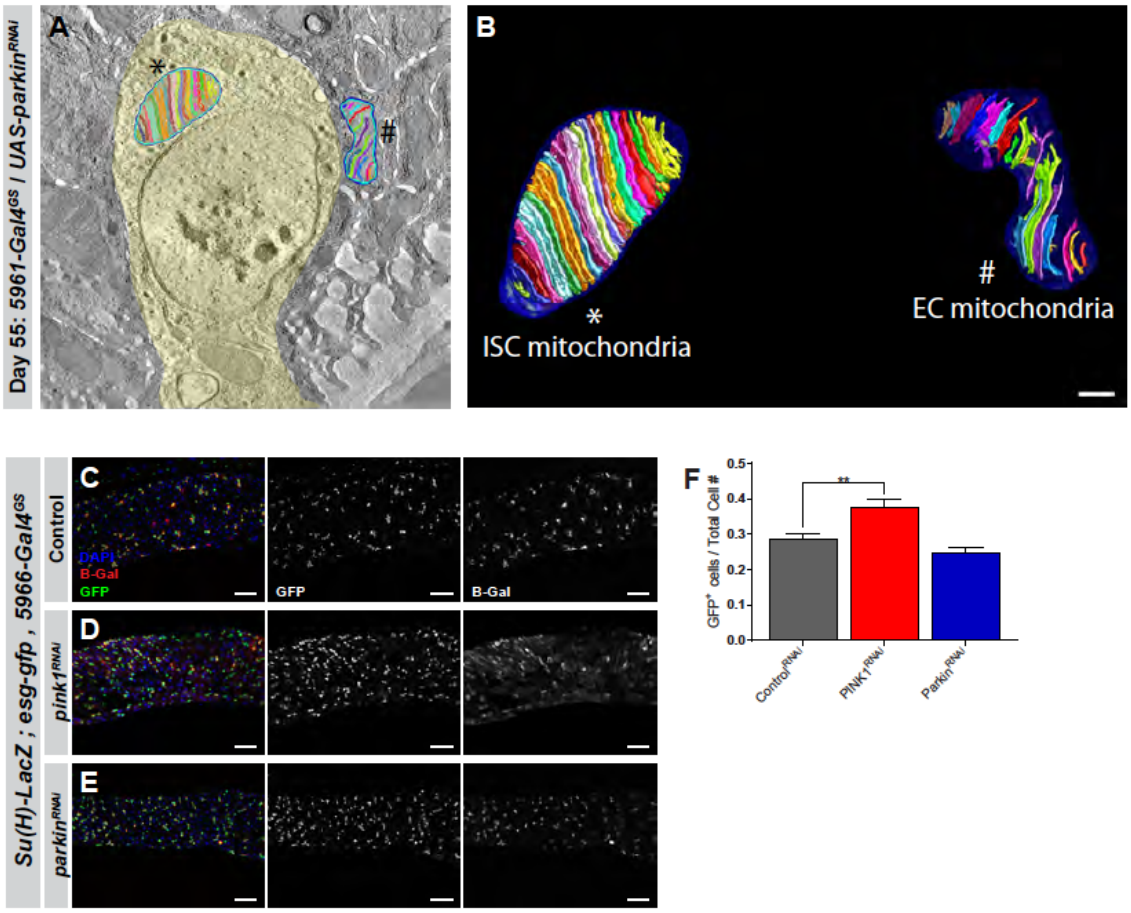

Supplementary Figure 4-1: The effects of progenitor-specific Pink1 or Parkin knockdown are limited to the ISC/EBs. **A**, transmission electron micrograph of a 55-day-old midgut ISC depleted of Parkin and a neighboring wildtype EC. The progenitor cell is pseudocolored light yellow, and the segmentation lines used to create a 3-D tomography of the mitochondria are shown. The * indicates the ISC mitochondria and the # marks the EC mitochondria. **B**, electron micrograph tomography of the mitochondria from **A**. A clear ultrastructural difference exists despite the close proximity of the cells. **C-E**, representative immunofluorescence images of posterior midguts from 50-day-old control (*Su(H)LacZ*; *esg-gfp,5966-Gal4^{GS}*/+;*UAS-mCherry^{RNAi}*), Pink1 knockdown (*Su(H)LacZ*; *esg-gfp,5966-Gal4^{GS}*/*UAS-pink1^{RNAi}*), or Parkin knockdown (*Su(H)LacZ*; *esg-gfp,5966-Gal4^{GS}*/*UAS-parkin^{RNAi}*). Scale bars = 50 μm. **F**,

quantification of the proportion of total cells that are positive for the esg-gfp reporter in **C-E**. One-way ANOVA with Dunnett's multiple comparison test used to determine significant differences. ** $P<0.01$.

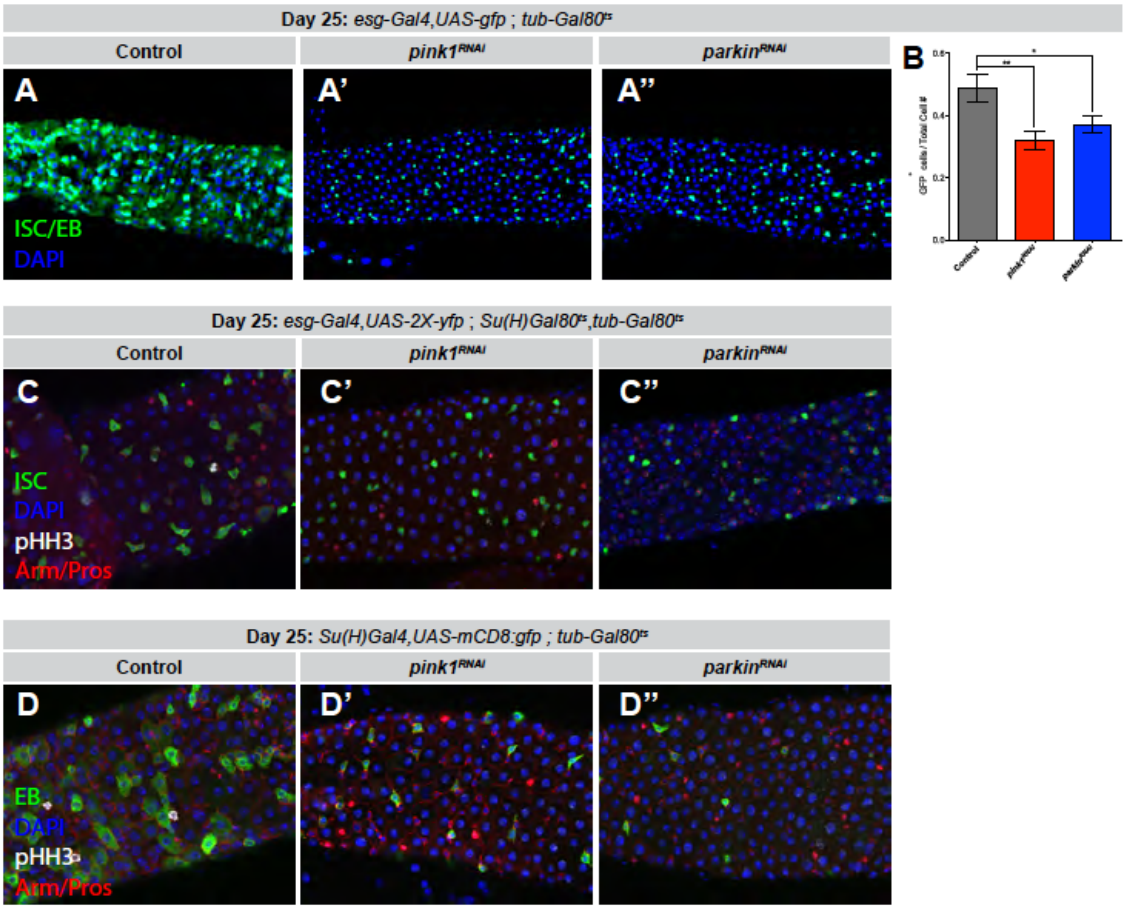

Supplementary Figure 4-2: ISC- or EB-specific knockdown of Pink1 or Parkin delays the tissue level aging phenotypes in the posterior midgut. A-A'' immunoflourescence images showing restriction of esgGal4 expression in 25-day-old flies upon progenitor-specific knockdown of Pink1 (**A'**) or Parkin (**A''**). **B**, quantification of the proportion of GFP-positive cells per total cell number from flies represented in **A-A''**. Statistically significant differences were determined with One-way ANOVA and a Dunnet's post test. * P<0.05 and ** P<0.01. **C-C''** representative images from data presented in **Fig 4-2 G-H**. **D-D''** representative images from data presented in **Fig 4-2 I-J**.

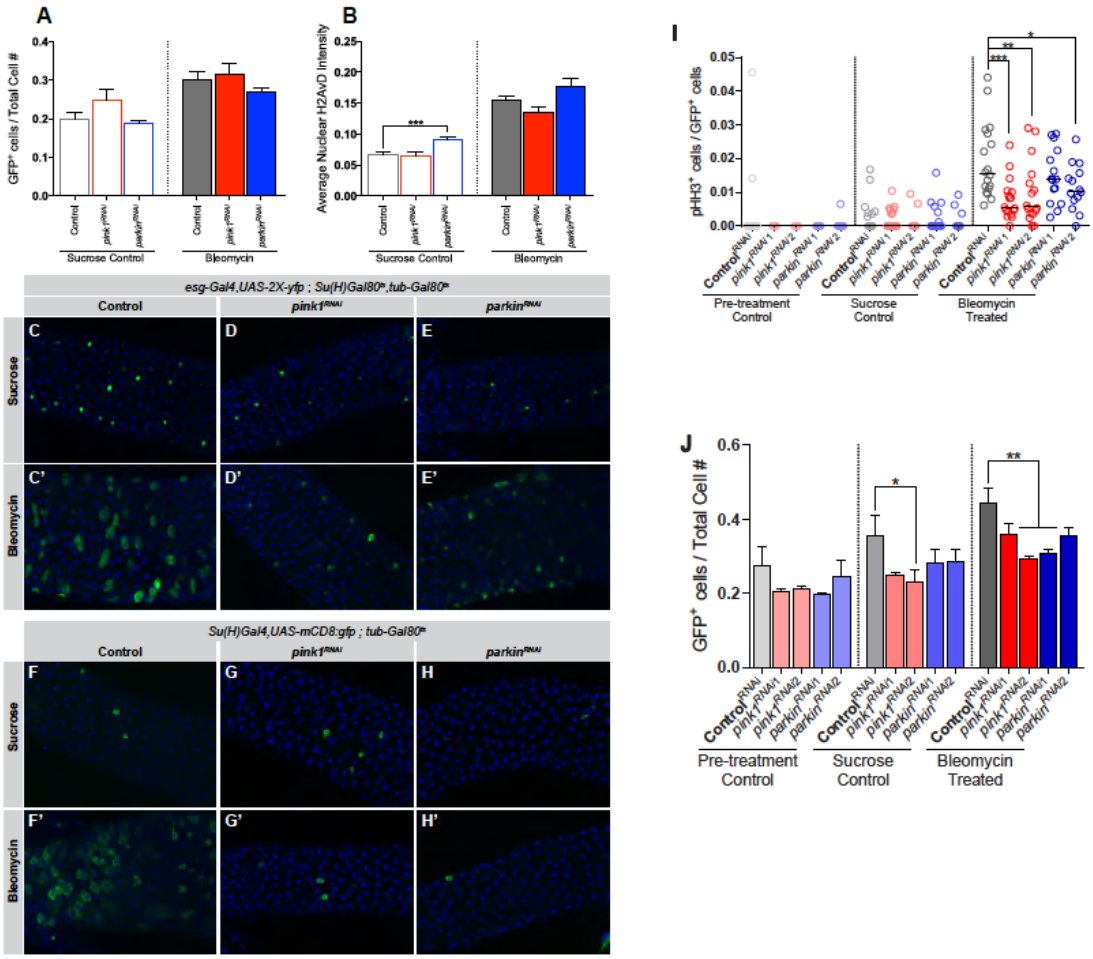

Supplementary Figure 4-3: Knockdown of Pink1 or Parkin in ISC/EBs limits the normal proliferative response during stress. **A**, quantification of the proportion of GFP-positive cells, or **B**, measure of the average H2AvD intensity in the uninduced (no RU486) samples from **Fig 4-3E-I**. **C-E'**, representative immunoflourescence images from quantified data in **Fig 4-3J-K**. **F-H'**, images representative of those used to quantify EB number and pHH3 upon EB-specific knockdown in **Fig 4-3F-H'**. **I**, quantification of the ratio of pHH3 cells per esg-GFP^{+} cells during bleomycin treatment using additional RNAi lines targeting *pink1* or *parkin*. Bleomycin treatments were carried out on 10-day-old flies as described previously. The indicated genotypes carried *Su(H)LacZ*;*esg-gfp,5961-Gal4*^{GS} in addition to: Control^{RNAi} (*UAS-luciferase*^{RNAi} – on II), *pink1*^{RNAi1} (*UAS-pink1*^{RNAi} – on III, BL31170), *pink1*^{RNAi2} (*UAS-pink1*^{RNAi} – on III,

BL31262), *parkin*^{RNAi1} (*UAS-parkin*^{RNAi} – on III, BL31259), or *parkin*^{RNAi2} (*UAS-parkin*^{RNAi} – on II, VDRC). **J**, quantification of esg-GFP^{+} cells in the posterior midgut of flies described in **I**. For **I** and **J**, each treatment group was analyzed independently using one-way ANOVA and Dunnett's multiple comparison test. One-way ANOVA and Dunnett's multiple comparison tests were used to assign significant differences. * P<0.05, ** P<0.01, *** P<0.001, **** P<0.0001.

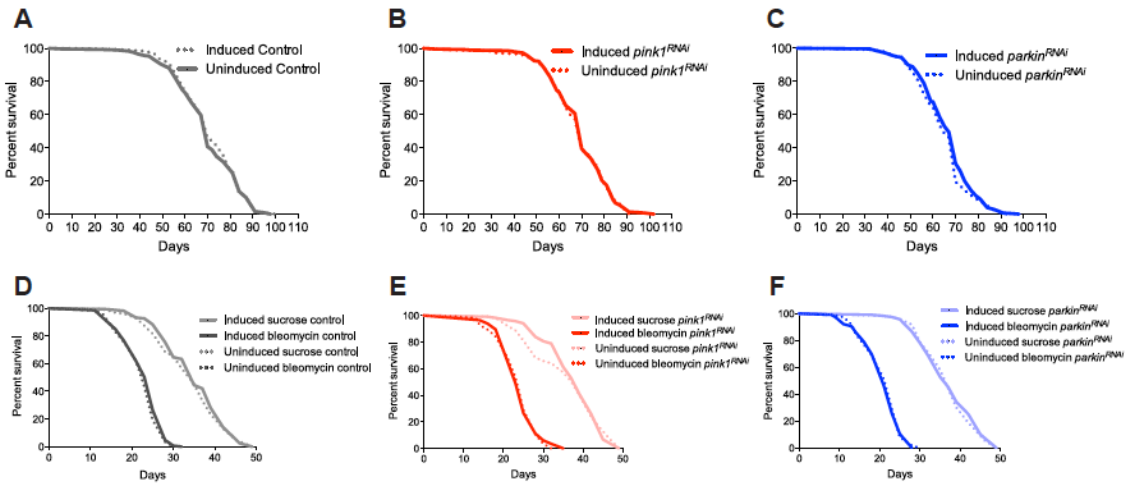

Supplementary Figure 4-4: Midgut progenitor-specific knockdown of Pink1 or Parkin does not change lifespan or survivorship in response to prolonged bleomycin feeding. Lifespan of male **A**,Control (*Su(H)LacZ*; *esg-gfp,5961-Gal4*^{GS}/+;*UAS-mCherry*^{RNAi}), **B**, Pink1 knockdown (*Su(H)LacZ*; *esg-gfp,5961-Gal4*^{GS}/*UAS-pink1*^{RNAi}), or **C**, Parkin knockdown (*Su(H)LacZ*; *esg-gfp,5961-Gal4*^{GS}/UAS-*parkin*^{RNAi}) raised at 25°C on standard molasses/cornmeal medium. Transgene expression was induced with 25 µg/ml RU486 incorporated into the food. Uninduced controls were fed standard food containing ethanol as a vehicle control. **D**-**F**, survivorship assay for flies exposed to bleomycin. Ten days after eclosion, flies were flipped to vials containing control (5% sucrose – black lines) or treatment (5 µg/ml bleomycin in 5% sucrose – red lines) solutions. Transgene expression was induced with 25 µg/ml RU486. Uninduced flies of the same genotype were used as controls. No significant difference in survivorship was observed for control (**D**, *Su(H)LacZ*; *esg-gfp,5961-Gal4*^{GS}/+;*UAS-mCherry*^{RNAi}), Pink1 knockdown (**E**, *Su(H)LacZ*; *esg-gfp,5961-Gal4*^{GS}/*UAS-pink1*^{RNAi}), or Parkin knockdown (**F**, *Su(H)LacZ*; *esg-gfp,5961-Gal4*^{GS}/UAS-*parkin*^{RNAi}).

References

1. Jones, D.L. and T.A. Rando, *Emerging models and paradigms for stem cell ageing.* Nature cell biology, 2011. **13**(5): p. 506-12.
2. Buchon, N., et al., *Morphological and molecular characterization of adult midgut compartmentalization in Drosophila.* Cell reports, 2013. **3**(5): p. 1725-38.
3. Marianes, A. and A.C. Spradling, *Physiological and stem cell compartmentalization within the Drosophila midgut.* Elife, 2013. **2**: p. e00886.
4. Micchelli, C.A. and N. Perrimon, *Evidence that stem cells reside in the adult Drosophila midgut epithelium.* Nature, 2006. **439**(7075): p. 475-9.
5. Ohlstein, B. and A. Spradling, *The adult Drosophila posterior midgut is maintained by pluripotent stem cells.* Nature, 2006. **439**(7075): p. 470-4.
6. O'Brien, L.E., et al., *Altered modes of stem cell division drive adaptive intestinal growth.* Cell, 2011. **147**(3): p. 603-14.
7. Liu, W., S.R. Singh, and S.X. Hou, *JAK-STAT is restrained by Notch to control cell proliferation of the Drosophila intestinal stem cells.* J Cell Biochem, 2010. **109**(5): p. 992-9.
8. Ohlstein, B. and A. Spradling, *Multipotent Drosophila intestinal stem cells specify daughter cell fates by differential notch signaling.* Science, 2007. **315**(5814): p. 988-92.
9. Takashima, S., et al., *Development of the Drosophila entero-endocrine lineage and its specification by the Notch signaling pathway.* Dev Biol, 2011. **353**(2): p. 161-72.
10. Maeda, K., et al., *E-cadherin prolongs the moment for interaction between intestinal stem cell and its progenitor cell to ensure Notch signaling in adult Drosophila midgut.* Genes Cells, 2008. **13**(12): p. 1219-27.

11. Biteau, B. and H. Jasper, *Slit/Robo signaling regulates cell fate decisions in the intestinal stem cell lineage of Drosophila.* Cell Rep, 2014. **7**(6): p. 1867-75.

12. Zeng, X. and S.X. Hou, *Enteroendocrine cells are generated from stem cells through a distinct progenitor in the adult Drosophila posterior midgut.* Development, 2015. **142**(4): p. 644-53.

13. Guo, Z. and B. Ohlstein, *Stem cell regulation. Bidirectional Notch signaling regulates Drosophila intestinal stem cell multipotency.* Science, 2015. **350**(6263).

14. Amcheslavsky, A., J. Jiang, and Y.T. Ip, *Tissue damage-induced intestinal stem cell division in Drosophila.* Cell Stem Cell, 2009. **4**(1): p. 49-61.

15. Amcheslavsky, A., et al., *Tuberous sclerosis complex and Myc coordinate the growth and division of Drosophila intestinal stem cells.* The Journal of cell biology, 2011. **193**(4): p. 695-710.

16. Amcheslavsky, A., et al., *Enteroendocrine cells support intestinal stem-cell-mediated homeostasis in Drosophila.* Cell Rep, 2014. **9**(1): p. 32-9.

17. Biteau, B. and H. Jasper, *EGF signaling regulates the proliferation of intestinal stem cells in Drosophila.* Development, 2011. **138**(6): p. 1045-55.

18. Buchon, N., et al., *Invasive and indigenous microbiota impact intestinal stem cell activity through multiple pathways in Drosophila.* Genes & Development, 2009. **23**(19): p. 2333-2344.

19. Buchon, N., et al., *Drosophila Intestinal Response to Bacterial Infection: Activation of Host Defense and Stem Cell Proliferation.* Cell Host and Microbe, 2009. **5**(2): p. 200-211.

20. Myant, K.B., et al., *Rac1 drives intestinal stem cell proliferation and regeneration.* Cell Cycle, 2013. **12**(18).

21. Tian, A. and J. Jiang, *Intestinal epithelium-derived BMP controls stem cell self-renewal in Drosophila adult midgut.* Elife, 2014. **3**: p. e01857.

22. Jiang, H. and B.A. Edgar, *EGFR signaling regulates the proliferation of Drosophila adult midgut progenitors.* Development, 2009. **136**(3): p. 483-493.

23. Jiang, H., et al., *Cytokine/Jak/Stat signaling mediates regeneration and homeostasis in the Drosophila midgut.* Cell, 2009. **137**(7): p. 1343-55.

24. Li, H., Y. Qi, and H. Jasper, *Dpp signaling determines regional stem cell identity in the regenerating adult Drosophila gastrointestinal tract.* Cell Rep, 2013. **4**(1): p. 10-8.

25. Lee, W.-J., *Bacterial-modulated host immunity and stem cell activation for gut homeostasis.* Genes & Development, 2009. **23**(19): p. 2260-5.

26. Rera, M., et al., *Modulation of longevity and tissue homeostasis by the Drosophila PGC-1 homolog.* Cell Metabolism, 2011. **14**(5): p. 623-34.

27. Greene, J.C., et al., *Mitochondrial pathology and apoptotic muscle degeneration in Drosophila parkin mutants.* Proceedings of the National Academy of Sciences of the United States of America, 2003. **100**(7): p. 4078-83.

28. Clark, I.E., et al., *Drosophila pink1 is required for mitochondrial function and interacts genetically with parkin.* Nature, 2006. **441**(7097): p. 1162-6.

29. Wei, H., L. Liu, and Q. Chen, *Selective removal of mitochondria via mitophagy: distinct pathways for different mitochondrial stresses.* Biochim Biophys Acta, 2015.

30. Zhu, J., K.Z. Wang, and C.T. Chu, *After the banquet: Mitochondrial biogenesis, mitophagy and cell survival.* Autophagy, 2013. **9**(11).

31. Springer, W. and P.J. Kahle, *Regulation of Pink1-Parkin-mediated mitophagy.* Autophagy, 2011. **7**(3): p. 266-78.

32. Youle, R.J. and D.P. Narendra, *Mechanisms of mitophagy.* Nature reviews. Molecular cell biology, 2011. **12**(1): p. 9-14.

33. Kashatus, D.F., et al., *RALA and RALBP1 regulate mitochondrial fission at mitosis.* Nature cell biology, 2011. **13**(9): p. 1108-15.

34. Poole, A.C., et al., *The mitochondrial fusion-promoting factor mitofusin is a substrate of the Pink1/parkin pathway.* PLoS ONE, 2010. **5**(4): p. e10054.

35. Poole, A.C., et al., *The Pink1/Parkin pathway regulates mitochondrial morphology.* Proceedings of the National Academy of Sciences of the United States of America, 2008. **105**(5): p. 1638-43.

36. Twig, G., et al., *Fission and selective fusion govern mitochondrial segregation and elimination by autophagy.* The EMBO journal, 2008. **27**(2): p. 433-46.

37. Yang, Y., et al., *Pink1 regulates mitochondrial dynamics through interaction with the fission/fusion machinery.* Proceedings of the National Academy of Sciences of the United States of America, 2008. **105**(19): p. 7070-5.

38. Benard, G. and R. Rossignol, *Ultrastructure of the mitochondrion and its bearing on function and bioenergetics.* Antioxidants & redox signaling, 2008. **10**(8): p. 1313-42.

39. Westermann, B., *Bioenergetic role of mitochondrial fusion and fission.* Biochimica et biophysica acta, 2012.

40. Henchcliffe, C. and M.F. Beal, *Mitochondrial biology and oxidative stress in Parkinson disease pathogenesis.* Nat Clin Pract Neurol, 2008. **4**(11): p. 600-9.

41. Benard, G. and R. Rossignol, *Ultrastructure of the mitochondrion and its bearing on function and bioenergetics.* Antioxid Redox Signal, 2008. **10**(8): p. 1313-42.

42. Hackenbrock, C.R., *Ultrastructural bases for metabolically linked mechanical activity in mitochondria. I. Reversible ultrastructural changes with change in metabolic steady state in isolated liver mitochondria.* The Journal of cell biology, 1966. **30**(2): p. 269-97.

43. Wang, L., C.J. McLeod, and D.L. Jones, *Regulation of adult stem cell behavior by nutrient signaling.* Cell Cycle, 2011. **10**(16): p. 2628-34.

44. Hur, J.H., et al., *Increased longevity mediated by yeast NDI1 expression in Drosophila intestinal stem and progenitor cells.* Aging, 2013.

45. Wang, L., et al., *Integration of UPRER and oxidative stress signaling in the control of intestinal stem cell proliferation.* PLoS Genet, 2014. **10**(8): p. e1004568.

46. Zeng, X., C. Chauhan, and S.X. Hou, *Characterization of midgut stem cell- and enteroblast-specific Gal4 lines in Drosophila.* Genesis (New York, NY : 2000), 2010.

47. Clarkson, M.J., et al., *Regions of variant histone His2AvD required for Drosophila development.* Nature, 1999. **399**(6737): p. 694-7.

48. Abramov, A.Y., et al., *Bioenergetic consequences of Pink1 mutations in Parkinson disease.* PLoS One, 2011. **6**(10): p. e25622.

49. Sykiotis, G.P. and D. Bohmann, *Keap1/Nrf2 signaling regulates oxidative stress tolerance and lifespan in Drosophila.* Dev Cell, 2008. **14**(1): p. 76-85.

50. Hochmuth, C.E., et al., *Redox regulation by keap1 and nrf2 controls intestinal stem cell proliferation in Drosophila.* Cell Stem Cell, 2011. **8**(2): p. 188-99.

51. Lee, A.C., et al., *Ras proteins induce senescence by altering the intracellular levels of reactive oxygen species.* J Biol Chem, 1999. **274**(12): p. 7936-40.

52. Nakamura, M., S. Ohsawa, and T. Igaki, *Mitochondrial defects trigger proliferation of neighbouring cells via a senescence-associated secretory phenotype in Drosophila.* Nat Commun, 2014. **5**: p. 5264.

53. Coppe, J.P., et al., *Senescence-associated secretory phenotypes reveal cell-nonautonomous functions of oncogenic RAS and the p53 tumor suppressor.* PLoS Biol, 2008. **6**(12): p. 2853-68.

54. Passos, J.F., et al., *Feedback between p21 and reactive oxygen production is necessary for cell senescence.* Mol Syst Biol, 2010. **6**: p. 347.

55. Correia-Melo, C., et al., *Mitochondria are required for pro-ageing features of the senescent phenotype.* EMBO J, 2016. **35**(7): p. 724-42.

56. Roman, G., et al., *P[Switch], a system for spatial and temporal control of gene expression in Drosophila melanogaster.* Proc Natl Acad Sci U S A, 2001. **98**(22): p. 12602-7.

57. Osterwalder, T., et al., *A conditional tissue-specific transgene expression system using inducible GAL4.* Proc Natl Acad Sci U S A, 2001. **98**(22): p. 12596-601.

58. McGuire, S.E., Z. Mao, and R.L. Davis, *Spatiotemporal gene expression targeting with the TARGET and gene-switch systems in Drosophila.* Sci STKE, 2004. **2004**(220): p. pl6.

59. Nicholson, L., et al., *Spatial and temporal control of gene expression in Drosophila using the inducible GeneSwitch GAL4 system. I. Screen for larval nervous system drivers.* Genetics, 2008. **178**(1): p. 215-34.

Chapter 5: Conclusions

Aging is characterized by the accumulation of cellular damage and a concomitant decline in tissue homeostasis. Once homeostatic conditions are sufficiently altered, organ function fails and ultimately leads to the death of an organism. In tissues capable of regeneration or turnover, populations of resident stem or progenitor cells are responsible for maintaining tissue homeostasis through controlled proliferation, self-renewal, and daughter cell differentiation. As stem cell function declines with age, so too does the ability of a tissue to regenerate or turnover. Despite the clear importance of stem cell function on organismal health, it is still unclear if the decline in stem cell function is a major causative factor of aging.

Many reports implicate cellular metabolism as the main factor that drives the advancement of the aging phenotype. Furthering this hypothesis, previous studies have shown that introduction of mtDNA mutations and deletions into the mitochondria of stem and progenitor cells of mice can lead to progeriod phenotypes including alopecia, general wasting, and decrease fertility [1, 2]. These reports indicate that the causative factor of aging could be mitochondrial dysfunction of stem and progenitor cell populations. This led us to investigate the possible roles of increased mitochondrial biogenesis (Chapter 2), increased ETC function (Chapter 3), or altered mitochondrial dynamics (Chapter 4) in the regulation of intestinal stem cell function in *Drosophila melanogaster*; we sought to determine if changes in the cellular metabolism of specific stem cells within the fly could have an impact on stem cell function, tissue homeostasis, and, therefore, lifespan of the fly [3, 4].

In Chapter 2, we investigated the role of dPGC-1 (a functional homologue of PGC-1α and master regulator of mitochondrial biogenesis) in ISC function during aging. We found that PGC-1 expression declined with age in the *Drosophila* intestine, leading us to question if decreased PGC-1 expression had an effect on declining tissue homeostasis with age. Through

intestinal progenitor-specific overexpression of dPGC-1, we show that mitochondrial activity is enhanced throughout the entire midgut of the fly. This enhanced mitochondrial function led to prolonged epithelial homeostasis and increased lifespan. In addition to enhancing mitochondrial function, overexpression of dPGC-1 in the ISC/EBs led to decreased ROS levels in the progenitor cells. In addition to being implicated as a causative factor of aging, ROS levels have also been shown to regulate stem cell self-renewal and differentiation [5-9]. In *Drosophila* ISCs, *CncC* (a master regulator of cellular redox state) promotes expression of antioxidant genes to maintain low ROS levels in order to maintains quiescence [10]. It is possible that enhanced mitochondrial function in the intestinal progenitor cells leads to proliferative homeostasis through the maintenance of low ROS levels late into the life of the fly. This study provides evidence that specific metabolic interventions in distinct stem cell populations is sufficient to increase the lifespan of *Drosophila*, and it would be interesting to investigate if this function is conserved in other organisms.

Chapter 3 expands on the results of Chapter 2 by narrowing the mechanism of action for prolonged lifespan from enhanced mitochondrial biogenesis to enhanced electron transport chain function. In this study, we overexpress *Ndi1* (the yeast homologue to Complex I of the ETC) in the stem and progenitor cells of the *Drosophila* midgut. *Ndi1* expression leads to enhanced ETC function via increased mitochondrial NADH dehydrogenase activity. Similar to *dPGC*-1 overexpression, *Ndi1* overexpression in the ISC/EBs led to a delay in intestinal barrier dysfunction, increased tissue homeostasis, and increased lifespan [3]. Interestingly, although the *Ndi1* overexpressing flies displayed prolonged lifespans, they also consumed more food than controls; this was, to our knowledge, the first report in which a lifespan extending intervention also correlated with increased food intake. These results show that the enhancement of NADH dehydrogenase activity in ISC lineages is a plausible strategy to delay intestinal aging, prolong tissue homeostasis, and increase the lifespan of fruit flies. *Ndi1* can be expressed in mammalian cells without causing an immune response [11-14]. Therefore, our

study provides an interesting strategy to improve stem cell function and tissue homeostasis in mammals through the stem cell-targeted overexpression of *ndi1*.

Chapter 4 builds on the findings of the previous chapters and investigates any possible roles of mitochondrial dynamics on ISC function with age. We find that RNAi-mediated knockdown of either Pink1 or Parkin (two mitophagy-related genes) in the ISCs of the *Drosophila* midgut results in decreased proliferation during either stress or aging. Specifically, we show that, upon knockdown of Pink1 or Parkin, the mitochondria of the ISCs undergo an orthodox to condensed transition, which is related to increased OXPHOS activity and increased ROS production. Indeed, the ISC/EBs that had been depleted of Pink1 or Parkin maintained higher levels of ROS. This led to the increased expression of several senescence associated markers including heterochromatic protein 1 (HP1) and sensence-associated β-galactosidase (SA-β-Gal). We then demonstrated that some of the ISCs that had been depleted were, in fact, functionally senescent as they could not respond to pro-proliferative cues even after the resumption of normal *pink1* or *parkin* expression. Taken together, our results indicate that progenitor-specific mitochondrial dysfunction uncouples cellular and tissue aging, in part, through induction of ISC senescence and suggest that ISCs utilize mitophagy as one strategy to maintain a healthy complement of mitochondria. The role of mitochondria in enhancing the onset of senescence has been recently reported in mammals [15], and our data reveal a similar relationship is present in invertebrates.

All of the studies in this manuscript were carried out using *Drosophila melanogaster* as a model organism. One major advantage of the *Drosophila* system with regards to the *in vivo* study of stem cells is the abundance of Gal4 drivers that allow spatiotemporal expression of transgenes in particular cell types. Despite the existence of ISC-specific drivers for transgene expression, more intense metabolic studies are hampered by the necessity for the use of mitochondrial dyes and an inability to carry out large-scale metabolomic studies. New protocols for the detection of ROS in dissected midguts [16] or H_2O_2 in living flies [17, 18] could aid in the

characterization of metabolic changes in the *Drosophila* ISCs. Furthermore, several groups have successfully sorted ISCs from *Drosophila* ISCs [19-21]. How well mitochondrial function can be preserved during the rather harsh dissociation protocol is yet to be determined. Regardless, mass spectrometry from stem, progenitor, and differentiated cell populations from young or aged midguts could provide useful insight into pathways that are most heavily affected during aging.

Mounting evidence suggests that mtDNA damage and mitochondrial dysfunction can play a causative role in aging phenotypes. Some of the hallmarks of aging include the loss of tissue homeostasis and a decline in stem cell function. In *Drosophila*, increased proliferative homeostasis of the intestinal stem cells can lead to increased lifespan. Interventions that enhance proliferative homeostasis often cause increased mitochondrial function within the stem cells. As methods to characterize changes in the metabolites of ISCs throughout aging improve, the comparison between young and old metabolic profiles will present new and exciting targets of study. Given the importance of consistent stem cell function on tissue homeostasis, and, in turn the vital nature of tissue homeostasis on lifespan, these findings will likely give insight into the cell-specific interventions that could drastically impact lifespan.

References

1. Ahlqvist, K.J., et al., *Somatic progenitor cell vulnerability to mitochondrial DNA mutagenesis underlies progeroid phenotypes in polg mutator mice.* Cell Metabolism, 2012. **15**(1): p. 100-9.
2. Vermulst, M., et al., *DNA deletions and clonal mutations drive premature aging in mitochondrial mutator mice.* Nat Genet, 2008. **40**(4): p. 392-4.
3. Hur, J.H., et al., *Increased longevity mediated by yeast NDI1 expression in Drosophila intestinal stem and progenitor cells.* Aging, 2013.
4. Rera, M., et al., *Modulation of longevity and tissue homeostasis by the Drosophila PGC-1 homolog.* Cell Metabolism, 2011. **14**(5): p. 623-34.
5. Owusu-Ansah, E. and U. Banerjee, *Reactive oxygen species prime Drosophila haematopoietic progenitors for differentiation.* Nature, 2009. **461**(7263): p. 537-41.
6. Ito, K., et al., *Reactive oxygen species act through p38 MAPK to limit the lifespan of hematopoietic stem cells.* Nature medicine, 2006. **12**(4): p. 446-51.
7. Ito, K., et al., *Regulation of oxidative stress by ATM is required for self-renewal of haematopoietic stem cells.* Nature, 2004. **431**(7011): p. 997-1002.
8. Smith, J., et al., *Redox state is a central modulator of the balance between self-renewal and differentiation in a dividing glial precursor cell.* Proc Natl Acad Sci U S A, 2000. **97**(18): p. 10032-7.
9. Tothova, Z. and D.G. Gilliland, *FoxO transcription factors and stem cell homeostasis: insights from the hematopoietic system.* Cell Stem Cell, 2007. **1**(2): p. 140-52.
10. Hochmuth, C.E., et al., *Redox regulation by keap1 and nrf2 controls intestinal stem cell proliferation in Drosophila.* Cell Stem Cell, 2011. **8**(2): p. 188-99.
11. Marella, M., et al., *No immune responses by the expression of the yeast Ndi1 protein in rats.* PLoS One, 2011. **6**(10): p. e25910.

12. Santidrian, A.F., et al., *Mitochondrial complex I activity and NAD+/NADH balance regulate breast cancer progression.* J Clin Invest, 2013. **123**(3): p. 1068-81.

13. Seo, B.B., et al., *Molecular remedy of complex I defects: rotenone-insensitive internal NADH-quinone oxidoreductase of Saccharomyces cerevisiae mitochondria restores the NADH oxidase activity of complex I-deficient mammalian cells.* Proc Natl Acad Sci U S A, 1998. **95**(16): p. 9167-71.

14. Seo, B.B., et al., *Use of the NADH-quinone oxidoreductase (NDI1) gene of Saccharomyces cerevisiae as a possible cure for complex I defects in human cells.* J Biol Chem, 2000. **275**(48): p. 37774-8.

15. Correia-Melo, C., et al., *Mitochondria are required for pro-ageing features of the senescent phenotype.* EMBO J, 2016. **35**(7): p. 724-42.

16. Luo, L., A.R. Reedy, and R.M. Jones, *Detecting Reactive Oxygen Species Generation and Stem Cell Proliferation in the Drosophila Intestine.* Methods Mol Biol, 2016. **1422**: p. 103-13.

17. Cocheme, H.M., et al., *Using the mitochondria-targeted ratiometric mass spectrometry probe MitoB to measure H2O2 in living Drosophila.* Nat Protoc, 2012. **7**(5): p. 946-58.

18. Cocheme, H.M., et al., *Measurement of H2O2 within living Drosophila during aging using a ratiometric mass spectrometry probe targeted to the mitochondrial matrix.* Cell Metab, 2011. **13**(3): p. 340-50.

19. Dutta, D., J. Xiang, and B.A. Edgar, *RNA expression profiling from FACS-isolated cells of the Drosophila intestine.* Curr Protoc Stem Cell Biol, 2013. **27**: p. Unit 2F 2.

20. Korzelius, J., et al., *Escargot maintains stemness and suppresses differentiation in Drosophila intestinal stem cells.* EMBO J, 2014. **33**(24): p. 2967-82.

21. Loza-Coll, M.A., et al., *Regulation of Drosophila intestinal stem cell maintenance and differentiation by the transcription factor Escargot.* EMBO J, 2014. **33**(24): p. 2983-96.